

Structural Modelling of Textile Reinforced Concrete (TRC) Sandwich Panels

Master's Thesis in the Master's Programme Structural Engineering and Building Technology

Guðlaugur Már Guðmundsson
Óskar Bragi Guðmundsson

MASTER'S THESIS 2015:81

Master's Thesis in the Master's Programme Structural Engineering and Building Technology

Guðlaugur Már Guðmundsson

Óskar Bragi Guðmundsson

Department of Civil and Environmental Engineering

Division of Structural Engineering

Research Group Concrete Structures

CHALMERS UNIVERSITY OF TECHNOLOGY

Göteborg, Sweden 2015

Master's Thesis in the Master's Programme Structural Engineering and Building Technology

Guðlaugur Már Guðmundsson

Óskar Bragi Guðmundsson

© GUÐLAUGUR MÁR GUÐMUNDSSON, ÓSKAR BRAGI GUÐMUNDSSON,
2015

Examensarbete 2015:81/ Institutionen för bygg- och miljöteknik,
Chalmers tekniska högskola 2015

Department of Civil and Environmental Engineering

Division of Structural Engineering

Research Group Concrete Structures

Chalmers University of Technology

SE-412 96 Göteborg

Sweden

Telephone: + 46 (0)31-772 1000

Cover:

FE-models of different test-setups for concrete sandwich panels.

Chalmers Repro Service / Department of Civil and Environmental Engineering

Göteborg, Sweden, 2015

Master's thesis in the Master's Programme Structural Engineering and Building Technology

Guðlaugur Már Guðmundsson

Óskar Bragi Guðmundsson

Department of Civil and Environmental Engineering

Division of Structural Engineering

Research Group Concrete Structures

Chalmers University of Technology

ABSTRACT

In modern construction industry, reinforced concrete is one of the most widely used building materials. By replacing the conventional steel reinforcement with high strength textile fibre mesh, the risk of reinforcement corrosion is eliminated, which provides a possibility to reduce the cover thickness and thus the overall size of the structural members without losing the element's strength and ductility. This is beneficial in many aspects such as reduction of the environmental footprint from cement production, lighter structural elements, easier transportation and installation as well as reduced overall cost.

Prefabricated concrete sandwich panels (PCSP) have been produced and used for structural applications for decades. As sandwich panels have shown to be structurally and thermally efficient and since the prefabricated elements have been increasingly used in construction projects, the implementation of textile reinforced concrete (TRC) in PCSP has become an important research topic.

To enable the composite action between the inner and outer concrete panels of a PCSP, a load transferring connection system is needed. Because of reduced thickness in TRC panels, the design of such connection is a challenge which makes up the primary focal point of this study. The purpose of this Master's thesis is to develop a FE-model for the design of TRC sandwich panels with particular emphasis on connection systems ensuring robust composite action.

The objectives of this thesis were (1) to investigate and compare different connection solutions, and (2) to develop a 3D FE-model of an experimental set-up for performance evaluation of connection systems. Several types of connectors were studied and modelled. Uncertainties and difficulties in the modelling of the connectors were identified and the gained knowledge was then applied to the development of a detailed FE-model of more complex connectors in TRC panels.

The results of 3D FE-models combined with test results of different commercially available connectors showed that the bond between concrete and connectors may strongly influence the strength and stiffness of a TRC sandwich panel. A modified shear plate connector and pin connectors made of fibre reinforced polymers (FRP) were then examined as a promising solution for TRC sandwich panels.

Key words: TRC, textile reinforcement, carbon fibre, alkali resistant glass FE-modelling, FRP, sandwich panels, PCSP, bond slip, connector

Svensk översättning av titeln
Underrubrik (om sådan finns)

Examensarbete inom masterprogrammet Structural Engineering and Building
Technology

Guðlaugur Már Guðmundsson
Óskar Bragi Guðmundsson
Institutionen för bygg- och miljöteknik
Avdelningen för Avdelningsnamn
Forskargrupsnamn
Chalmers tekniska högskola

SAMMANFATTNING

Sammanfattning på svenska. (If summary in Swedish is omitted, delete all text on this page and leave it blank.)

Nyckelord:

Contents

1	INTRODUCTION	1
1.1	Background	1
1.2	Objectives	2
1.3	Method	2
1.4	Limitations	2
2	SANDWICH PANELS	4
2.1	Textile reinforced sandwich panels	5
3	MATERIALS	6
3.1.1	Concrete	6
3.1.2	Textile reinforcement	6
3.1.3	Connectors	8
3.1.4	Insulation material	9
4	CONNECTING DEVICES	10
4.1	Functions and requirements	11
4.2	Load-bearing behaviour	14
4.2.1	Pin-connectors	14
4.2.2	Diagonal shear connectors	15
4.2.3	Shear grids	16
4.2.4	Shear plate connector	18
4.3	Testing	19
5	FE-MODELLING	21
5.1	Verification model	21
5.1.1	Geometry	21
5.1.2	Material properties	24
5.1.3	Mesh and element types	27
5.1.4	Boundary conditions	28
5.1.5	Loading and analysis method	30
5.1.6	Correlation and calibration	31
5.1.7	Test Model 3	50
5.2	TRC panel model	51
5.2.1	Geometry	52
5.2.2	Material properties	54
5.2.3	Mesh and element types	54
5.2.4	Boundary conditions	54
5.2.5	Loading and analysis method	55
5.2.6	Results	55

6	DISCUSSIONS	70
7	CONCLUSIONS	71
7.1	Conclusions	71
7.2	Further research	71
8	REFERENCES	73
9	APPENDICES	75
9.1	Appendix A – DIANA .dat file	75
9.2	Appendix B - Material properties calculations	81

Preface

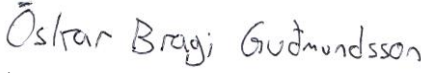
In this study, FE-models of shear tests were created and compared with experimental results from TRC sandwich panel. The work presented in this thesis was carried out from January 2015 to June 2015 at the Department of Civil- and Environmental Engineering, Division of Structural Engineering, Concrete Structures, Chalmers University of Technology, Sweden.

We would like to thank our supervisor Kamyab Zandi and our examiner Filip Nilenius for guiding us through the project and giving us helpful advice through the whole thesis work.

We would also like to thank our office colleagues Jón Pétur Indriðason and Vésteinn Sigmundsson for their support.

Göteborg, June 2015


Guðlaugur Már Guðmundsson


Óskar Bragi Guðmundsson

1 Introduction

In modern construction industry, concrete is one of the most widely used building material. When reinforced with high tensile strength material to compensate for its low tensile strength, it becomes suitable for many structural applications, though its vulnerability to deterioration and corrosion of steel reinforcement have shown to be an issue. Another disadvantage with extensive use of concrete is the highly energy consuming process of cement production, which is a major component of concrete. With increased environmental revival, the urge to diminish the environmental footprint from cement production grows.

With the objective to minimize these disadvantages, different measures are being examined. One of those is to replace conventional steel reinforcement with textile fibre meshes. By excluding the steel reinforcement and replacing it with high strength textile fibres the risk of reinforcement corrosion is eliminated which also opens a possibility for reducing the cover thicknesses and thus the overall thickness of the structural members. By arranging the high strength fibres in an effective way the textile reinforced concrete (TRC) can allow for the design of slender structural members and permits more freedom in the structure form (Bramshuber 2006).

Prefabricated concrete sandwich panels (PCSP) have been produced and used for structural applications for decades. First as non-composite elements, with one structural panel which is usually referred to as a wythe, and one non-structural “weather” layer and later as a composite type panel where both wythes are utilized structurally by connecting them with a load transferring connectors or insulation material (Benayoune et al. 2007).

1.1 Background

As sandwich panels have shown to be structurally and thermally efficient and the method of using prefabricated elements in construction projects is increasingly utilized, the implementation of TRC in PCSPs has become an interesting research topic. The possibility of decreasing the wythe thicknesses and thus the overall thickness of an element by replacing the steel reinforcement with a noncorrosive fibre material, motivates researchers in development of this more slender and lightweight application with high durability (Shams, Hegger et al. 2014).

To enable a robust composite action between the inner and outer wythes, a well-designed connection system is needed. The optimal connector should be noncorrosive, have low thermal conductivity and be able to transfer a considerable amount of load while not requiring a great embedment depth. Because of the reduced thickness in TRC panels, the design of such connectors is a challenge.

There are a number of commercially available sandwich panel connectors, which are generally used in conventional steel reinforced PCSPs. These connectors have to be tested in TRC sandwich panels and might have to be modified for optimal performance.

1.2 Objectives

The main aim of this Master's thesis was to develop a FE-model for the design of TRC sandwich panels, focusing on the connection system between the two wythes.

This principal aim was divided into the following sub-objectives:

- Investigate and discuss different connection solutions
- Develop a non-linear 3D FE-model of an experimental set-up to evaluate the performance of the connection system
- Identify uncertainties and difficulties in FE-modelling of a connection system
- Identify critical issues connecting thin TRC layers
- Develop a FE-model of a promising connection system for TRC sandwich Panels for further investigation and experimental testing

1.3 Method

Methodology used to achieve the different sub-objectives:

- Documentation regarding currently available connectors used for conventional concrete as well as existing scientific articles concerning TRC sandwich panels were collected. Different solutions were discussed and compared
- Experimental set-ups of different connection systems were studied and appropriate material properties were collected. Test results from experimental testing regarding the bond between concrete and connector were studied
- A non-linear 3D FE-model of different test set-ups were made and the corresponding failure modes were identified. The model was then calibrated using the results from experiments available in literature
- A non-linear 3D FE-model of a promising connection system for TRC panels was made and the corresponding failure modes and structurally critical regions were identified and discussed

1.4 Limitations

The following limitations are encountered in this study:

- For the FE-model of experimental test set-ups, the compressive strength and elastic modulus that were used in the analyses had been experimentally evaluated. Other input parameters for the concrete were calculated according to existing recommendations, they may however differ from the actual values.
- The material properties for the insulation material in the test set-up had not been provided, but only the insulation type had been given. Therefore properties from a certain manufacturer were assumed. As these properties differ to some extent between manufacturers, this could cause a small discrepancy.
- Results from pull-out tests on modelled connectors only included their maximum pull-out capacity. Because of that, the bond-slip relation was assumed and calibrated.

- Test results from the modelled connections system for the TRC panels was not available at the time of this work, so the identified behaviour and failure modes could not be verified. Nevertheless, the Swedish Cement and Concrete Research Institute (CBI) are planning to do experiments in the near future with a similar TRC sandwich panel and connecting system as described in this Master's thesis.

2 Sandwich panels

Precast concrete sandwich panels (PCSP) have been used as exterior walls for the last 50 years (Sopal et al. 2013). PCSP are made up of two concrete layers called wythes, which are parted by a insulation material which is usually an insulation foam, an example of a sandwich panel can be seen in Figure 2-1. Due to the insulation layer, a high thermal resistance can be achieved with the panels and by utilizing a composite action between the two wythes, they will act together to resist vertical and horizontal loads. Such elements, often referred to as sandwich panels, have proven to be a viable solution for many building applications due to its good structural and thermal performance (Benayoune et al. 2007).



Figure 2-1 Sandwich panel, two concrete wythes parted by an insulation layer (Mountain view – pre-cast concrete©, 2015).

To achieve the desired composite behaviour it is important to have stiff and strong connection between the two wythes (J . Finzel , U . Häussler-Combe, 2003). By increasing the density of the insulation foam, the load bearing capacity as well as the shear resistance and elastic modulus will increase (Shams, Hegger et al. 2014b). The degree of composition is usually divided into three categories: fully composite, semi-composite and non-composite. A PCSP that has fully composite behaviour will act as one single unit and resist the load until failure, this can be achieved by enabling shear transfer between the wythes. This way the reinforcement will yield or the concrete will be crushed before the connectors fail. A PCSP that is partially composite have connectors that can only transfer a small portion of the shear in the longitudinal direction. Because of this, the connectors will fail before the wythe's reinforcement or concrete have reached their capacities. If on the other hand, the PCSP has non-composite behaviour, the connectors do not transfer shear in the longitudinal direction, but only perpendicular between the two wythes, who will act as two separate units (A. Benayoune et al. 2008). The shear force diagram in Figure 2-2 shows how the different degrees of composition affects the distribution of shear forces in the sandwich panel.

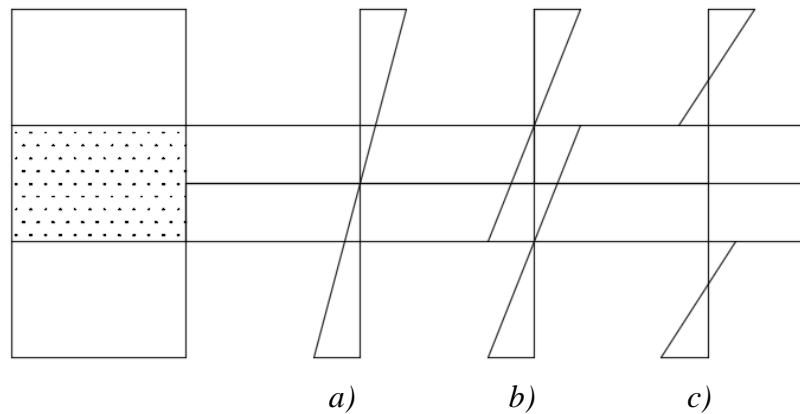


Figure 2-2 Shear force diagram of a sandwich panel, a) fully composite, b) semi-composite, c) non-composite.

In the past, these shear transfer mechanisms were achieved by casting solid concrete zones and ribs or alternatively placing trusses made of steel between the wythes. These methods can work well if they are properly designed, however they have a negative effect on the thermal insulation since it will cause thermal bridges (Sopal et al. 2013). Hence, it is desirable to find a new method to transfer shear to obtain a composite behaviour.

2.1 Textile reinforced sandwich panels

The classical PCSP can be thick and heavy, which is due to the fact that they have a large concrete cover thickness to prevent corrosion in the steel reinforcement. By using high-strength textiles that do not corrode it is possible to decrease the cover thickness immensely (J. Finzel & Häußler-Combe, 2003). These textile reinforced concrete (TRC) sandwich panels will then be able to carry loads in an efficient way while maintaining a slender figure. However, there are some restrictions regarding the thickness of the panels, they have to be thick enough to fulfil the demands for load-bearing capacity, ductility, deformation and safety against cracking. A PCSP with textile reinforcement can have 2 cm - 4 cm thick wythes, while the thickness for normal steel reinforced wythes are often 8 cm -14 cm with at least a 3 cm concrete cover (Portal et al. 2014) and (Shams, Horstmann et al. 2014). By using these slender TRC wythes, the thickness of the entire sandwich panels decreases significantly which will result in a lighter, slimmer and more economically and environmentally friendly structure (Shams, Horstmann et al. 2014).

Although the strength of each material within the panel is a very important factor when it comes to durability and ultimate strength, there are other parameters that can affect the performance of the sandwich panel. For optimal performance the bonding between materials within the sandwich panel is an important aspect to study. Studies have shown that the bond between the insulation material and the wythes can have great influence on the stiffness of the element. It can be problematic to achieve a sufficient bond between those parts as some types of insulation materials have very smooth surfaces (Sopal et al. 2013). Nevertheless, a stiff and robust connecting devise can compensate for that, but to achieve full function of such device, it is vital that the connecting device has a proper bond to the concrete. Subsequently, by using well designed connecting system it is possible to get a sufficient bond between these layers (Shams, Hegger et al. 2014).

3 Materials

3.1.1 Concrete

Concrete is considered to be an essential structural material and can be found in most structures. It has a great compressive strength but lacks the tensile strength. Therefore steel reinforcement is often used to compensate for the low tensile strength. (Domone & Illston 2010). Other advantages of concrete is the low cost and versatility while steel is more expensive and has the risk of corrosion (Obrien et al. 2012). Plain concrete without reinforcement can also be used in structures if it will not be exposed to tensile forces, for example in foundations, short columns and simple walls (Engström 2014). But in cases where the concrete has to transfer forces, both compressive and tensile, as in load-bearing sandwich panels, it is necessary to have sufficient amount of reinforcement.

Concrete is made by mixing cement, water, fine aggregate (<4 mm) and course aggregate (>4 mm). Often a part of the cement is replaced by admixtures to enhance some of the properties of the concrete. Many experiments for conventional sandwich panels have been conducted and there are many different types of concrete used. Ordinary Portland cement with 10 mm crushed aggregate, a water-cement ratio of 0,55, a compressive strength of $f_c = 24,15$ MPa and an elastic modulus of $E_c = 22,45$ GPa can for instance be used according to a test setup described in (A. Benayoune et al 2008). The diameter of the steel reinforcement used was 6 mm with a yield strength of $f_y = 250$ MPa and an elastic modulus of $E_s = 215$ GPa.

For TRC sandwich panels, there are other limitations to be considered when selecting the ingredients and material parameters. Since the textile reinforcement consists of a mesh with small openings, there are some limitations on the grain size; it has to be small enough so the concrete will be able to penetrate the reinforcement. The small cover thickness can also limit the grain size, as the concrete needs to be able to flow between the reinforcement and the moulds. Low viscosity for the concrete is also preferred. Using fine grained concrete will result in a lower modulus of elasticity and larger deformations than regular concrete with the same compressive strength (Hegger & Voss 2008). Thus, it is important to study which concrete mix is most suitable for each situation.

3.1.2 Textile reinforcement

Textile reinforcement consists of fibres in a bundle that contain a large number of filaments, see Figure 3-1. These filaments are woven together and are referred to as strands if they are straight or yarns if they are twisted (Mallick 2008). There are two common methods to knit these fibres, warp knitting and weft knitting. Warps are the yarns that lay lengthwise and parallel to the selvage and they are interwoven with the weft which runs from selvage to selvage perpendicular to the warps. Weaving can be defined as the crossing of warps and wefts (Purnell & Brameshuber 2006). Hundreds, up to thousands, of filaments are roved into a yarn and shaped into a grid-like formation. These materials usually consist of alkali resistant glass (AR-glass) or carbon fibres which are not vulnerable to corrosion (Shams, Hegger et al. 2014).

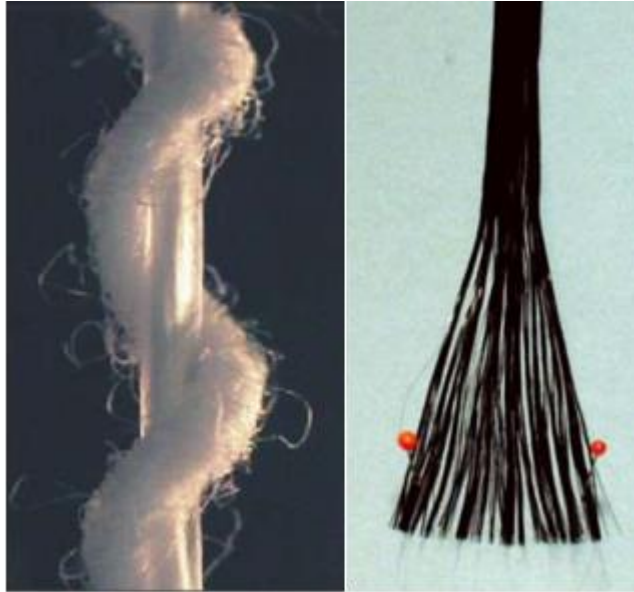


Figure 3-1 Fibre filaments (Purnell & Brameshuber 2006).

The main material in AR-glass is silica sand (SiO_2) and usually about 15% zircon (ZrO_2). It will therefore resist the corrosive alkaline solution in concrete made from standard cement.

The main material of carbon fibres is polyacrylonitrile (PAN) and meso phase pitch. The carbon fibres will not have as good adhesion to the concrete as the AR-glass. (Purnell & Brameshuber 2006).

When selecting a suitable reinforcement material there are some features that has to be considered, for example the material properties, temperature resistance, bond quality between reinforcement and concrete, the environmental impact, low cost and easy production. It is also essential to find the right reinforcement ratio and a suitable placement of the reinforcement to get the best composite performance (Williams Portal 2013). A typical reinforcement mesh can be seen in Figure 3-2.

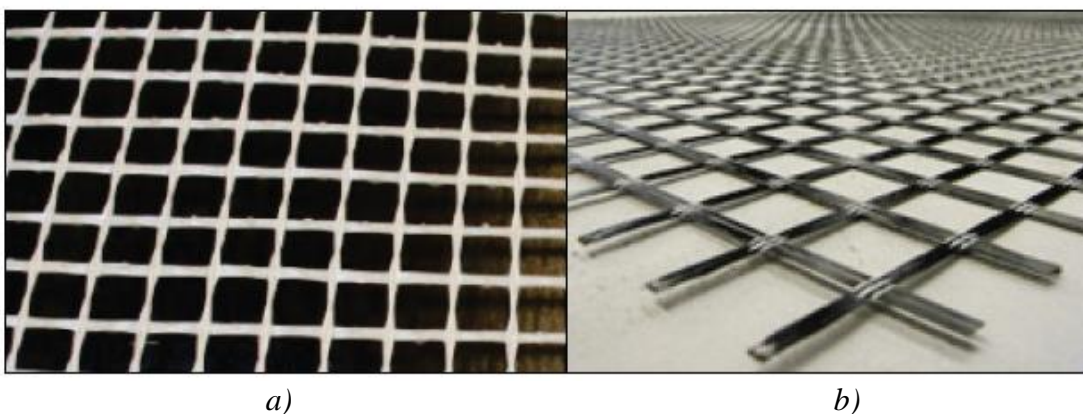


Figure 3-2 a) AR-Glass mesh, b) carbon mesh (Williams Portal, 2013).

The textile reinforcement should have a modulus of elasticity that is considerably higher than of the concrete to minimize the negative effect on the stiffness when cracking occurs. The location and interaction between the filaments will affect the stress-strain relation of the filament yarn, it is preferable to have the filaments parallel

and drawn (Purnell & Brameshuber 2006). The filaments in the yarn consist of two sets which get separated, inner and outer filaments. In the outer filaments, the fibres are in direct contact with the concrete which leads to a fully embedded bond. The inner filaments are bonded internally by friction between the filaments. Therefore there are two sorts of bonds that has to be considered: firstly the bond between the outer filaments and concrete and secondly the bond between the inner filaments (Häußler-Combe & Hartig 2007). The concrete will not be able to penetrate to the inner filaments. Thus, the inner filaments are not fully activated for load transfer. This can be solved by soaking the yarn in an epoxy resin which will yield a homogenous cross-section where practically all of the filaments participate in load transfer (Shams, Hegger et al. 2014). Tests performed on single filaments showed that the stress-strain curve had nearly a linear behaviour until failure. At failure the filaments had shown low strain and a brittle failure mode. Since there is no yielding in the filaments, damage can occur in production and manufacturing if the material is not handled properly. The strength of each fibre filament can vary, therefore a few filaments might break when loaded by a relatively low tensile force while the majority of the filaments in the yarn will be able to carry a high tensile force without failing (Mallick 2008). In Table 3-1 some material properties for textile reinforcement obtained from tensile tests on single filaments are shown (Hegger & Voss 2008).

Table 3-1 Material properties of textile reinforcement.

Material	Tensile strength [Mpa]	Elastic modulus [GPa]	Maximum strain [‰]
Carbon	3912	235,6	16,5
AR-glass	2018	70	28,8

3.1.3 Connectors

Connectors are essential to the composite behaviour of a sandwich element. Their material properties influence the stiffness and ultimate strength as well as affect the thermal resistance of the element as the connectors penetrate through the insulation creating a risk of a thermal bridging.

Many types of commercial connectors are available, made of various materials providing different functionality, depending on their intended application. In this Master's Thesis the focus was set on connectors made of low thermal conductive and non-corrosive fibre-reinforced polymers (FRP). In general there are two types of FRP that have shown potential to be suitable for this application. (Shams, Horstmann et al. 2014). Glass fibres, that has shown to have low thermal conductivity, average thermal expansion, low thermal resistance and is highly resistant to corrosion. And secondly carbon fibres, with average thermal conductivity, low thermal expansion, high thermal resistance and high corrosion resistance (Williams Portal 2013).

In this thesis the focus will be on connectors made of glass fibres, in particular electrical/chemical resistant glass fibres (E-CR-glass) impregnated with vinyl ester matrix to make a solid composite. This composition is used in a commercial connectors from Thermomass (Thermomass® 2012).

3.1.4 Insulation material

Insulation material, similar to the connectors, plays a vital role in the structural behaviour of a PCSP. Rigid foam material with high thermal resistance and low thermal conductivity is usually used as insulation material. The overall stiffness of the sandwich element depends highly on the density of the insulation material and its shear stiffness (Gopinath et al. 2014).

The shear flow capacity of the insulation material is also highly dependent on the bond between the concrete and the insulation material (Sopal et al. 2013).

Different types of rigid foam material are commercially available. In the paper (Sopal et al. 2013), results from experimental testing on a large number of panels with different insulation materials and connector spacing, were analysed with regards to the connectors/foam shear flow capacity. The foam materials that have been included in this study were: Expanded Polystyren (EPS), Extruded Polystyren (XPS) and Polyisocyanurate (POLY-ISO). Since the surface of the XPS had previously shown to have low bond strength due to its smooth coating, an effort was made to roughen the surface using sand blasting and plastic rollers.

The results showed that EPS and XPS with sandblast roughened surface showed a decrease in shear-flow capacity with an increased foam thickness, which indicates that failure was not due to sliding of the bonded interface. For the POLY-ISO and the rolled XPS the shear-flow capacity was not influenced by the foam thickness, which suggests a weaker bond interface for the latter two.

In the 3D FE analysis of the tests reported by Naito et al, 2012, which are presented in Chapter 4, XPS with untreated surfaces had been used as insulation material.

4 Connecting devices

Apart from keeping the two concrete wythes together, the main purpose of connecting devices is to transfer the loads between them. Depending on the connection, the behaviour and degree of composite action can be utilized as desired by the designer. Typically, the loads are transferred between the wythes either perpendicular to the wythes surface, with a pin-like behaving device, or parallel with a shear transferring device. Such connecting device enables the composite behaviour of a sandwich element discussed in Chapter 2.

Most often in a façade sandwich element, the inner wythe is thicker than the outer. The inner wythe is then assumed to support the vertical load from a roof or above structures and the self-weight of the outer wythe. The outer wythe works as a weather shield transferring horizontal forces from wind or impact to the inner wythe that supports it structurally, see Figure 4-1 a). Connecting devices in such elements mostly consists of pin-like connectors but a shear transfer is also needed for transferring the self-weight of the outer wythe to the inner one and for stabilising the whole sandwich element.

Another arrangement is when the two wythes are of similar thickness. Vertical load is then carried by one or both wythes and by implementing enough composite behaviour, the horizontal load is supported through a truss like action, with one wythe working in compression and the other in tension, see Figure 4-1 b).

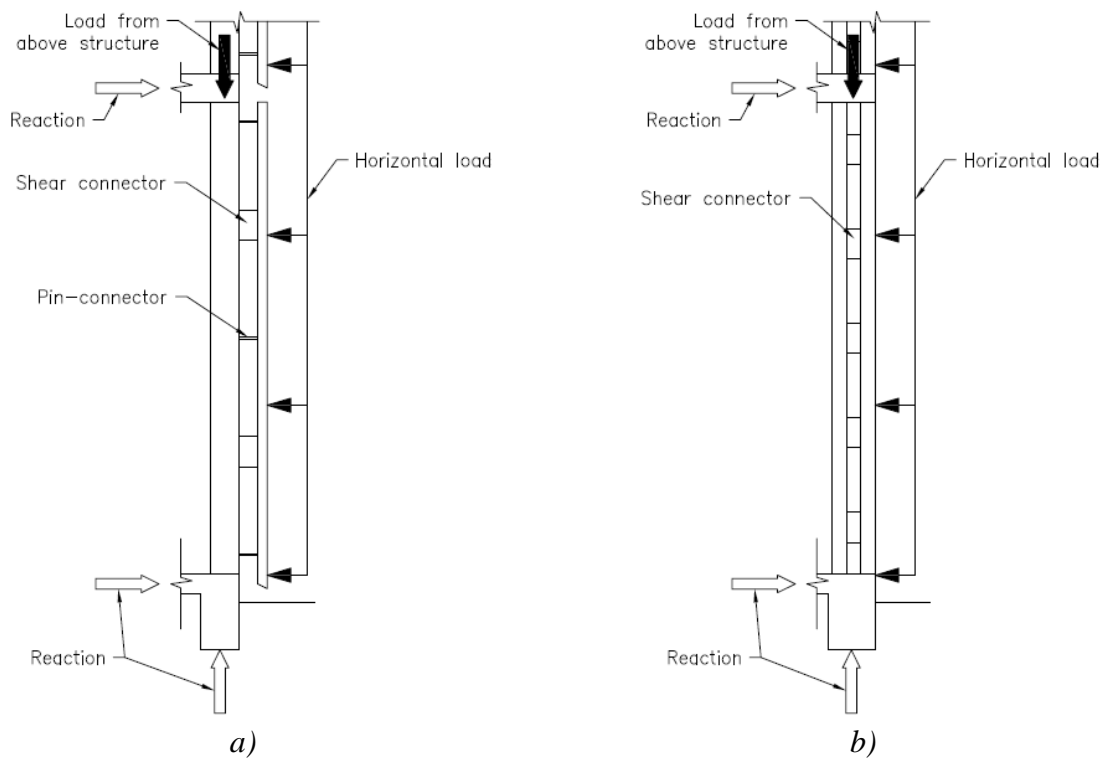


Figure 4-1 Different types of sandwich panels, a) Non-(or semi) composite, b) fully composite.

The main advantage of using TRC for the wythes, as discussed earlier, is the possibility of having thin and slender concrete elements. On the other hand, the thin concrete wythes can set restrictions in design of the connecting devices both by limiting possible anchorage length for the connector as well as making the wythes vulnerable to punching shear failure. An optimal anchorage behaviour is obtained if the connector fails before the embedded part.

4.1 Functions and requirements

As discussed in Naito et al. 2012, the composite action influences the flexural behaviour and the ultimate capacity of the element. For full composite flexural capacity, the connectors need to carry the shear forces in direction perpendicular to the load, see Figure 4-2.

Different methods can be used to determine the magnitude of needed shear resistance of the connectors, throughout the length of an element. The Precast/Prestressed Concrete institute (PCI Sandwich Wall Committee 1997) recommends a method, most often used in design of PCSP, where the required shear resistance is calculated from the flexural resistance of the section (Naito et al. 2012). The maximum compression or tension capacity of each wythe at mid-span is computed and the smaller value is used as a minimum shear resistance of the connectors as can be seen in Figure 4-2 and Equations 4-1 to 4-3.

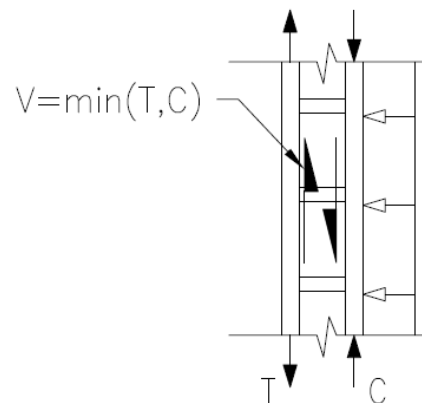


Figure 4-2 Simplified force pattern within an element from horizontal loading.

$$V_{required} = \text{minimum}(T, C) \quad \text{Eq. 4-1}$$

$$T = \text{tension} = A_{ps}f_{ps} + A_s f_y \quad \text{Eq. 4-2}$$

$$C = \text{compression} = 0,85f'_c b t_c \quad \text{Eq. 4-3}$$

Where :

- A_{ps} is the area of pre-stressing steel in tension wythe
- f_{ps} is the stress in pre-stressing steel at ultimate flexural strength
- f'_c is the compressive strength of the concrete
- b is the width of the element

t_c is the thickness of the compression wythe

The number of shear connectors required to keep full flexural composition, $n_{required}$ can then be described with Equation 4-4.

$$n_{required} > \frac{V_{required}}{V_{single\ connector\ capacity}} \quad \text{Eq. 4-4}$$

For simplification of calculations, this method assumes the entire depth of each wythe is either in compression or tension, see Figure 4-3.

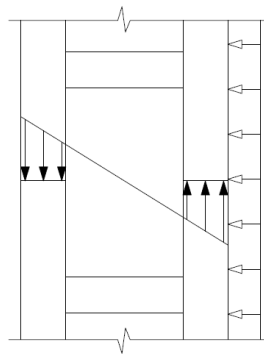


Figure 4-3 Stress distribution in the concrete wythes.

Non-shear transferring connecting devices transfer normal forces between the two wythes. For wall elements, these forces can be from wind or accidental load such as explosion or collision. The magnitude depends on the load and distance between the connectors. As wind load can work both as suction and pressure, these connectors can be subjected to both compression and tension. Failure of the connector itself is not necessarily decisive for the capacity, but anchorage to the concrete can be critical (Shams, Horstmann et al. 2014b). This can especially be the case in a thin TRC wythe, as discussed above.

A common method to prevent an anchorage (slip/pull out) failure is to mechanically anchoring the connectors either by tying them to the wythe reinforcement, see Figure 4-4 a), or by shaping the embedded part in a way that increases the bond between the concrete and the connector, see Figure 4-4 b).

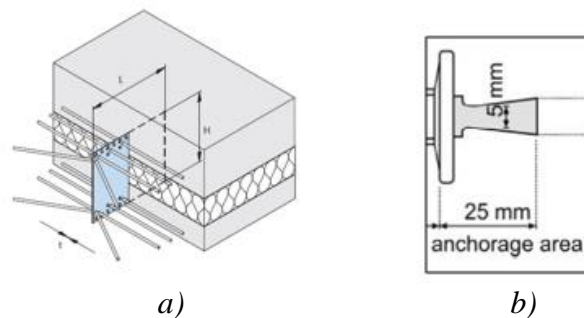


Figure 4-4 Examples of anchorage, a) plate anchored with reinforcement bars (Halfen©, 2015), b) cone shaped embedded part (Shams, Horstmann et al. 2014).

The punching shear resistance of the thin concrete faces can be increased by altering the shape of the connector. A beneficial shape for such resistance is one that maximizes the cone shaped punching shear failure surface. Increased cover thickness behind the loaded object and size of loaded area increases the size of the failure surface and thus the resistance, as shown in Figure 4-5 (Shams, Horstmann et al. 2014). Concrete strength and type as well as the amount of reinforcement may also affect the punching shear resistance.

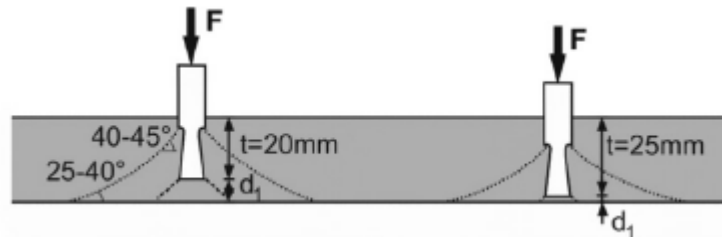


Figure 4-5 Influence of cover thickness and shape on punching-shear failure surface (Shams, Horstmann et al. 2014).

For calculation of the pull-out resistance of a the pin-connector shown in Figure 4-6, Equation 4-5 is given in Shams, Horstmann et al. 2014:

$$F_{calc} = k \cdot t_{TM}^{1,5} \cdot f_{cm}^{0,5} \quad \text{Eq. 4-5}$$

Where:

- $k = 8,6$ is the empirical factor, for conical anchorage end of the pin connectors
- t_{TM} is the embedment depth of the pin-connectors, $15 \text{ mm} \leq t_{TM} \leq 30 \text{ mm}$
- f_{cm} is the mean experimental compressive strength of concrete

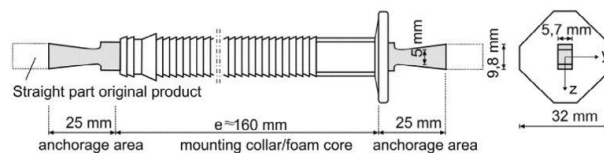


Figure 4-6 MC/MS-series connector with modified anchorage area (Shams, Horstmann et al. 2014).

On account of the conical end of the pin-connectors tested in Shams, Horstmann et al. 2014 and the fact that the test specimen had no flexural reinforcement, Equation 4-6 for the punching shear capacity is given by the same equation as the pull out since it shows the same cone failure mechanism:

$$N_{TM} = 13,5 \cdot (h^{1,5} - d_1^{1,5}) \cdot f_{cm}^{0,5} \quad \text{Eq. 4-6}$$

Where:

- d_1 is the concrete cover
- h is the thickness
- f_{cm} is the mean experimental compressive strength of concrete

4.2 Load-bearing behaviour

4.2.1 Pin-connectors

Tests have been conducted on TRC sandwich panels with pin connectors as shown in Shams, Horstmann, et al. 2014. A few test setups for sandwich panels are described in section 4.3. In the tensile tests, experiments showed that with increasing embedment depth of the pin-connectors, the load-bearing capacity increased. An increased tensile strength of the concrete also had a positive effect on the load-bearing capacity. The test results showed that the main failure of samples with less than 25 mm anchorage depth was pull-out, while the main failure of samples with more than 25 mm was shear failure. The pin-connectors used in the tests are the Thermomass MC/MS series shown in Figure 4-7.



Figure 4-7 Thermomass MC/MS-series pin-connector (Thermomass©, 2015).

In Figure 4-8, it can be seen how the pin-connector is embedded in the sandwich panel.

The pin-connectors will increase the bearing capacity for tensile loads perpendicular to the wythes surface, while they will only have minor influence on the stiffness and bearing capacity in shear and bending.

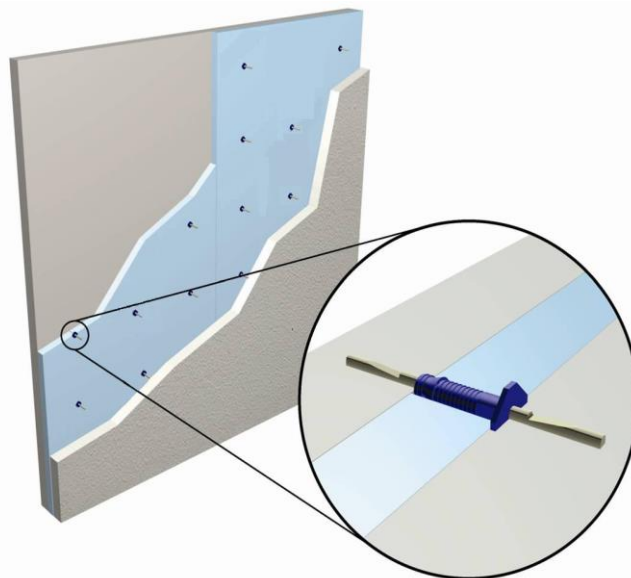


Figure 4-8 Thermomass pin-connector embedded in a sandwich panel (Composite Global Solution, 2011).

Among the main advantages of using pin-connectors in TRC sandwich panels is the increased capacity for tensile and compressive loads perpendicular to the panel as well as their small contribution to the composite action within the panel. Flexural testing on TRC elements with only pin-connectors and insulation material have shown that though the connectors do not contribute much to stiffness and ultimate capacity,

they provide noticeable capacities to the element after the insulation had failed (Shams, Horstmann et al. 2014). Using FRP, instead of steel, for the connector material will decrease the risk of corrosion and thermal bridging, while maintaining suitable strength properties. However, there is a risk of pull-out failure if the embedment depth is insufficient and punching shear failure if the cover thickness behind the connector is inadequate. Although there are more types of pin-connectors commercially available, only the Thermomass MC/MS series will be studied in this Master's thesis. Other types of pin-connectors can however be seen in Figure 4-9.

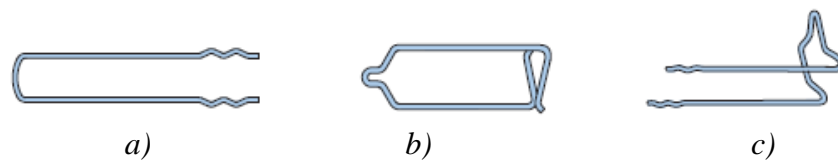


Figure 4-9 Different types of pin-connectors, a) connector pin, b) clip-on stirrup, c) clip-on pin.(Halfen© 2015).

4.2.2 Diagonal shear connectors

In addition to transferring horizontal forces between the two wythes a diagonal connector also transfers shear forces.

Diagonal connection can be implemented in different ways. One effective way is by arranging separate pins or loops diagonally between the wythes and anchoring them to the wythes reinforcement, see Figure 4-10 a) and b). Another way is by bending a bar to form a helical shape with approximately 45 degrees inclinations and fixing it to the concrete wythes by threading it with a reinforcing bars, see Figure 4-10 c).

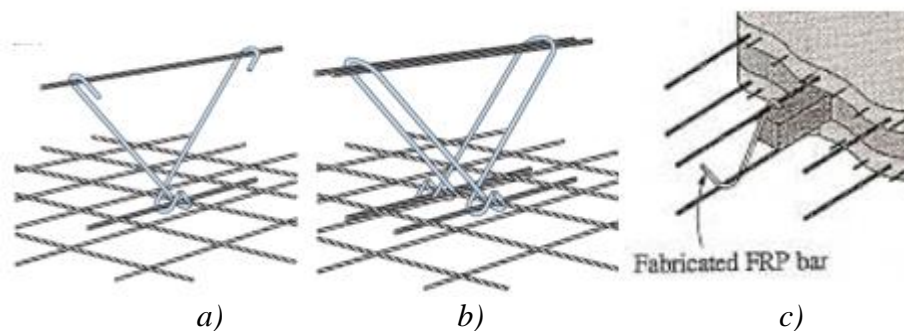


Figure 4-10 Different types of diagonal shear connectors, a) single V-shape anchor, b) double V-shape anchor (Halfen© 2015), c) Diagonally bent FRP bar (Einea et al. 1994).

The inclined connectors transfer load only longitudinally to their direction, thus in the yarn direction which is favourable if made from FRP yarn.

The use of bent FRP bars as connectors have been studied by experimental testing and with FE analysis in Einea et al. 1994. Conventional steel reinforced concrete elements had been cast and their behaviour under both shear- and flexural loading had been

examined. This study concluded that even though the FRP was not a ductile material, it showed a very ductile behaviour in the test performed. This has been explained by cracking in the concrete around the bent connector leading to gradual loss of composite behaviour. Another observation had been made that the initial stiffness of the panel system was less than what was anticipated in the analysis due to the slippage of the bent connectors at their anchorages.

The main advantages of a diagonal shear connector is a great ultimate strength and ductile behaviour. Nonetheless, the low initial stiffness of the connectors can be considered as the main disadvantage.

4.2.3 Shear grids

Shear grids are made by cutting a textile grid into strips with a 45° angle to the mesh. These strips are then used as a connector between the wythes, see Figure 4-11. As the rovings (yarns) in the textile mesh have very high tensile capacity, the critical part of such connectors is the anchorage into the concrete. To examine the anchorage capacity, pull-out tests of the rovings have been done to obtain the minimum embedment depth which will yield the highest tensile strength of the shear grids. Test results have shown that for plainly anchored rovings, the tensile failure occurred at an embedment depth of 40 mm while the hooked anchorage failed at 30 mm. Tests have also shown that by using shear grids it was possible to approximately double the bearing capacity as well as increasing the stiffness and ductility compared with only using pin-connectors. The shear grids performed as ties of a truss system while the foam insulation showed the behaviour of struts, which made it possible to resist shear deformation. When the shear grids are combined with a stiff insulation material, the stiffness and bearing capacity of the connection will increase for tensile, shear and bending loads. With an increased stiffness of the insulation material the shear grids will perform more efficiently with regard to the ultimate load (Shams, Hegger et al. 2014a).

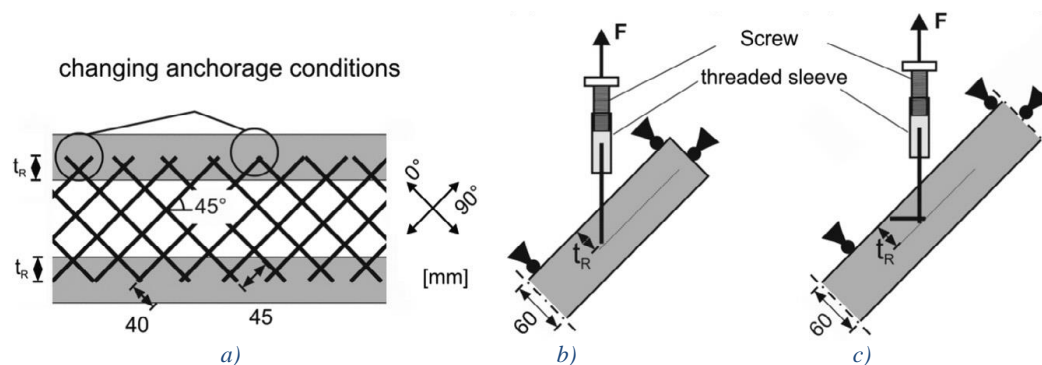


Figure 4-11 a) Changing anchoring conditions, b) plain anchorage, c) hooked anchorage (Shams, Horstmann et al. 2014).

The bond between the connections, insulation material and concrete will affect the ultimate strength and degree of composite action. The type and thickness of the insulation material and the distance between the rows of shear grids are believed to affect shear flow capacity (Sopal et al. 2013). A typical set-up of shear grid reinforcement is shown in Figure 4-12. Test results have shown that the overall shear flow strength of panels with EPS and XPS-SB (XPS with sandblasted surface) foam

increases with increasing spacing between shear flow grids, due to a larger bonded area between concrete and insulation. On the other hand, test results for XPS-R (XPS with rolled surface) foam showed that the spacing between grid connectors has a negligible effect on the shear flow strength, this is due to the low bond strength between the concrete and insulation foam (Sopal et al. 2013).

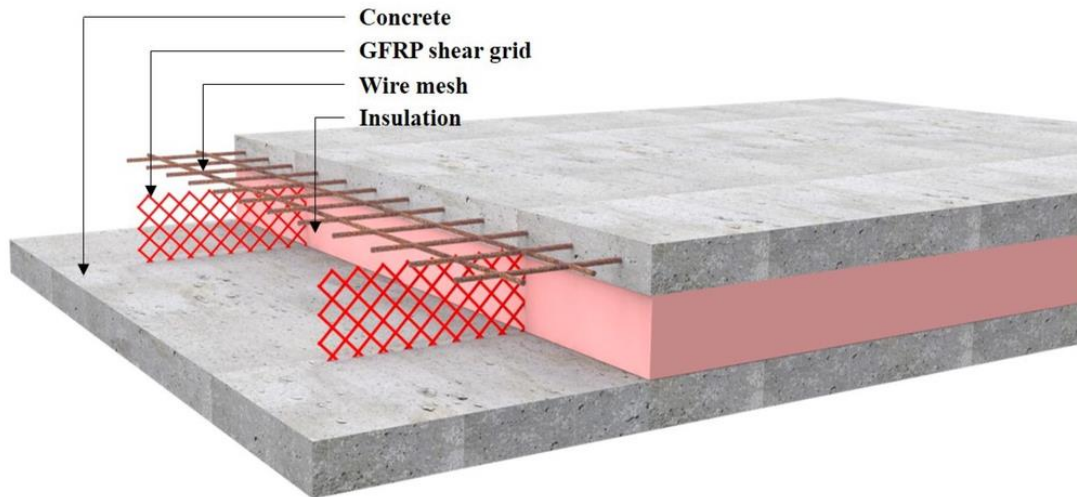


Figure 4-12 Shear grid reinforcement in a sandwich panel (Kim & You 2015).

The failure mechanisms for the grid, when properly anchored, were either rupturing of the yarn in tension or buckling of compression chords. It has also been observed that the yarn tends to rupture either near the yarn joints in the mesh or near the connection to the concrete. This has been explained by an angular deformation in the grid nodes and a deviation from original embedded angle of the chords, when the wythes deformed under the load, see Figure 4-13 (Shams, Horstmann, et al. 2014).

Because of this phenomenon, tests have shown utilization ratio of the ultimate tensile strength to be 77% - 91% in shear tests depending on insulation thickness and 63% for tensile tests, independent of insulation thickness (Shams, Hegger et al. 2014a).

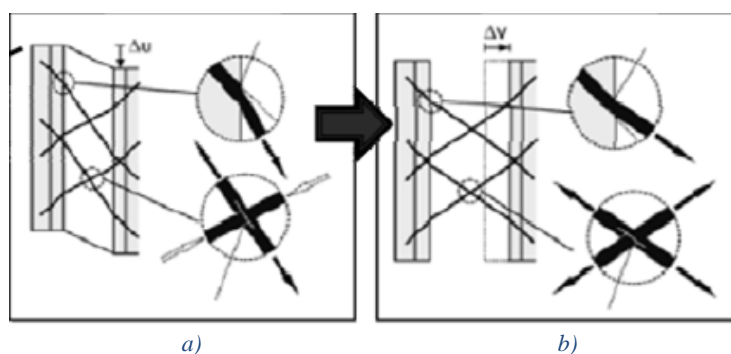


Figure 4-13 Angular deformation of grid nodes under load, a) shear, b) tension (Shams, Horstmann et al. 2014).

The advantages of using shear grid connectors are their high ultimate strength because of the dense spacing of the chords. The possibility of using the same textile grid as used for reinforcement in the wythes can also be considered efficient.

On the other hand, the rather large embedment depth can pose a problem when using with the thin TRC panels. Also the loss of tensile strength due to oblique-angles when deforming and its dependency on insulation material for stiffness can be considered a drawback.

4.2.4 Shear plate connector

Different types of flat plate connectors are commercially available and widely used as shear transferring anchors. For use with conventionally steel reinforced concrete sandwich panels their geometry makes them easy to embed into the wythes, see Figure 4-14. Structurally, they transfer shear forces differently between the wythes than the aforementioned types, who transfer the forces mostly as tension in the ties. The plate connectors transfer the load rather through shear and bending.

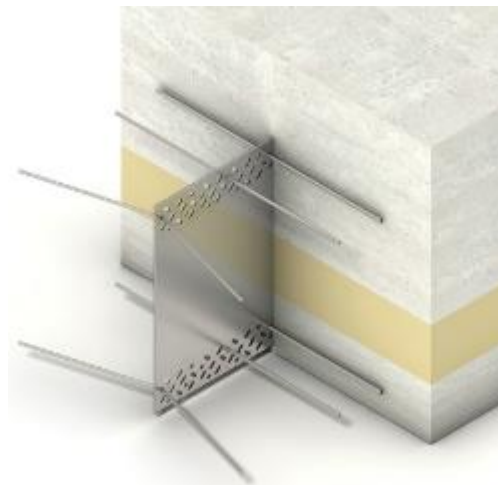


Figure 4-14 Halfen sandwich panel anchor (Ancon© 2015).

Many different types of connectors have been experimentally tested and their behaviour and capacity compared, including a CC Series fibre composite connectors from Thermomass, see Figure 4-15 (Naito et al. 2012). The material of the Thermomass CC-series connectors, as described in section 3.1.3, is thermally non-conductive and has high strength. If on the other hand, the material of the plate is vulnerable against alkaline attack or has a thermal coefficient of expansion that exceeds that of concrete, then it is not recommended to use the material as connectors for sandwich panels.



Figure 4-15 Thermomass CC-series connector (Thermomass©, 2015).

The CC-series connectors anchoring grooves and their high strength material makes them suitable to provide composite action in a sandwich panel. Their thermal properties and durability also makes them an attractive choice. The short embedment length of the CC-series connector anchored into a thin TRC wythe can be considered

an issue as (i) there is not much space for anchoring grooves, and (ii) the smooth surface of the FRP may provide little bond strength to the concrete.

4.3 Testing

When a full panel is uniformly loaded as shown in Figure 4-16, it can be seen that the connectors at both ends are subjected to the largest shear deformation. For a connector that can resist a sufficient amount of shear but is remarkably flexible, the panel will not be able to reach a full composite behaviour. Thus, the inner and outer wythes will act as two individual panels and resist the flexural load separately (a. Benayoune et al. 2008).

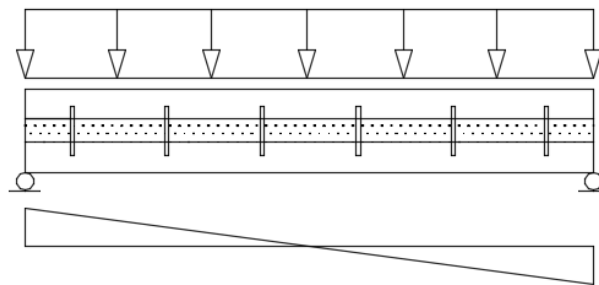


Figure 4-16 Sandwich panel under uniformly distributed flexural load, shear diagram.

Two tests are most often used to examine the structural behaviour of sandwich panels; they are also used to evaluate the efficiency of different connecting device. Firstly, direct shear test, that provides a pure shear response of the connector and/or insulation material, see Figure 4.17 a). Secondly, flexural test, that gives the flexural behaviour of the composite panel, see Figure 4-17 b) and lastly tensile test which gives the load bearing capacity of the pin connectors.

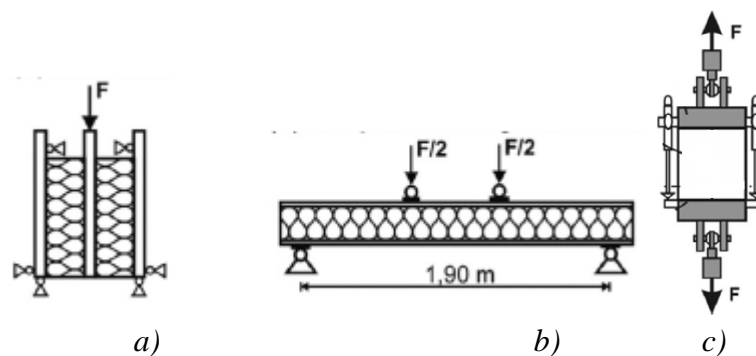


Figure 4-17 Test setup, a) direct shear test, b) flexural test, c) Tensile test (Shams, Horstmann et al. 2014).

Methods have been developed to predict the flexural behaviour of a panel with data from direct shear test. With that perspective, a simplified trilinear curve has been developed, as is shown in Figure 4-18, to study the behaviour of plate connectors from shear tests (Naito et al. 2012). The curve is divided into 3 parts: elastic, plastic and unloading. As shown in Figure 4-18, the elastic part is defined as $0,75V_{max}$, the yield displacement Δy is defined as the point at the ultimate load, V_{max} . The ultimate displacement, Δu is the point where the ultimate load has been decreased by 50%.

Lastly, Δ_m is the displacement at failure. The simplified trilinear curve can then be used to predict the behaviour of the sandwich panel under flexural loading.

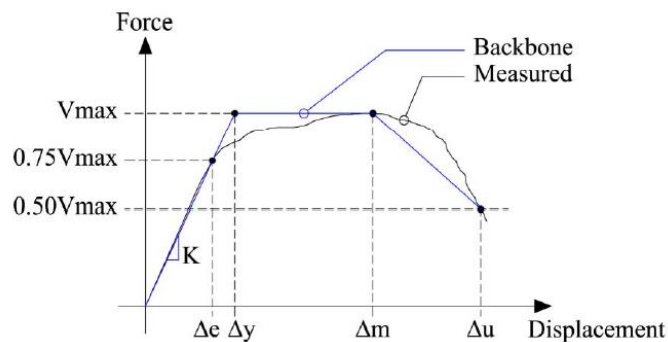


Figure 4-18 Simplified trilinear curve (Naito et al. 2012).

As described in Naito et al. 2012, the ultimate flexural capacity of concrete sandwich panels is dependent on the stiffness and failure mode of the shear connector. Experiments have shown that the shear response of a connector affected the failure mode of the sandwich panel. Furthermore, different types of ties exhibited a variation in slip and ultimate capacity of the sandwich panels. With increasing stiffness of the ties, the overall flexural strength of the panel increased. Before the panel was loaded it was defined as a fully composite sandwich panel. When loading is initiated, the shear ties and insulation material start to slip with respect to the outer wythe, causing a partially composite behaviour and in some cases where the ties fail the panel will have a non-composite behaviour (Naito et al. 2012).

5 FE-Modelling

Four different models were created. Firstly, two models of experimental test setups published in two different papers were made, to verify if the chosen modelling method would show reasonable results. That method was then implemented in modelling of connectors in a TRC sandwich panel.

The experimental tests used as a reference were introduced in Naito et al. 2012 and Shams, Horstmann et al. 2014b. Shear tests have been made on panels connected with different types of commercially available connectors made for typical reinforced concrete (Naito et al. 2012). Of those connectors, a plate CC-series connector from Thermomass, which is discussed in section 4.2.4, was assumed suitable to adapt to the thin wythes of a TRC panels and thus chosen for reference. This model will be noted as Test Model 1 in the following discussion.

Shear tests have also been made on panels connected with MC/MS-series pin-connectors from Thermomass (Shams, Horstmann et al. 2014b). These panels were made of TRC and since the Thermomass connectors are only commercially available for typically reinforced concrete, they were modified to fit the thin TRC panels. This model will be noted as Test Model 2 in the following discussions.

Furthermore, a model denoted as Test Model 3 was made. This model resembles Test Model 1, except that it only has two concrete wythes compared to three in Test Model 1 and 2. A two wythe model can be beneficial as it saves computational time and enables a more easy extension of the model into model of a full scale panel. Consequently, the purpose with this model was to establish the boundary conditions, which would yield correlating results to Test model 1. Thereafter, these boundary conditions would be used to model the TRC panel panel.

Lastly, after the modelling method was verified, a bigger and more complex model was made, called the TRC panel model. There, a proposed connector system for a TRC panel was modelled and the results were analysed.

5.1 Verification model

5.1.1 Geometry

The geometry of the FE-models replicates the geometry of both experimental setups of the shear tests.

5.1.1.1 Test Model 1

Test Model 1 has three unreinforced concrete wythes, with the middle one thicker than the other ones, as it has two connectors embedded. The connectors are placed in the middle of the wythe, see Figure 5-1 and 5-2.

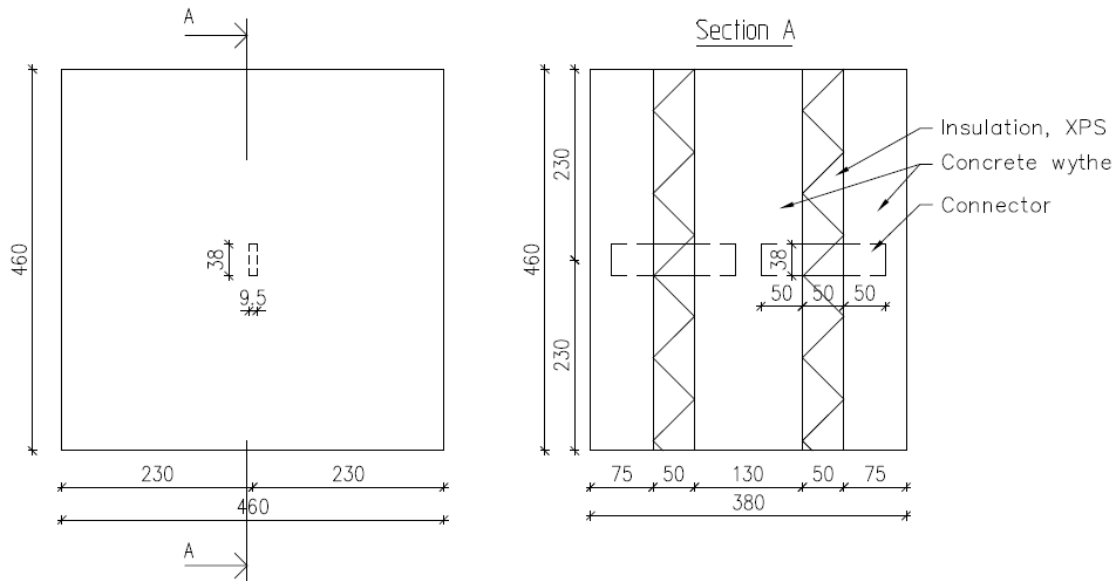


Figure 5-1 Geometry of Test model 1, dimensions are in mm.

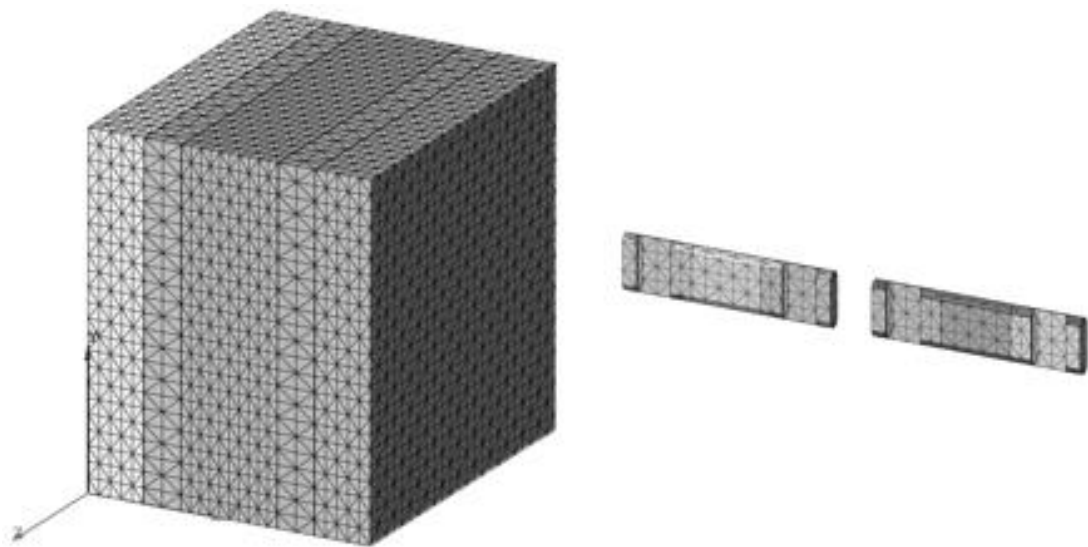


Figure 5-2 Test model 1.

The connectors dimensions are obtained from manufacturer's data (CC-series connector from Thermomass), except for the depth and size of the anchoring grooves, as well as the rounded edges, which were assumed, see Figure 5-3.

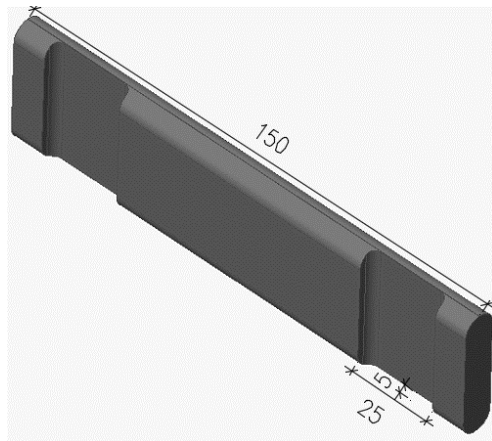


Figure 5-3 Plate connector.

5.1.1.2 Test Model 2

Test Model 2 has three textile reinforced concrete wythes, with the middle one thicker than the other ones, as it has two connectors embedded. Two connectors are placed between each wythe and positioned as shown in Figure 5-4.

The connectors are modified for this test by shortening the embedded part to be suitable for the thin TRC panels (Shams, Horstmann et al. 2014). Modified dimensions are obtained from the report. Conical anchoring ends of the pins are modelled as straight, see Figure 5-5.

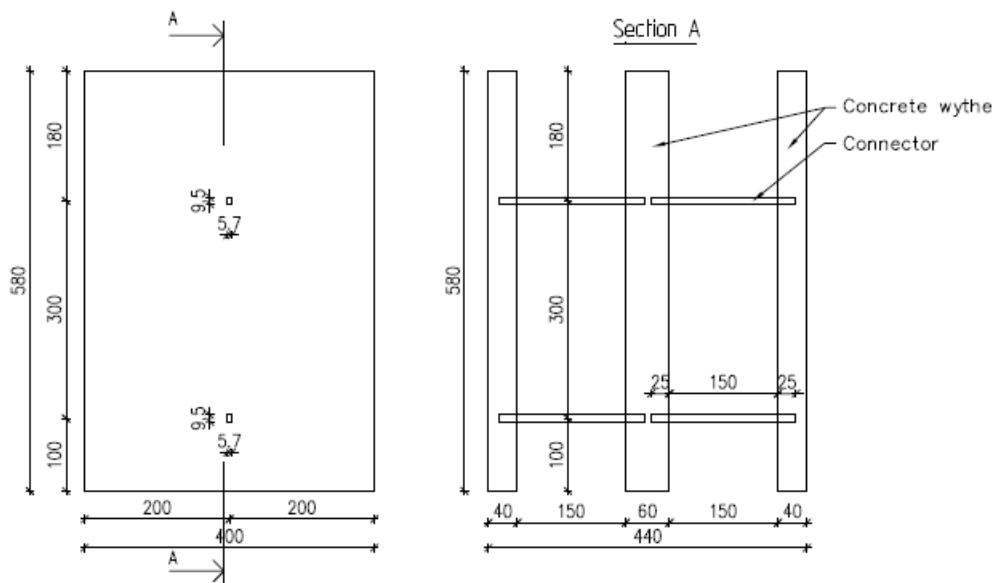


Figure 5-4 Geometry of Test model 2, dimensions are in mm.

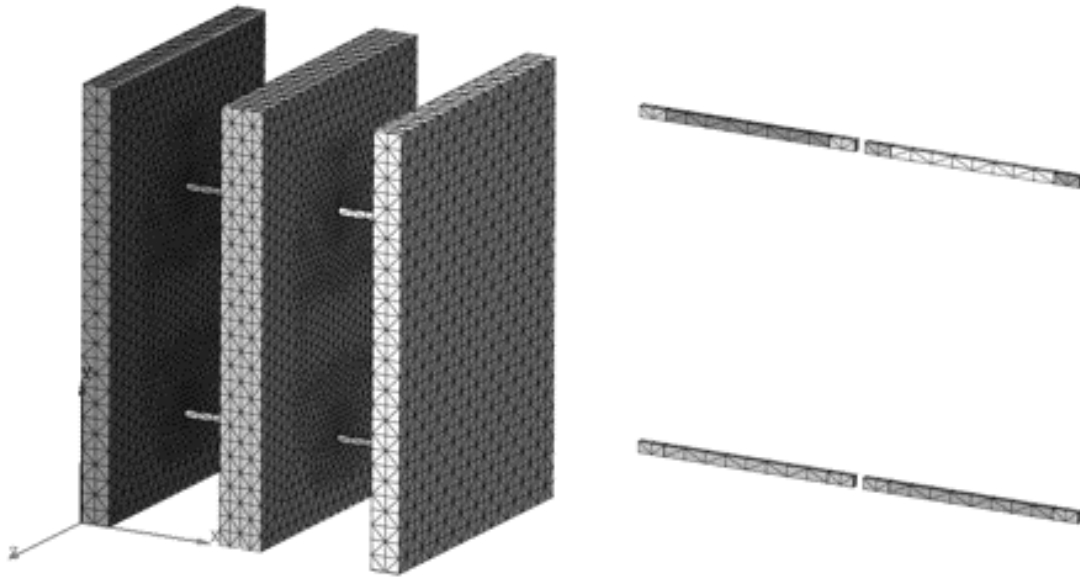


Figure 5-5 Test model 2.

5.1.2 Material properties

5.1.2.1 Test Model 1

Three cylinder compression tests have been conducted and the concrete compressive strength for each specimen measured according to ASTM Standard C39, resulting in a mean value of $f_{cm} = 47,4$ MPa. Additional necessary material properties of the concrete shown in Table 5-1 were calculated according to (Model Code 2010) see 9.2.

Table 5-1 Material properties for concrete, Test Model 1.

Compressive strength	f_{cm}	47,4 MPa
Tensile strength	f_{ctm}	3,5 MPa
Elastic modulus	E_{cm}	36,1 GPa
Fracture energy	G_f	146,2 N/m

For the compressive behaviour of the concrete, a modified Thorenfeldt curve was used. The original Thorenfeldt curve describes the stress-strain relationship of a 300 mm long cylindrical concrete specimen. As the strain values in the curve are dependent on the specimen length, the strain needs to be modified to the length of the crushing elements in the model according to (Hanjari et al. 2011), see Figure 5-6. In general, the element sizes in the model are 20 mm, as will be described in section 5.1.3. However, the mesh size condenses down to 3,5 mm around the embedded connectors. It is assumed that crushing occurs in one element row above or below the embedded connectors and therefore the Thorenfeldt curve is modified to the appropriate size of 3,5 mm.

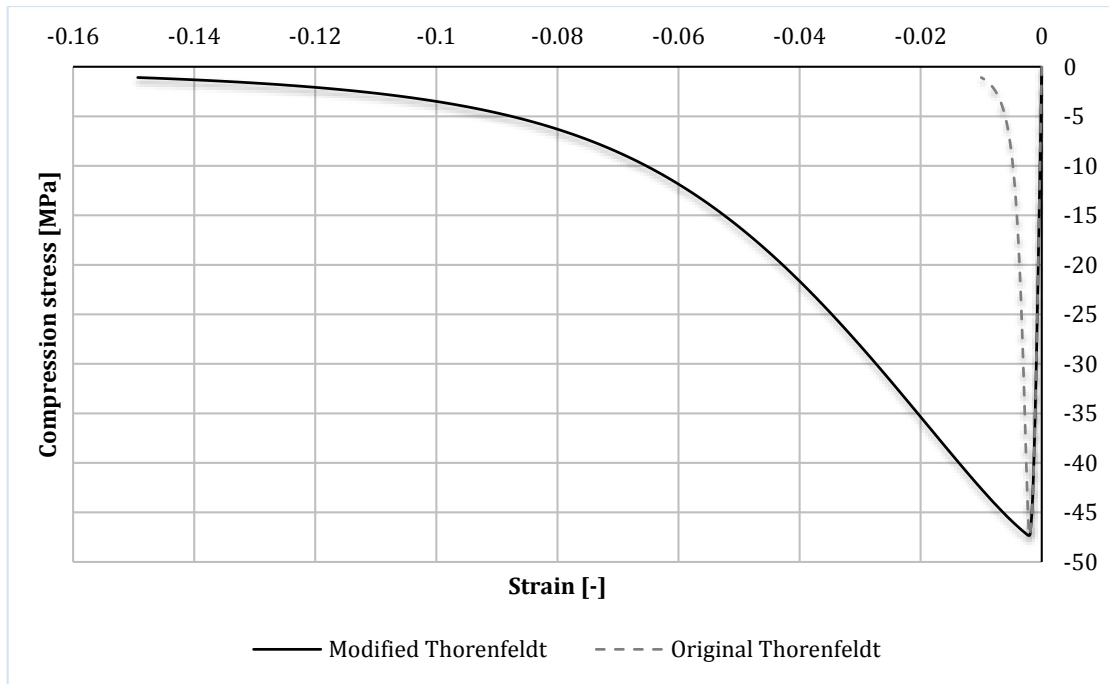


Figure 5-6 Original and modified Thorenfeldt curve.

For tensile behaviour of the concrete, the tension softening was taken into account using a predefined Hordijk's curve in DIANA as can be seen in Figure 5-7.

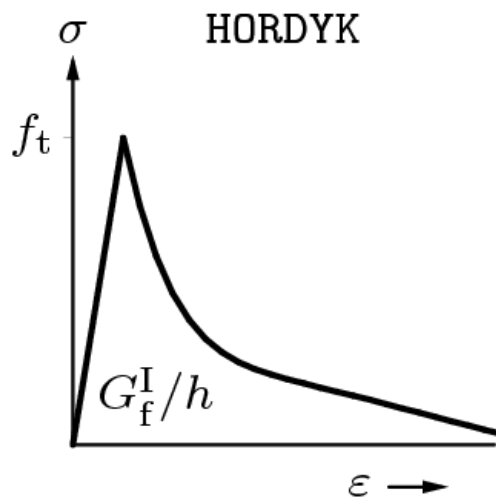


Figure 5-7 Hordijk's curve (TNO DIANA©, 2015)

The crack model chosen for the concrete was a total strain based model with rotating crack approach. The effective bandwidth length was assumed to match the element sizes, as recommended in the DIANA user's manual.

The FRP connector material properties were obtained from manufacturers data, see Table 5-2. The connectors were modelled as fully embedded in the concrete using non-linear elastic-fully plastic Von Mises constitutive model with the flexural strength as the initial yield stress limit using Poisson's ratio 0,2.

Table 5-2 Material properties for CC-series connectors.

Flexural strength	f_f	827 MPa
Flexural elastic modulus	E_f	30 GPa

The insulation material used in the test presented in (Naito et al. 2012) was extruded polystyrene (XPS). As XPS insulation boards have shown to give little friction between insulation and concrete because of the smooth coating on the surface (Sopal et al. 2013), shear transfer through the intersection is assumed to be negligible. Consequently, in Test Model 1, the insulation was modelled using an orthotropic material, with stiffness only assigned to the direction perpendicular to the wythes surfaces. The material was modelled as linear elastic with an elastic modulus obtained from material producer's datasheet, $E_{XPS} = 12$ MPa.

5.1.2.2 Test Model 2

Elastic modulus, E_{cm} and compressive strength, $f_{cm,cube}$ for the concrete have been specified as a mean 28 days mean values (Shams, Horstmann et al. 2014b). Corresponding concrete cylinder strength and other necessary material properties of the concrete specimen were then calculated according to (Model Code 2010), see Table 5-3 and section 9.2.

Table 5-3 Material properties for concrete, Test Model 2.

Compressive strength	f_{cm}	61,4 MPa
Tensile strength	f_{ctm}	4,26 MPa
Young's modulus	E_{cm}	37,23 GPa
Fracture energy	G_f	153,2 N/m

As described in section 5.1.1.1, the compressive behaviour of the concrete is described with a modified Thorenfeldt curve assuming possible crushing of the concrete above or below the embedded connectors, were the same condensation of the mesh occurs, as described for Test Model 1.

The tensile behaviour is described with Hordijk's curve and a total strain based crack model with rotating crack approach, using the element sizes as the effective bandwidth length.

The FRP connector material properties were obtained from (Shams, Horstmann et al. 2014b), see Table 5-4. The connectors were modelled as fully embedded in the concrete using non-linear elastic-fully plastic Von Mises constitutive model with the tensile strength as the initial yield stress limit using Poisson's ratio 0,2.

Table 5-4 Material properties for MC/MS-series connectors.

Tensile strength	F_y	948 MPa
Elastic modulus	E_f	30 GPa

Material properties for the carbon fibre mesh reinforcement were obtained from Shams, Horstmann et al. 2014b, see Table 5-5. The spacing of the yarn in the mesh is 40 mm in one direction (0°) and 45 mm in the other (90°). The reinforcement was modelled as non-linear using elastic-fully plastic Von Mises constitutive model with the tensile strength as the initial yield stress limit.

Table 5-5 Material properties for Carbon fibre mesh (C-grid).

Tensile strength in concrete	f_t	2276 MPa
Elastic modulus	E	171 GPa
Cross sectional area (0°/90°)	A	0,46/0,51 cm ² /m

5.1.3 Mesh and element types

For concrete and insulation the general mesh size of 20 mm was chosen both for Test Models 1 and 2 however the mesh size condenses down to 3,5 mm around the embedded connectors as described in section 5.1.2.1. It is assumed that crushing occurs in one element row above or below the embedded. Appropriate thickness division was chosen for each part as shown in Figures 5-8 and 5-9. For plate connectors in Test Model 1 a mesh size of 10 mm was chosen and 20 mm for the pin connectors in Test Model 2, see Figure 5-10.

To merge and get an interaction between the mesh set of different components in the model, the “embed solid” option in midas FX+ for DIANA was used. By using this option, the connectors and concrete in the panel will share nodes in the mesh.

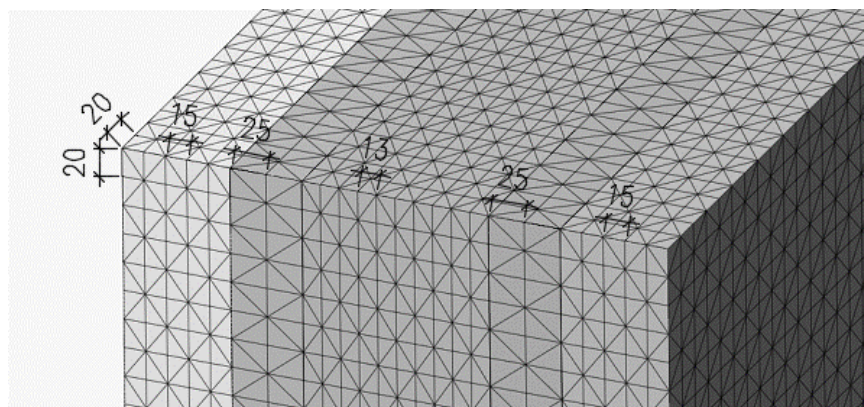


Figure 5-8 Mesh size of Test Model 1, dimensions are in mm.

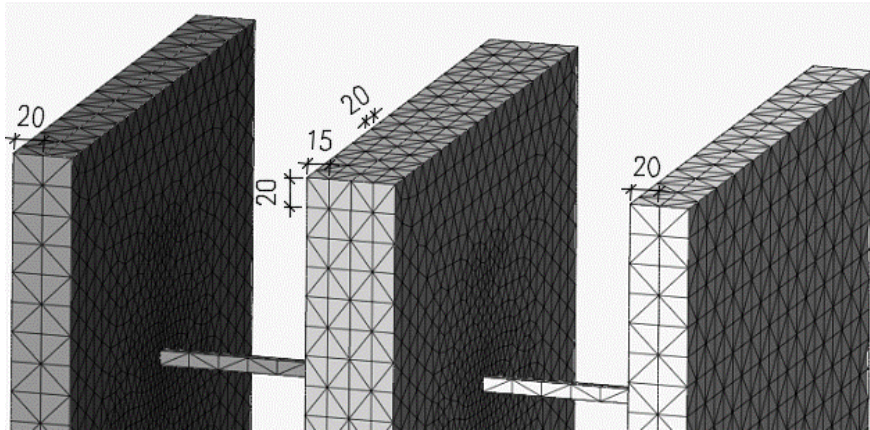


Figure 5-9 Mesh size of Test Model 2, dimensions are in mm.

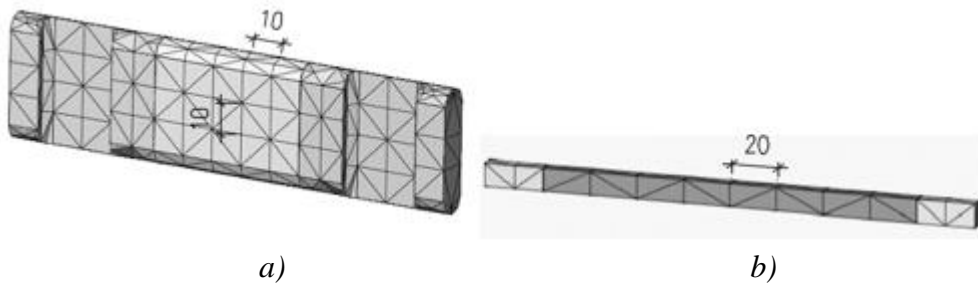


Figure 5-10 Mesh sizes, a) Test Model 1, b) Test Model 2, dimensions are in mm.

For both models the concrete, insulation and connectors are modelled with a four-node, three-side isoparametric solid pyramid elements called TE12L in DIANA. It is based on non-linear and numerical integration. The default option of 1-point integration scheme over the volume was used.

The textile reinforcement in Test Model 2 is modelled as grid reinforcement, embedded in solid elements. The reinforcement amount is prescribed as an equivalent thickness, t_{eq} , i.e. the area of cross-section per unit length, in each direction, see Figure 5-11. Calculations on t_{eq} , can be seen in section 9.2.

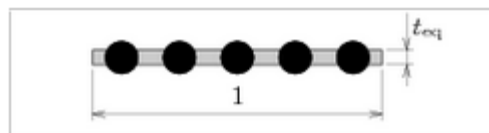


Figure 5-11 Equivalent thickness as an input for reinforcement amount (TNO DIANA©, 2015)

5.1.4 Boundary conditions

The boundary conditions for both Test Model 1 and 2 were chosen to correspond to the actual condition in each test setup, see Figures 5-12 and 5-13. For both cases, the

two outer wythes were supported on a flat steel plate. For Test Model 2 the upper part of the outer wythes were also supported for horizontal translation.

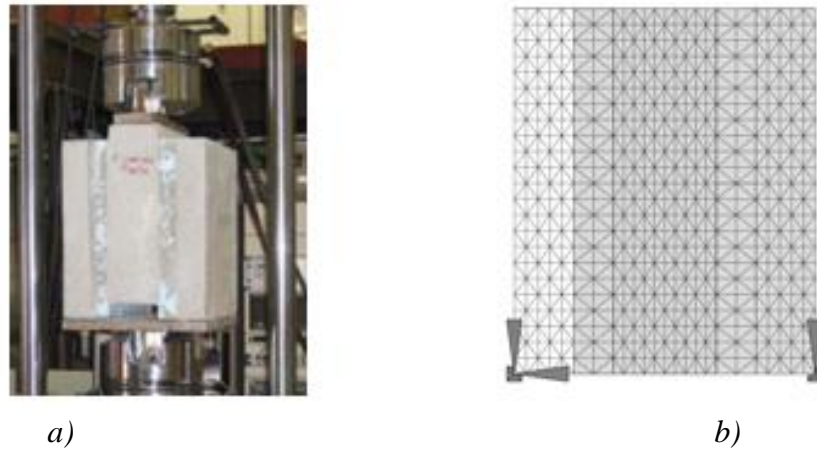


Figure 5-12 a) Test setup 1 (Naito et al. 2012), and b) Test Model 1.

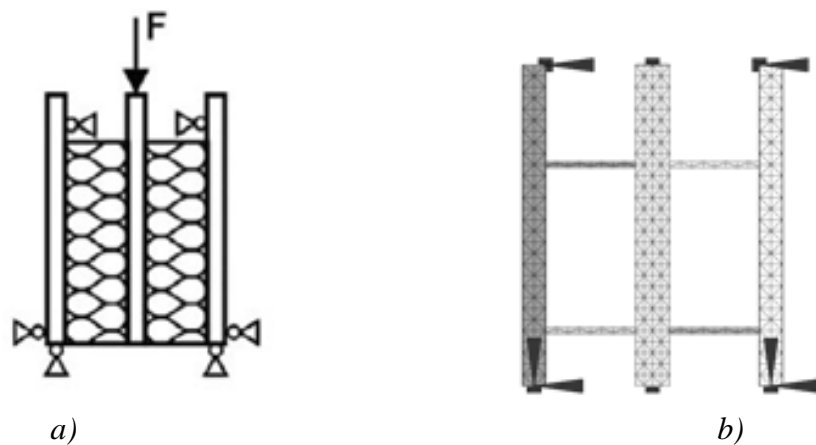


Figure 5-13 a) Schematic figure of Test setup 2 (Shams, Horstmann et al. 2014), and b) Test Model 2.

To implement support and loading plates into the models, nodes on each surface are tied together using the element link option in midas FX+ for DIANA. One node on each surface is then chosen to be a master node and all other linked as slave nodes to the master node, sharing the same behaviour, see Figures 5-14 and 5-15.

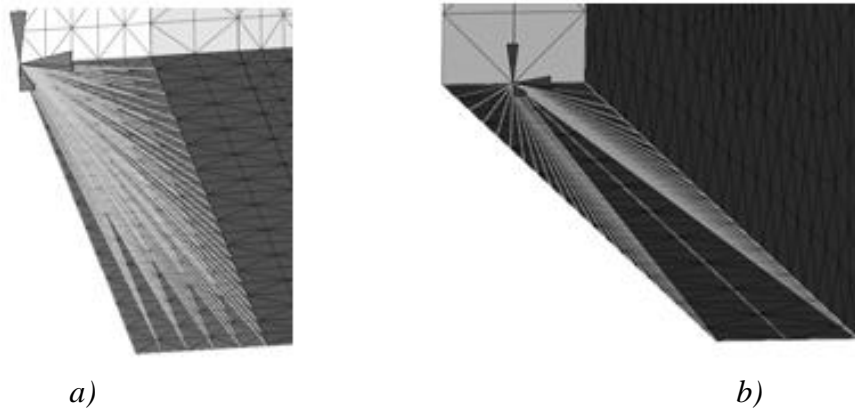


Figure 5-14 Link elements and boundary conditions, a) Test Model 1, and b) Test Model 2.

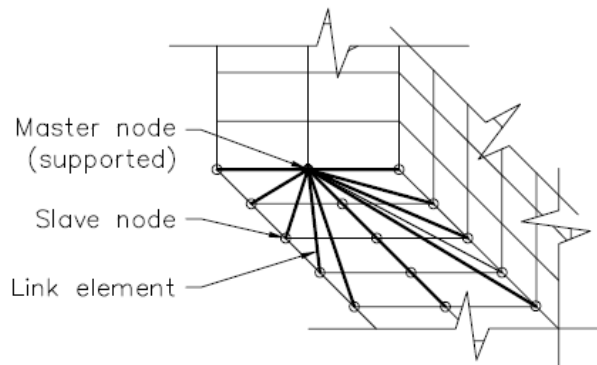


Figure 5-15 Illustration of linked nodes for supports.

5.1.5 Loading and analysis method

Similar to the supports, the loading on the middle wythe in both models was applied with a flat steel plate. As shown in Figure 5-16, the same linking procedure was used to implement that into the model as discussed in section 5.1.4.

The load was applied with deformation controlled loading. This method enables accurate and detailed behaviour to be followed during the different stages of response. The deformation was applied in step size of 0,1 mm and 0,2 mm for Test Model 1 and Test Model 2, respectively. For each step, the load needed to induce the applied deformation is calculated.

In analysis of both models, Quasi-Newton (Secant) tangential iteration method was used to find equilibrium in each step. Energy convergence norm was used with a tolerance of 0,01. When a solution within this tolerance is met, the analysis continues to the next step. If on the other hand, divergence occurs, the analysis terminates.

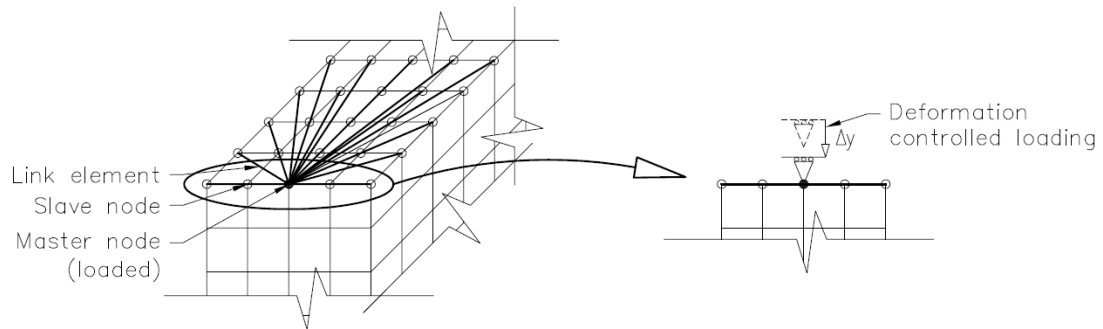


Figure 5-16 Illustration of linked nodes for load application.

5.1.6 Correlation and calibration

In Figure 5-17 and 5-18 the diagrams show load vs. vertical displacement of middle wythe, from numerical analysis of both models. It can be seen that both models show considerably higher initial stiffness and ultimate capacity than the tests results presented in Naito et al. 2012 and Shams, Horstmann et al. 2014b.

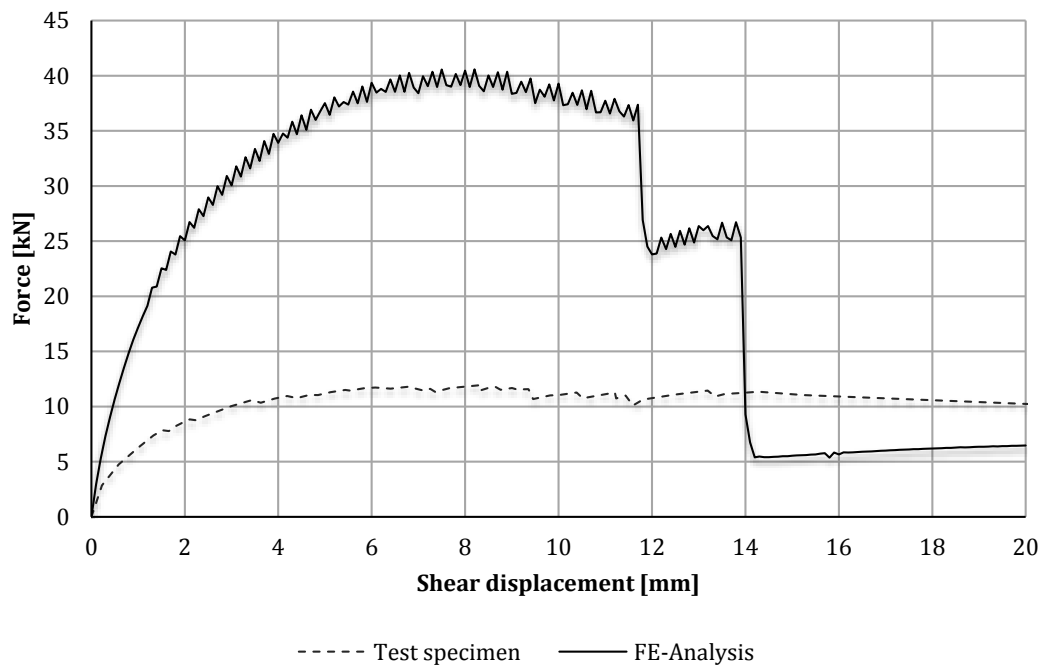


Figure 5-17 FE-results. Load vs. displacement of middle wythe, Test Model 1.

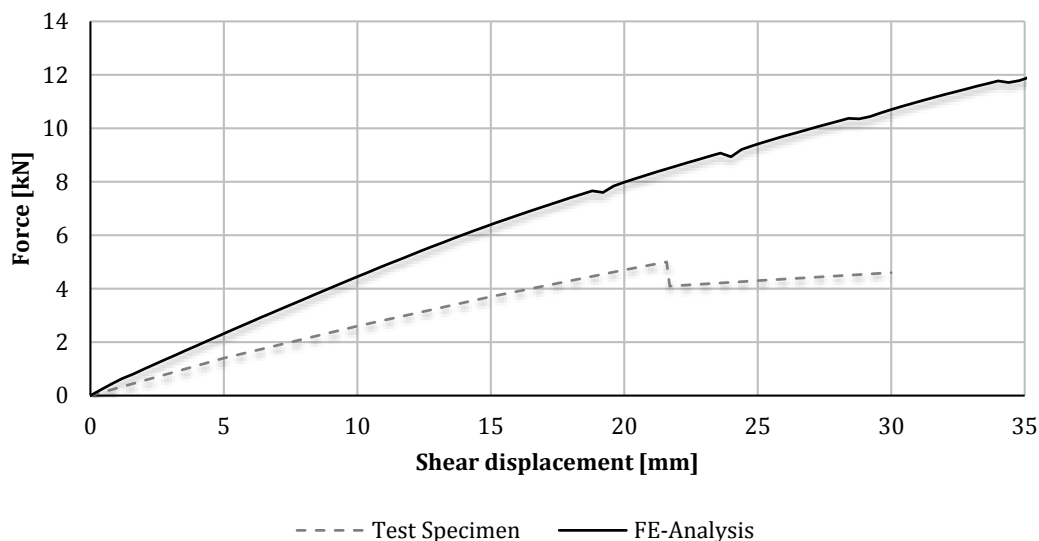
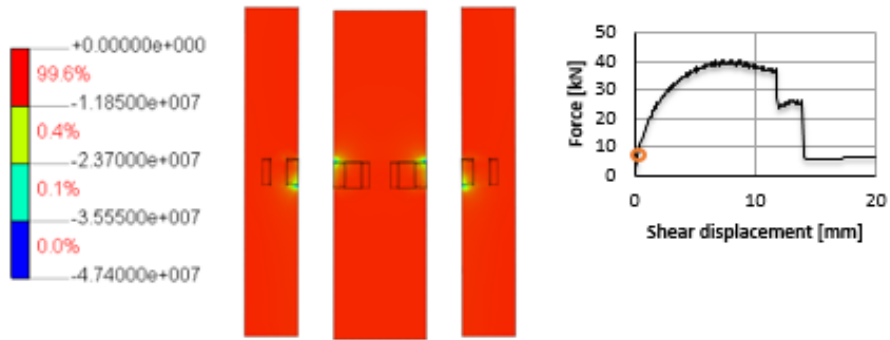


Figure 5-18 FE-results. Load vs. displacement of middle wythe, Test Model 2.

In Test Model 1, stress concentrations occur at the compressive side, above and below the connecting plates, resulting in the concrete reaching its full compressive capacity, locally, at approximately 21 kN and crushing occurs. With a local crush the concentrated stress spreads out with increased load until full capacity is reached at approximately 40 kN. The connector plate begins to yield at approximately 34 kN where the cross section is smallest (at the anchoring groove), but with stress redistribution within the plate it doesn't fail completely. At a displacement of approximately 11,5 mm, cracks starts to initiate in the outer concrete wythes resulting in a full horizontal crack through the whole width of wythes as well as punching shear failure from the connectors ends. This results in the first major capacity lost followed by another one, when the middle wythe cracks and the connector punches out at approximately 14 mm displacement. Stress and strain distributions in different stages are shown in Figures 5-19 to 5-24.

As the graph in Figure 5-17 indicates, the failure mode observed in the experiment was not the same as in the FE-model. In the experiment a laminar fracture of the connector and a flexure-tension failure at the concrete interface was observed.

Concrete compressive stress, S_3 [MPa]



Concrete strain, E_{ZZ} [-]

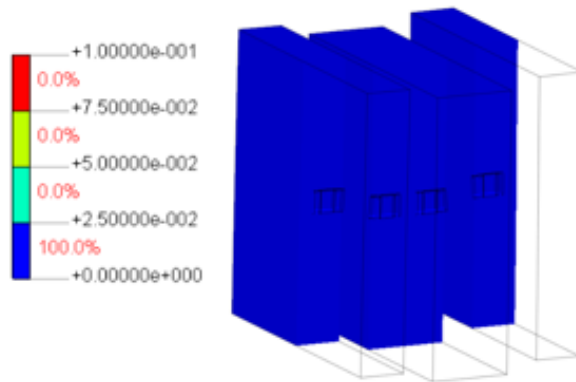


Plate connector, von Mises stress [MPa]

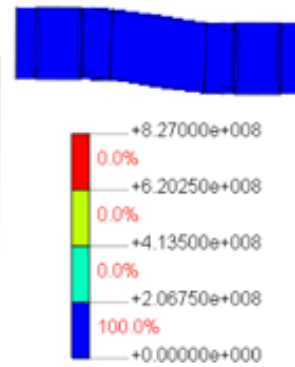


Figure 5-19 FE-results, initial state, Test Model 1.

Concrete compressive stress, S_3 [MPa]

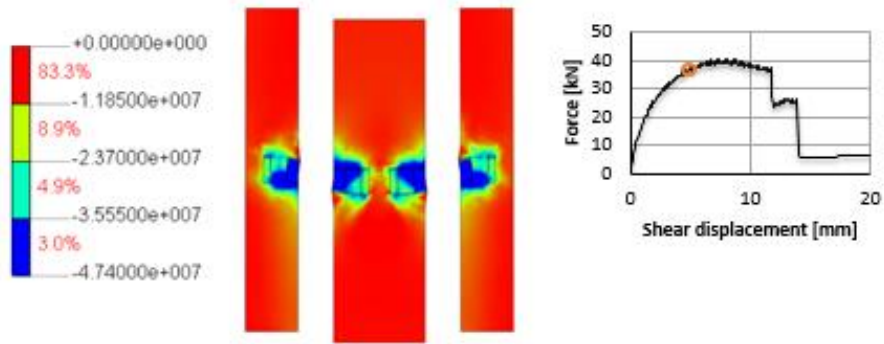


Figure 5-20 FE-results, connector starts to yield, Test Model 1.

Concrete compressive stress, S_3 [MPa]

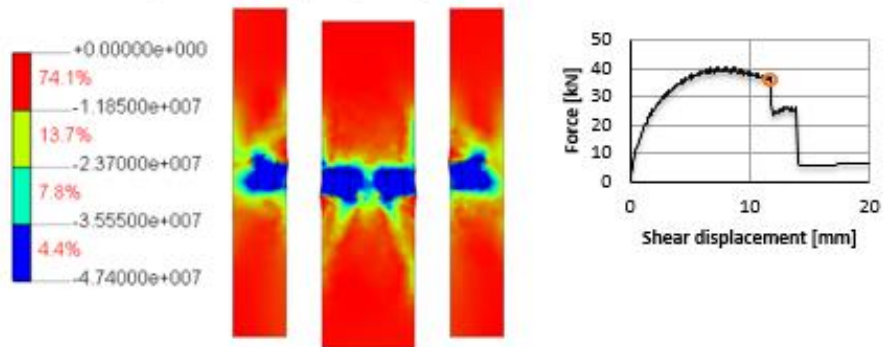
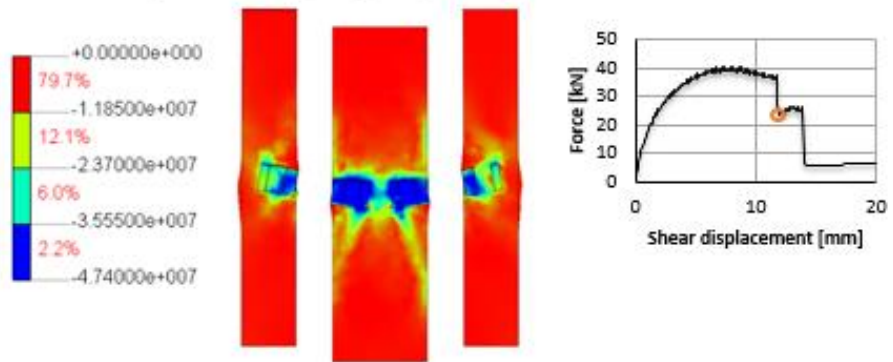


Figure 5-21 FE-results, before first crack, Test Model 1.

Concrete compressive stress, S_3 [MPa]



Concrete strain, \bar{E}_{ZZ} [-]

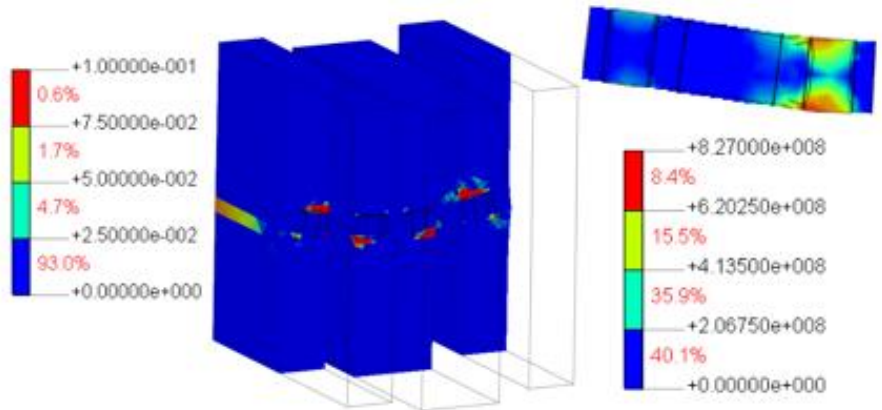


Figure 5-22 FE-results, after first crack, Test Model 1.

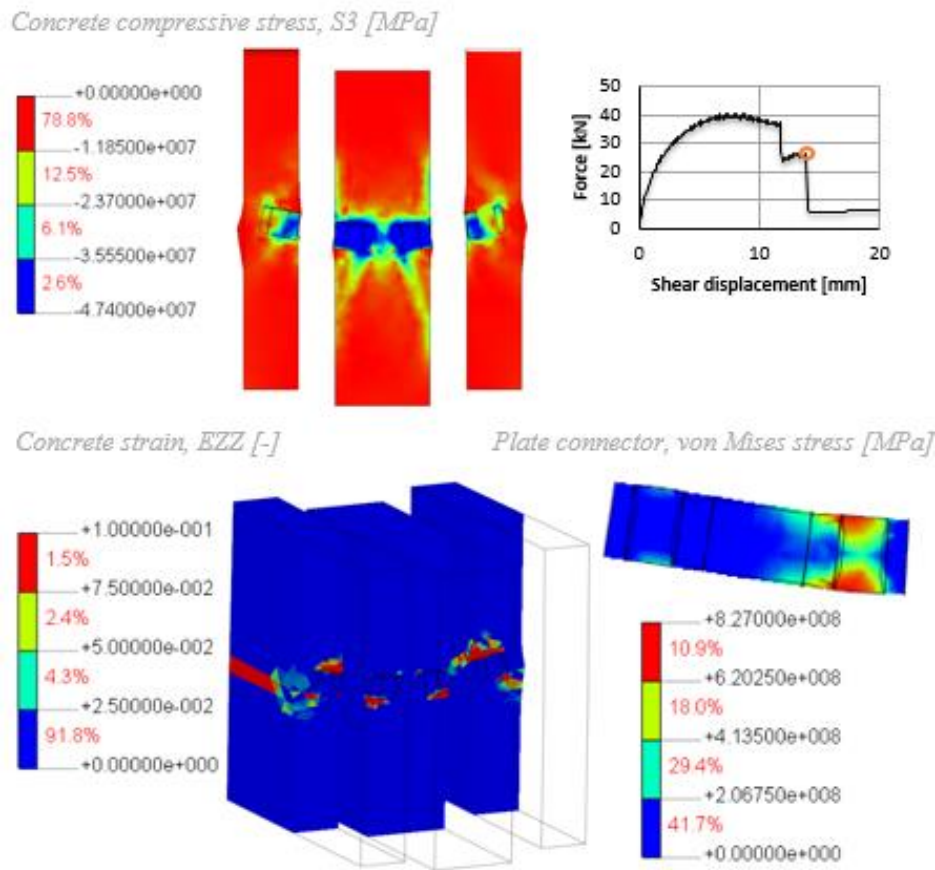


Figure 5-23 FE-results, before second crack, Test Model 1.

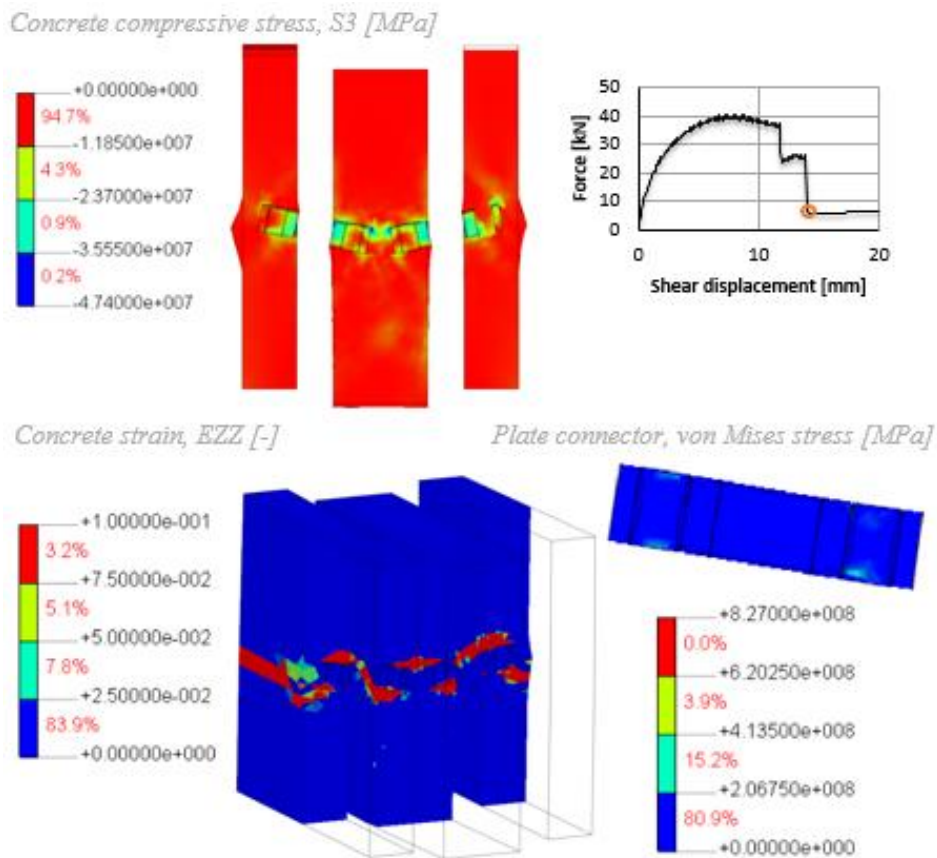


Figure 5-24 FE-results, after second crack, Test Model 1.

Figures 5-25 and 5-26 show the concrete strain perpendicular to the wythes surface (x direction), in the middle of the element, before and after the two major loss in capacity according to the graph in Figure 5-17. It can be seen how cracks firstly penetrate to the surface behind the connector causing a punching failure through the outer wythes and latter; how the cracking that have initiated at the connectors ends propagates to the surface below in the middle wythe.

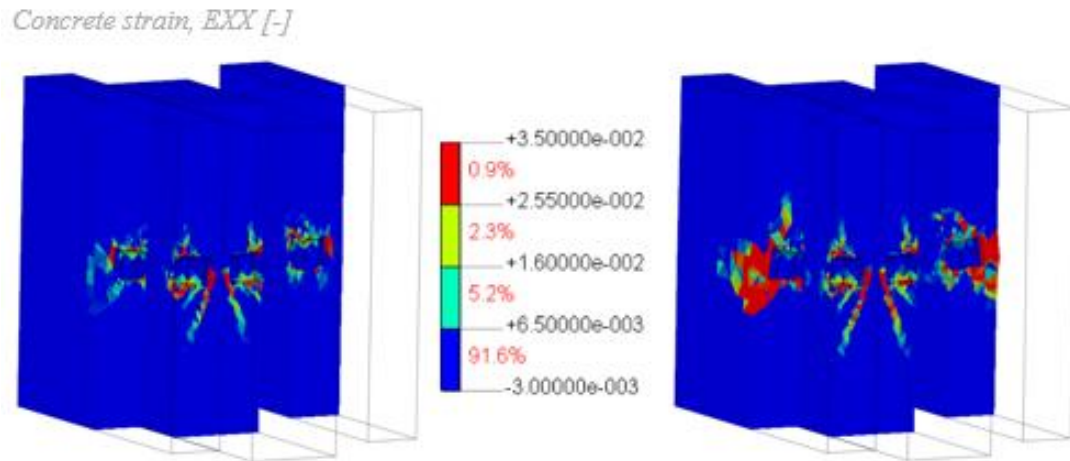


Figure 5-25 FE-results, before and after the first crack, Test Model 1.

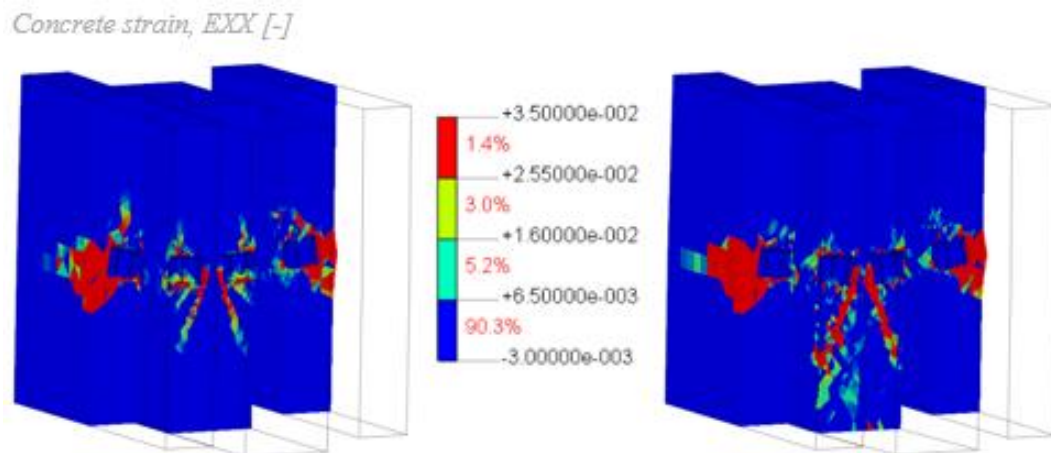


Figure 5-26 FE-results, before and after the second crack, Test Model 1.

Test Model 2 showed less stiffness, see Figure 5-18, as expected since the wythes are connected only with pin connectors, which are not intended to transfer much shear load and therefore provides low stiffness. At a force approximately 5 kN, stress concentration on the compressive side above and below the connectors reached the concretes compressive strength. As can be seen in the diagram shown in Figure 5-18, this had a very small influence on the stiffness as it was still governed by the soft connectors. With a local crush, the concentrated stress spreads out with increased load.

Behaviour after 30 mm displacement was not shown in Shams, Horstmann et al. 2014 though failure had not been reached. At that point in the FE-model tensile stresses in the connectors had reached approximately 540 MPa (~60% of f_y). The FE-analysis

were made up to 40 mm displacement, where tensile stresses in the connectors were 939 MPa (99% of f_y); however no global failure of the panel was observed.

To further examine the reason for the discrepancy in stiffness and capacity between the two models and the test results, different parameters were examined, such as:

- Insulation material
 - Altering stiffness properties
 - Replacing with spring elements
 - Removing
- Boundary conditions
 - Replacing “whole surface” boundaries with “boundary-lines”, to allow more free horizontal rotation of the wythes
 - Implementing spring elements to account for possible horizontal sliding of the wythes on the steel plate supports
- Connectors
 - Altering material properties assuming uneven stress distribution over the cross-section caused by the non-homogeneous FRP material
 - Implementing bond behaviour between connector and concrete

The conclusion from analysing the results of the above mentioned alternatives, was that the assumption of full interaction between the connectors and concrete is far from reality and could have led to too stiff and too high capacity in both FE analyses. In another words, a more precise description of the connector-concrete interaction could lead to a more realistic prediction of the stiffness and strength of the test specimens. To implement the bond behaviour, information on pull-out capacity and the associated bond-slip behaviour is important. Different methods of implementing the bond behaviour are discussed in the sections below.

5.1.6.1 Reduced material properties

Firstly, to establish if the behaviour was effected by the bonding conditions, a concept of reducing the material properties of the embedded part of the connectors was studied. As the connectors in this model were modelled as fully embedded into the concrete, full capacity of both the concrete and connector material are utilized in the analysis, with full load transfer between them. When examining test results from pull-out tests conducted on the connectors, it was observed that full utilization of the connector materials was not reached before the failure of the bonding surface occurs. This implied that modelling the connectors as fully embedded could be effecting the results from the FE-analysis.

In an attempt to implement this into the model without implementing interface elements, the ratio between the actual tensile capacity of the connector and the much lower pull-out strength (obtained from the manufacturer’s data for the CC-series connectors and calculated for the MC/MS-series connectors) was computed. The material properties of the embedded part of each connector was then reduced by the same ratio.

Furthermore, to establish if the concrete strength was influencing the load bearing behaviour, the same analyses were done with increased concrete compressive strength to see if that would increase the capacity, suggesting if capacity was rather controlled by the concrete strength rather than the bond strength.

5.1.6.1.1 Test Model 1

In Figure 5-27, the force vs. displacement graph shows good correlation to the test results by altering the material properties with the reduction factor μ_1 , which is calculated with Equation 5-1:

$$\mu_1 = \frac{F_{po1}}{T_{max1}} = 0,059 \quad \text{Eq. 5-1}$$

Where:

$F_{po1} = 15,3 \text{ kN}$ is the obtained ultimate tension pull-out capacity for CC-series connector
 T_{max1} is the maximum tensile capacity of the CC-series connector. Calculated with Equation 5-2:

$$T_{max1} = A_{FRP1} \cdot f_{yt1} = 259,3 \text{ kN} \quad \text{Eq. 5-2}$$

Where:

$A_{FRP1} = 313,5 \text{ mm}^2$ is the cross-sectional area of the CC-series connector
 $f_{yt1} = 827 \text{ MPa}$ is the tensile strength of the connectors material

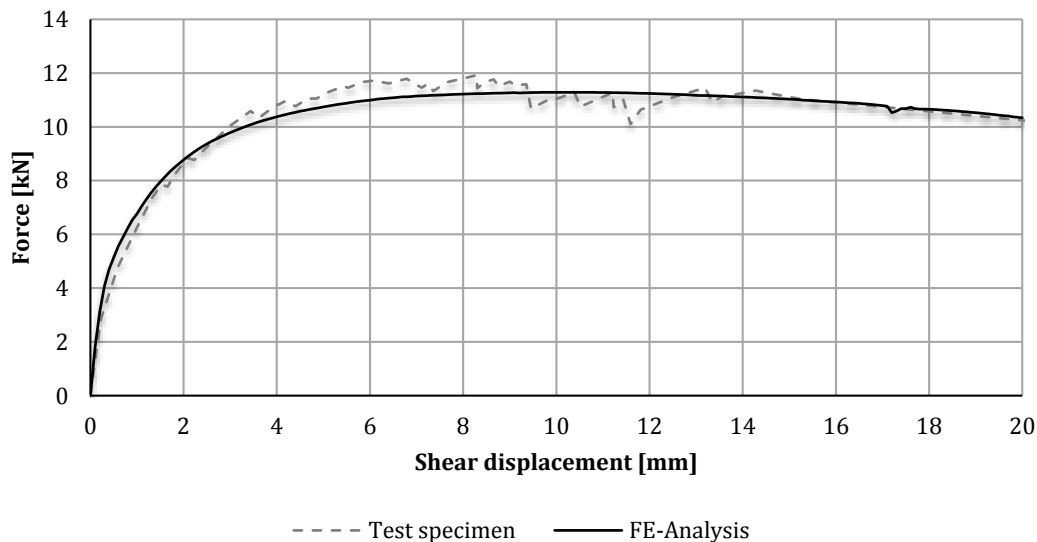


Figure 5-27 FE-results. Load vs. displacement of middle wythe. Test Model 1, with reduced material properties of embedded part of connector.

Figure 5-28 shows comparison of analysis with 10% increase in concrete compressive strength. The results shows a very small increase in the initial stiffness, but an approximately 1,4% reduction in the maximum capacity.

Calculated maximum tensile strength:

$$T_{max2} = A_{FRP2} \cdot f_{yt2} = 52,9 \text{ kN} \quad \text{Eq. 5-5}$$

Where:

$A_{FRP2} = 55,9 \text{ mm}^2$ is the cross-sectional area of the MC/MS-series connector
 $f_{yt2} = 948 \text{ MPa}$ is the tensile strength of the connectors material

As the embedded part of the MC/MS-series connectors were modified for the experimental test presented in Shams, Horstmann, et al. 2014, manufacturers data regarding their pull-out strength was not considered valid. In section 4.1 an equation on how to calculate pull-out resistance is introduced, including empirical factor, k, modified to be valid for the specific shape of the embedded part of this connector. Using that the ultimate pull-out capacity for the MC/MS-series connectors was calculated, see Equation 5-4.

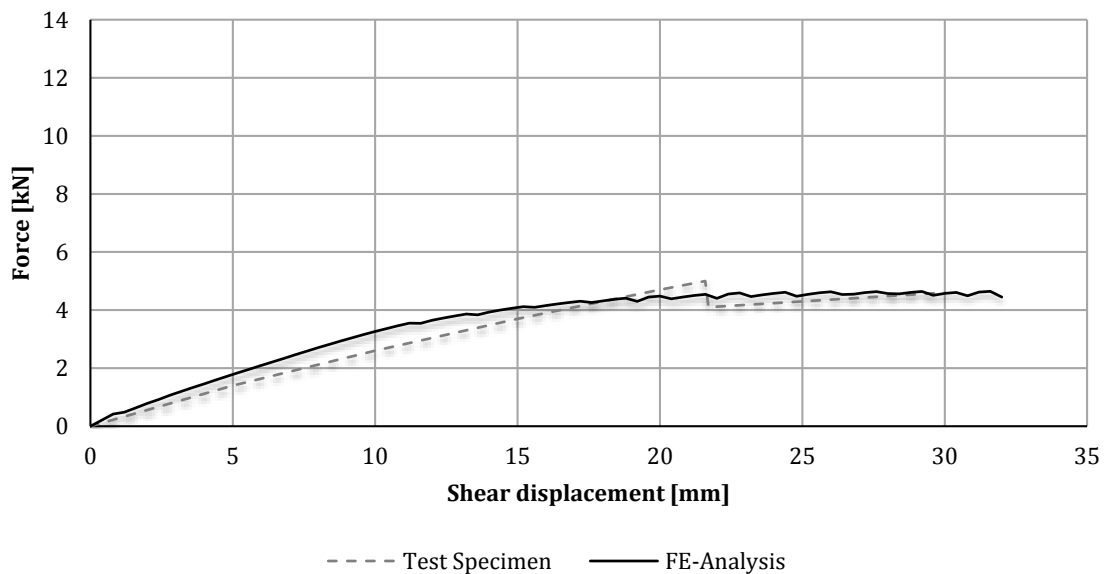


Figure 5-29 FE-results. Load vs. displacement of middle wythe. Test Model 2, with reduced material properties of embedded part of connector.

Figure 5-30 shows comparison of analysis with 10% increase in concrete compressive strength. The results shows the same initial stiffness, and an approximately 1,1% increase in the maximum capacity.

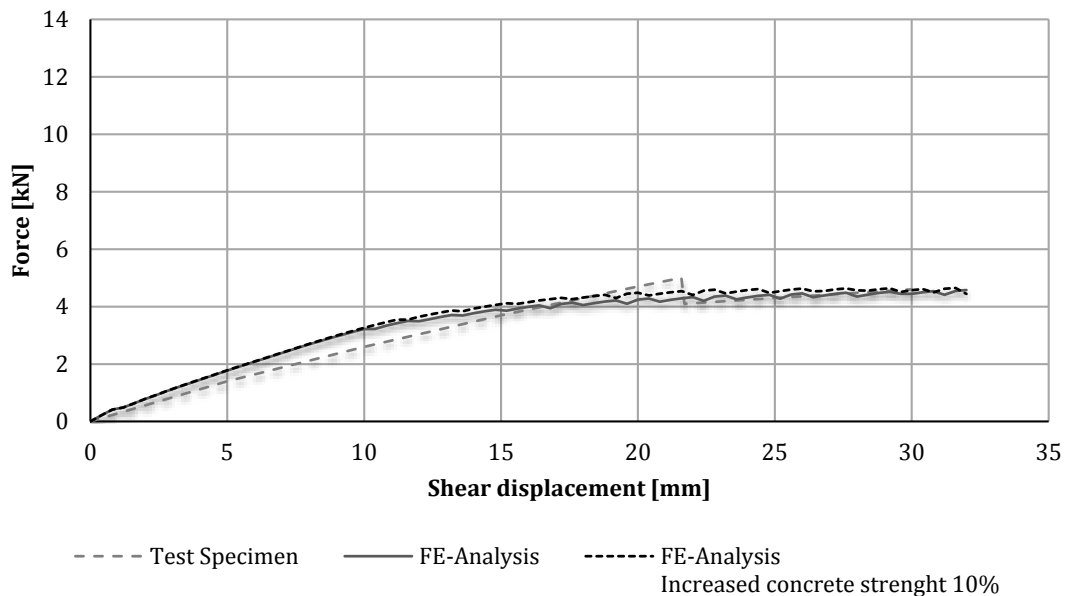


Figure 5-30 FE-results. Load vs. displacement of middle wythe. Test Model 2, with reduced material properties of embedded part of connector, increased concrete strength.

5.1.6.2 Outcome

The aforementioned results from analysis with modified material properties of a connector indicate that the pull-out capacity of a connector does affect the load bearing behaviour of the panel, reducing it's stiffness and ultimate capacity. Furthermore, analysis with modified concrete properties indicate little influence of the concrete strength on the overall behaviour of the panel.

Thus, studying the effect of the pull-out in a more detailed approach was considered an important aspect to further analyse the behaviour of the sandwich panel under shear load. As the pull-out capacity is governed by the bond-slip behaviour between the connector and the concrete an actual bond-slip relation was implemented into the FE-model using interface elements between the concrete and the connector, seeking a more realistic response in the FE-model.

5.1.6.3 Bond slip

To model the actual bond behaviour between the connector and the concrete, interface elements were implemented for the embedded parts of the connectors. When modelled without an interface element the concrete and the connector share the same nodes where they meet. By using interface, an element is created between the two planes separating their nodes, see Figure 5-31.

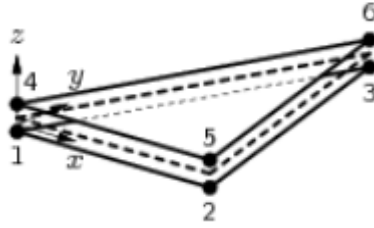


Figure 5-31 Illustration of interface element separating nodes (TNO DIANA©, 2015).

When implementing the interface elements into both models, the anchoring shape of the connectors were neglected, with the objective to implement its effect into the interface material properties. In Figures 5-32 and 5-33 the three separate components are shown, concrete wythe, interface and connector.

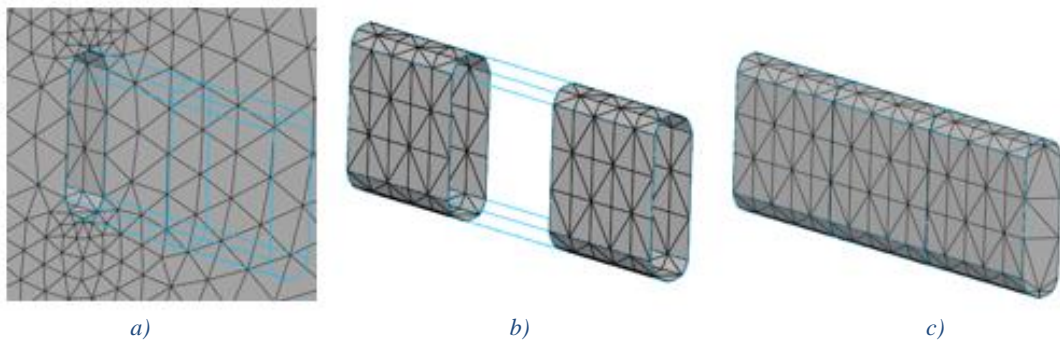


Figure 5-32 Test Model 1, a) slot in the concrete wythe, b) interface element, c) connector.

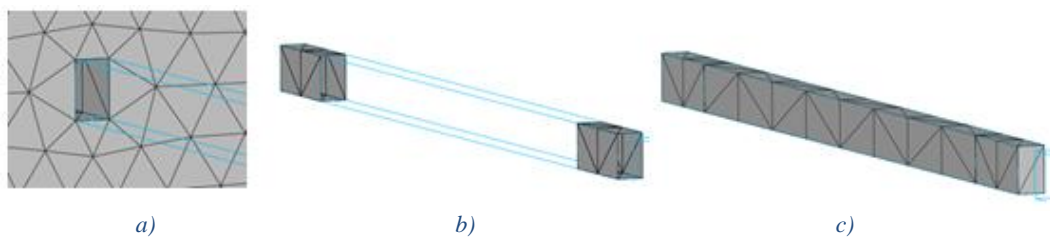


Figure 5-33 Test Model 2, a) slot in the concrete wythe, b) interface element, c) connector.

By assigning appropriate material properties for the interface element, the bond behaviour can be implemented. Interface elements called T18IF in DIANA were used. These elements are based on linear interpolation. The default 3-point integration scheme was used.

Material properties for the interface elements are defined with bond slip behaviour. Input parameters to describe the bond-slip are given as a relation between traction and relative displacement within the element, for both normal- and shear traction.

In DIANA, the relations between normal traction and normal relative displacement is kept linear, but the relations between shear traction and shear relative displacement is non-linear. Three models are available in DIANA to describe the non-linear behaviour, called cubic, power law and multi-linear, see Figure 5-34.

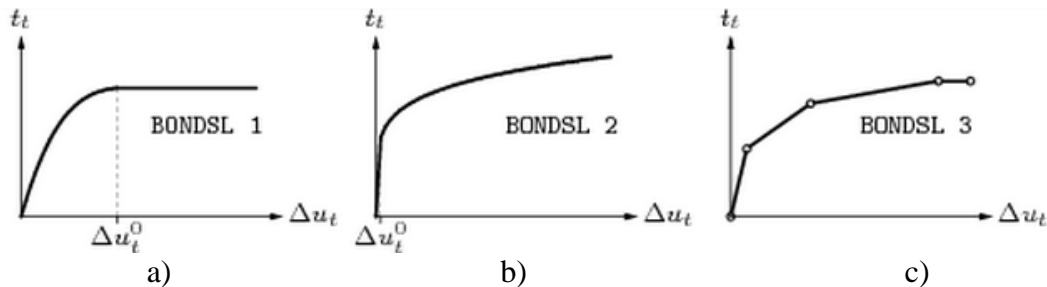


Figure 5-34 Different predefined bond-slip curves available in DIANA. a) cubic, b) Power Law, c) multi-linear (TNO DIANA©, 2015).

Bond slip curves are usually obtained from pull-out tests. Available information from pull-out testing of the two connector types only included the maximum pull-out capacity. The relative displacement, Δu_t was therefore assumed and calibrated to give correlating results to the load vs. displacement diagram from the experiments. As the embedded part of the two connector types have a certain shape, to improve their anchorage strength, the stiffness obtained from this calibration was assumed to be valid for their specific shape.

Equation 5-6 was used to obtain the maximum shear traction value t_t , with the approach to distribute maximum pull-out capacity over the bonding area:

$$t_t = \frac{F_{po}}{A_{bond}} \text{ [N/mm}^2\text{]} \quad \text{Eq. 5-6}$$

Where:

t_t is the maximum traction
 F_{po} is the maximum pull-out capacity
 A_{bond} is the interface area between concrete and connector

The linear normal stiffness was calculated with Equation 5-7:

$$k_n = \frac{t_t}{\Delta u_{tn}} \text{ [N/mm}^3\text{]} \quad \text{Eq. 5-7}$$

Where:

k_n is the normal stiffness
 t_t is the maximum traction
 Δu_{tn} is the relative normal displacement, see section 5.1.6.3.1

5.1.6.3.1 Test Model 1

The calculated maximum traction for the CC-connectors in Test Model 1, was $t_t = 3,22$ MPa. Calibration of the relative displacement resulted in a relative normal displacement, $\Delta u_{tn} = 0,00003$ m and relative shear displacement, $\Delta u_t = 0,003$ m.

Consequently, this resulted in a normal stiffness, $k_n = 1,0733 \cdot 10^{11}$ N/mm³ and the bond slip curve shown in Figure 5-35. The multi-linear function in DIANA was used to define the curve into to the model.

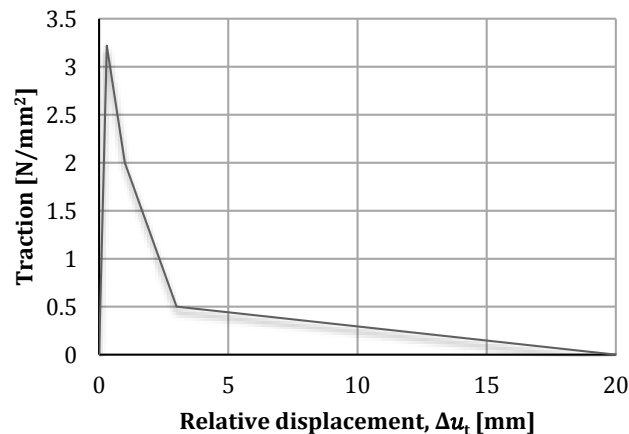


Figure 5-35 Bond-slip curve used in Test Model 1.

In Figure 5-36, the load vs. displacement diagram obtained from the FE-analysis including the bond slip behaviour, compared with results from the test set-up and FE-analysis without bond slip behaviour is shown. Including the bond slip with above stated values shows a slightly larger initial stiffness but almost the same ultimate capacity and similar ductility behaviour.

Analyses were also done with different definition of the bond slip curve; i.e. using the cubic function, assuming brittle failure of the bond and assuming perfectly plastic behaviour after maximum traction. Also different slopes of the descending branch of the curve were tested. Results from these analyses showed some, but not substantial difference in the load vs. displacement behaviour.

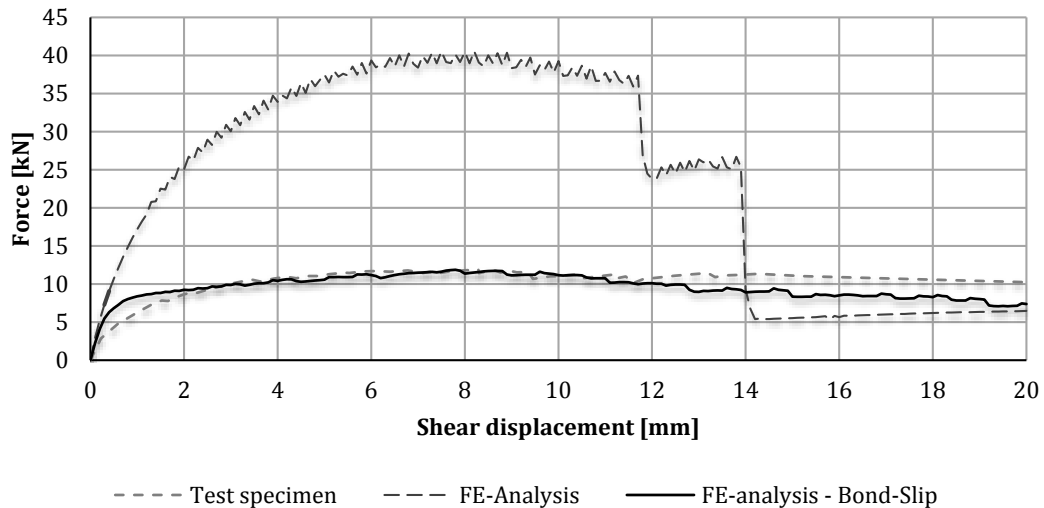


Figure 5-36 FE-results. Load vs. displacement of middle wythe. Test Model 1, with and without bond-slip interface.

Figure 5-37 shows stress distribution in different components after 0,4 mm displacement, where the load vs. displacement curve starts to separate from the curve from the FE-analysis without a bond-slip interface.

Concentrated compressive stresses in the concrete on either side of the connectors are reaching 47,3 MPa compared with 47,2 MPa at the same displacement in the original model. At this stage local crushing of the concrete has begun and the concentrated stresses are distributing. A big difference can be seen in tensile stresses in the connector, 131 MPa in this model compared with 366 MPa in the original test. This can be explained by a slip in the interface element, allowing for a release of the stresses in the fixed connector. This can be also be seen in the difference in deformed shape of the connectors between models.

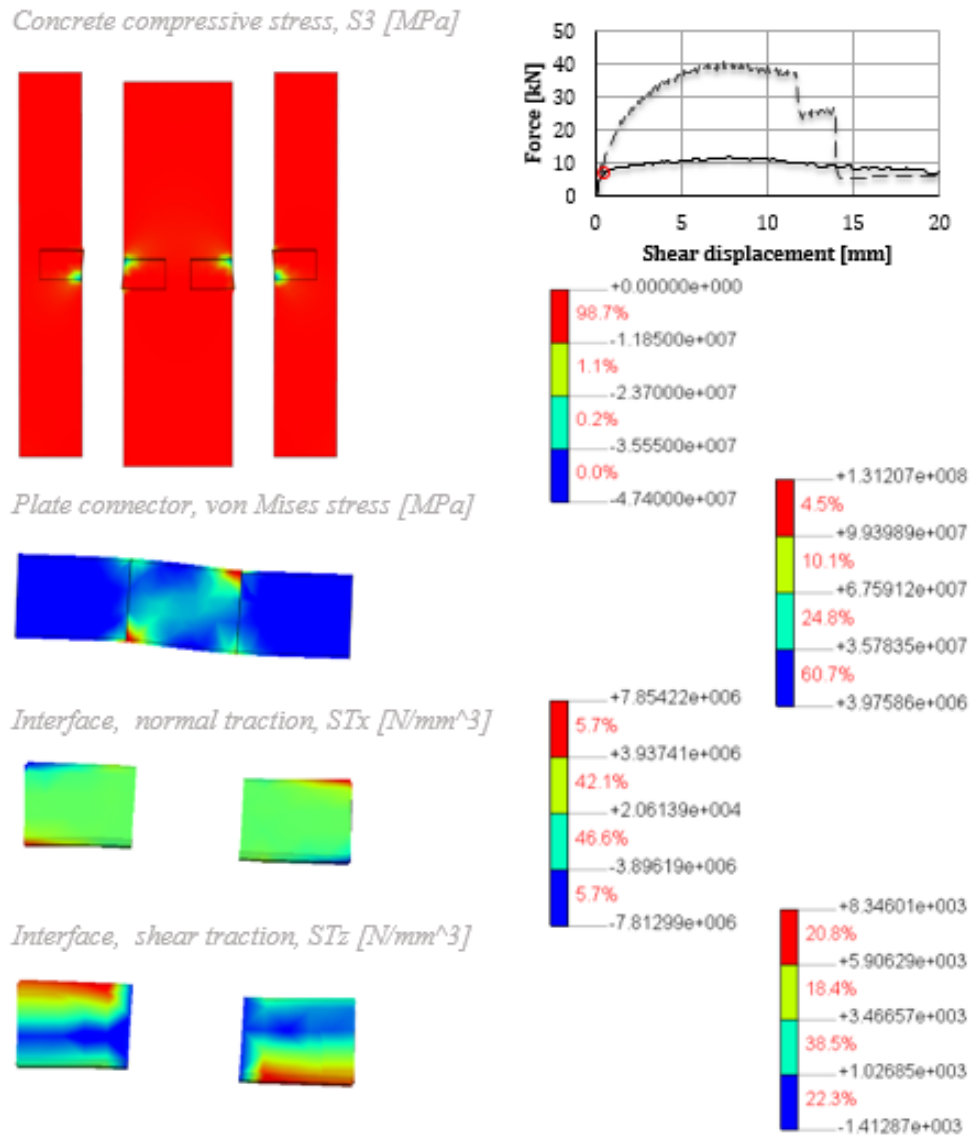


Figure 5-37 FE-results, Test Model 1. After 0,4mm displacement of middle wythe.

Figure 5-38 shows stress distribution after 7,9 mm displacement, at maximum capacity, which was at 7,5 mm displacement in the model without a bond-slip interface.

At this stage the concentrated stresses have distributed further and have reduced to 44,4 MPa. Again, a big difference can be seen in tensile stresses and the deformed shape of the connector, 250 MPa in this model compared with the connector already reaching its yield strength of 948 MPa in the original model.

The shear traction in the interface elements have reached 0,15 MPa of the 3,22 MPa maximum traction. At the end of the analysis it has reached approximately 1 MPa. This means that their displacement behaviour is not yet affected by the “after failure” part of the bond slip curve. The shear traction values further on and to the end of this analysis showed that they never reached this value. This could explain the fact that altering the shape of the bond-slip curve did not affect the load vs. displacement curve but to a limited extend. The shear tractions STy and STz (in the midas FX+ for

DIANA post-processor) acts in-plane of the element, indicated as u_y and u_x in Figure 5-39.

On the other hand, the normal traction has reached up to 139 MPa. As the normal traction is kept linear throughout the analysis, it has no assigned maximum value. The normal tractions, ST_x (in the midas FX+ for DIANA post-processor) acts out-of-plane to the element, u_z in Figure 5-39.

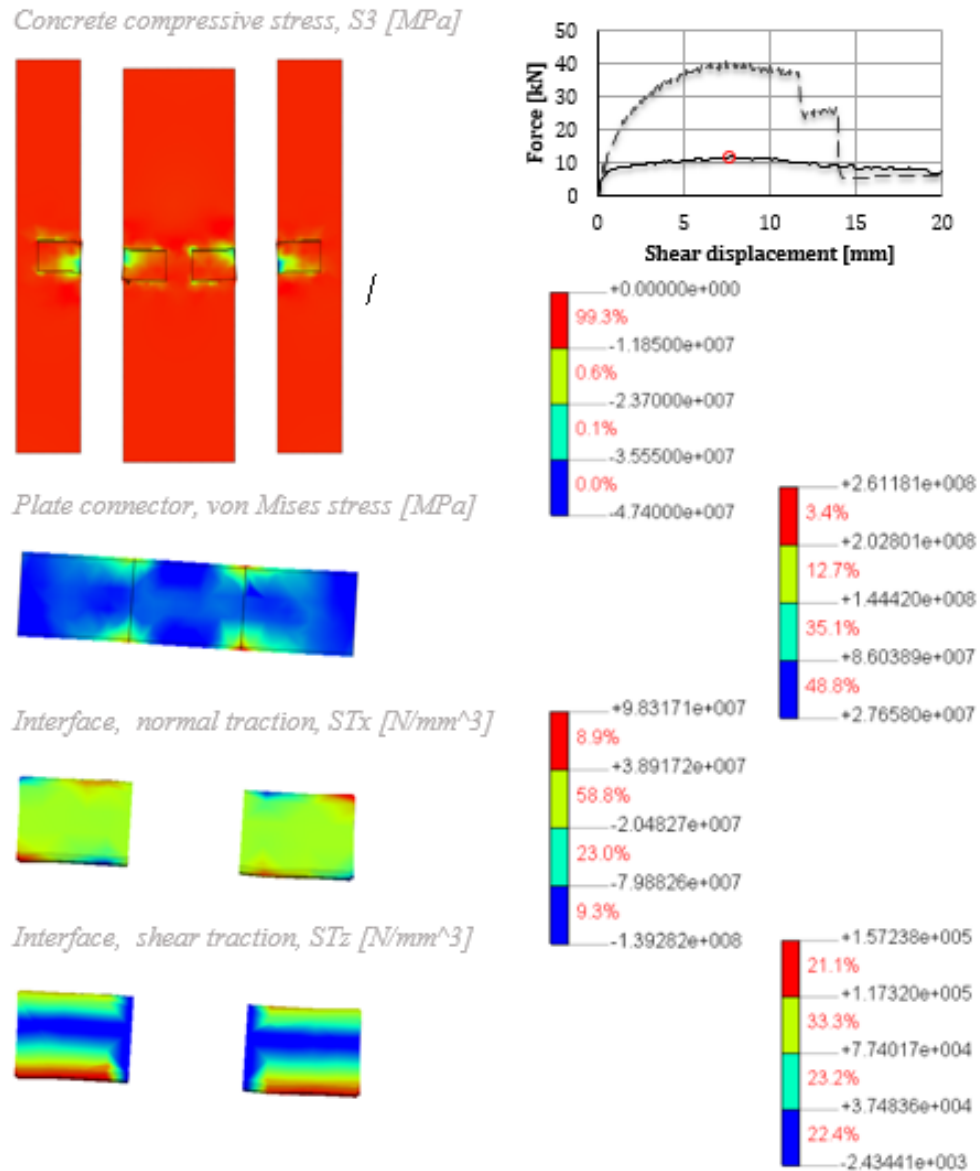


Figure 5-38 FE-results, Test Model 1. After 7,9 mm displacement of middle wythe.

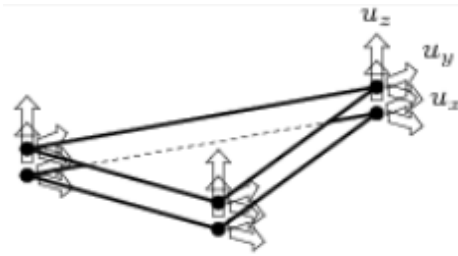


Figure 5-39 Illustration of normal- and shear directions in an interface element (TNO DIANA©, 2015)

5.1.6.3.2 Test Model 2

The calculated value maximum traction for the MC/MS-connectors in Test Model 2, was $t_t = 10,9$ MPa. Calibration of the relative displacement resulted in a relative normal displacement, $\Delta u_{tn} = 0,001$ m and relative shear displacement, $\Delta u_t = 0,001$ m.

Consequently, this resulted in a normal stiffness, $k_n = 1,09 \cdot 10^{10}$ N/mm³ and the bond slip curve shown in Figure 5-40. The multi-linear function in DIANA was used to define the curve into to the model.

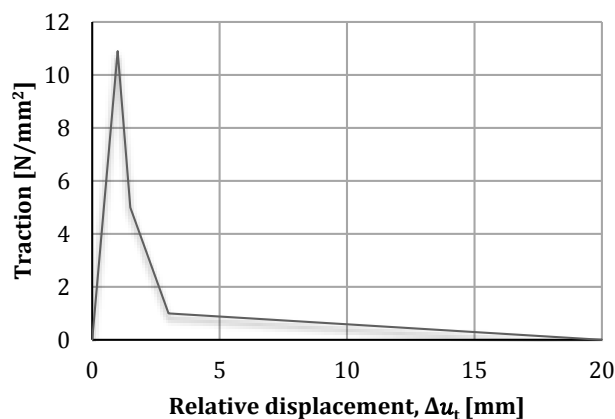


Figure 5-40 Bond-slip curve used in Test Model 2.

In Figure 5-41, the load vs. displacement diagram obtained from the FE-analysis including the bond slip behaviour, compared with that from the test set-up is shown. By including the bond slip with above stated values, the model shows a slightly larger initial stiffness which elevates the curve slightly above the test result curve, but after $\sim 0,2$ mm displacement the curves show similar stiffness. The ultimate capacity is close to the test results. At the end of the analysis the shear traction in the interface elements had reached approximately 5,3 MPa of the 10,9 MPa maximum capacity and the normal traction had reached about 27,4 MPa.

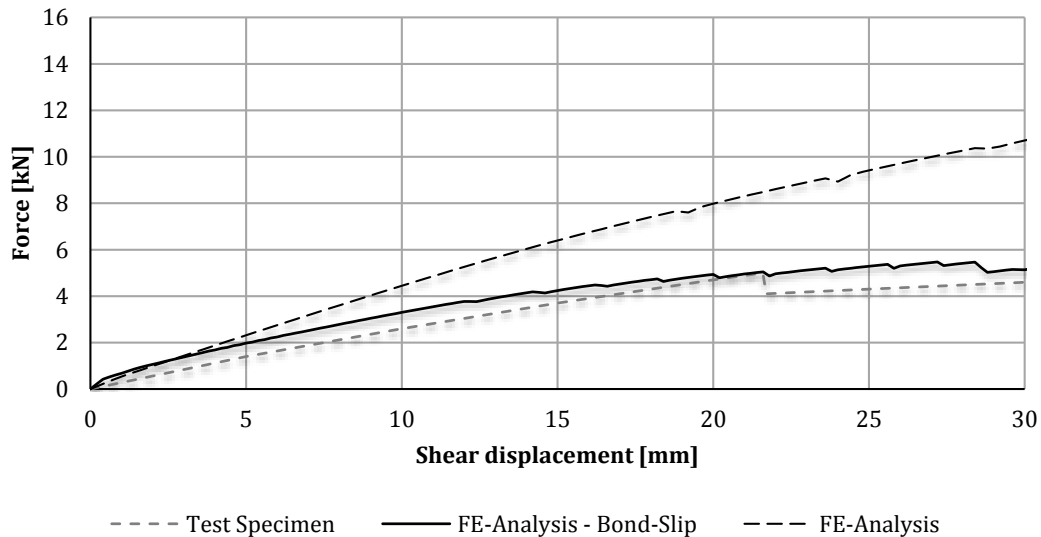


Figure 5-41 FE-results. Load vs. displacement of middle wythe. Test Model 2, with and without bond-slip interface.

5.1.7 Test Model 3

Test Model 3 consisted of two unreinforced concrete wythes with insulation and a CC-series plate connector placed in the middle of the wythe. The plate geometry and material properties are the ones which were described in sections 4.1.1.1 and 4.1.2.2 respectively. This is made exactly like Test Model 1 and takes advantage of its symmetry to provide a simpler model, see Figure 5-42. By establishing the boundary conditions that give the most correlating results, it is possible to implement them to the TRC panel model which should result in a comparable behaviour between the models. Nodes on the bottom surface of the left wythe were tied with a link and constrained in x-,y- and z- directions. The nodes in the top left corner of the same wythe were also tied with a link but constrained only in x-direction as can be seen in Figure 5-42. In Figure 5-43 it can be seen that these boundary conditions give a reasonable correspondence to the experimental results. Hence, these boundary conditions were used on the TRC model.

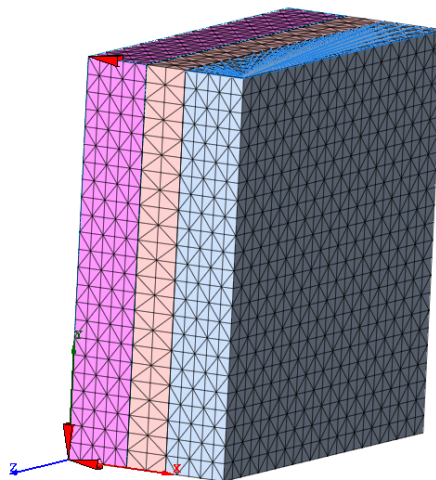


Figure 5-42 Test Model 3, including boundary conditions.

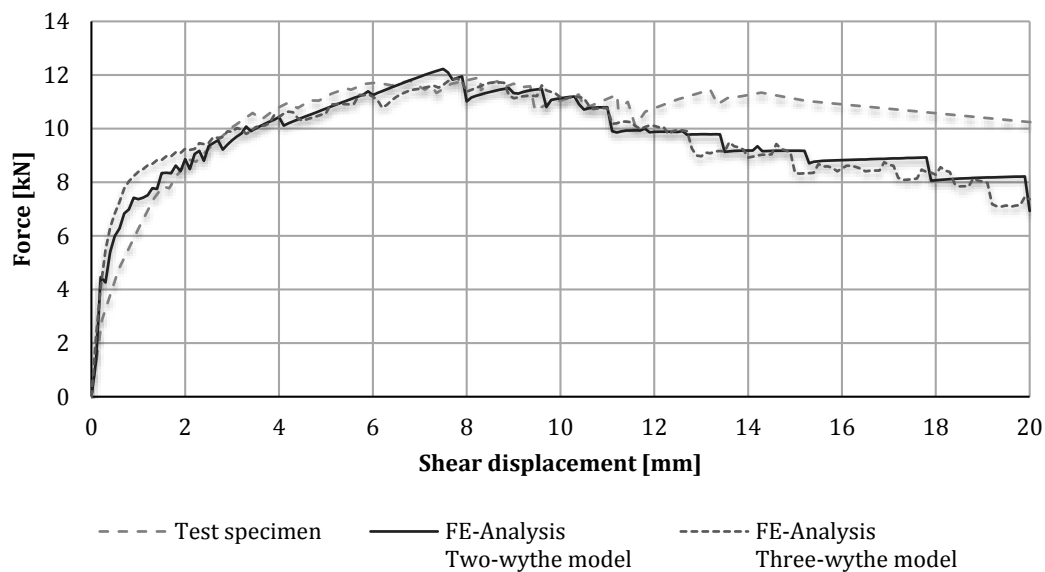


Figure 5-43 FE-results. Load vs. displacement of outer wythe. Test Models 1 and 3, with bond-slip interface.

5.2 TRC panel model

The TRC panel model consists of a 50mm “inner” wythe, 150mm XPS insulation and 20mm “outer” wythe, which was considered reasonable according to various reports concerning TRC sandwich panels (Williams Portal 2013), (Malaga 2011), (Shams, Horstmann et al. 2014). Both wythes are made of TRC. The connecting system in the model consists of two MC/MS-series pin-connectors, as modelled in Test Model 2 and a FRP plate which is anchored into the concrete with FRP bars as shown in Figure 5-44. The plate was designed and modelled with a commercially available plate anchor from the manufacturer Halfen. Material properties were chosen to be the same as used in the FRP connectors from Thermomass. Thus, the plate uses the anchorage technique from the Halfen plates but has the advantage of FRP instead of steel, which is considered to be an important factor for thin concrete panels.

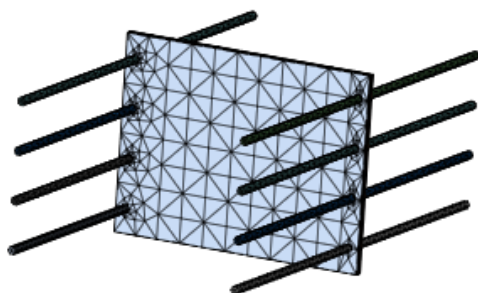


Figure 5-44 FRP plate connector with anchoring bars.

Due to the anchorage effect from the bars that are attached to the plate, bond slip was not considered for the plate. On the other hand, interface elements were added to implement bond slip for the pin-connectors mainly because they have a small embedment depth and no special anchoring effect. As can be seen on Figure 5-45 the interface element is only added on the surface of the embedded pin that is in contact with the concrete.

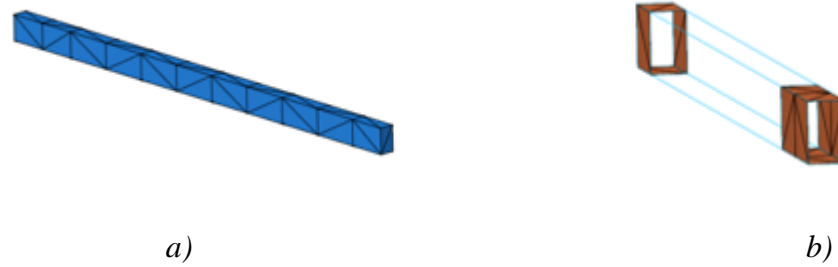


Figure 5-45 a) Pin-connector mesh, b) Interface element mesh.

5.2.1 Geometry

When the geometry of the sandwich panel model was chosen, one of the most important criteria was considered to be the thickness, since the main objective was to have the sandwich panel as thin as possible. Papers discussing different geometries for TRC sandwich panels were studied and a geometry which was considered reasonable was then selected (Finzel et al. 2003), (Gopinath et al. 2014). The modelled TRC sandwich panel, as shown in Figures 5-46 and 5-47 has a height of 1200 mm and a depth of 500 mm, the thickness of each element is shown in Table 5-6.

Table 5-6 Thickness of different components in the TRC panel model.

Panel	Thickness [mm]
Inner wythe	50
Insulation	150
Outer wythe	20
Total	220

A plate with a similar geometry as the plate from Test Model 1 was modelled and analysed. This was done to have a connecting device that is comparable to Test Models 1 and 3. The plate was modelled as 200 mm x 150 mm x 6 mm with 8 bars, as can be seen in Figure 5-47.

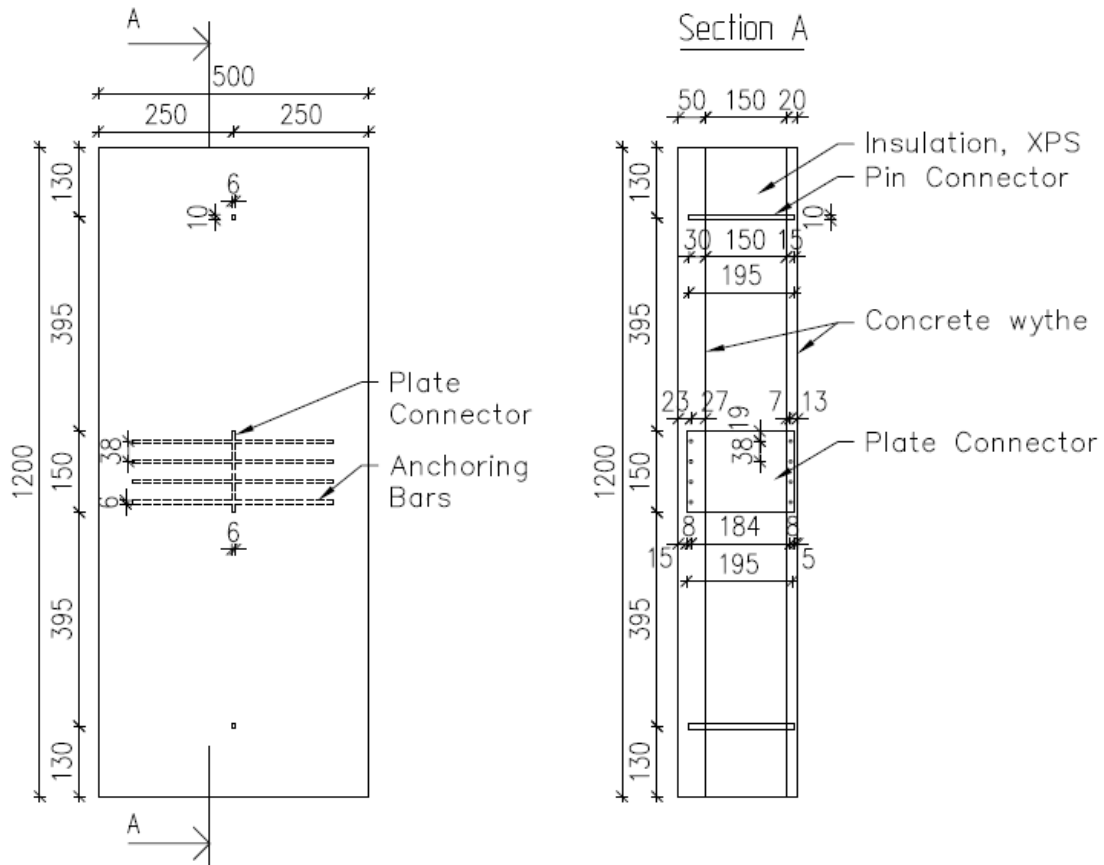


Figure 5-46 Geometry of the TRC panel model; dimensions are in mm.

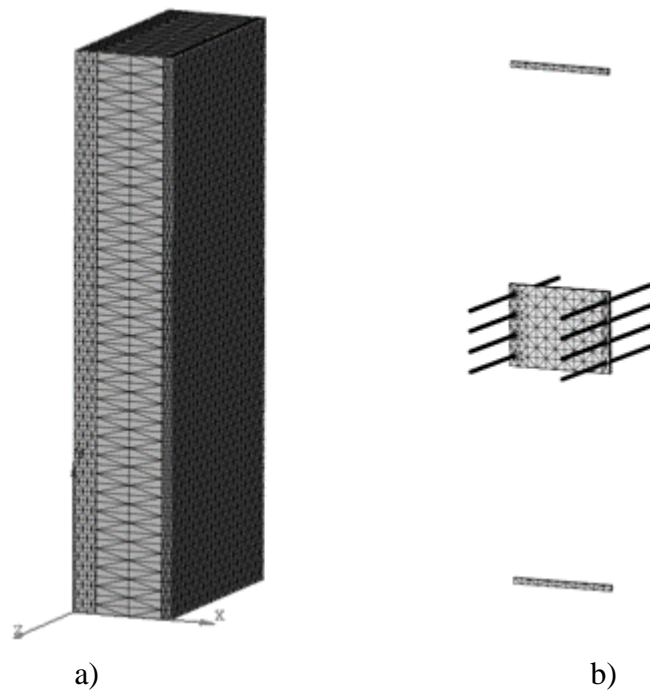


Figure 5-47 a) TRC panel model mesh , b) Connector mesh.

5.2.2 Material properties

High strength concrete (C80/90) was chosen to resist as much load as possible while maintaining a slim figure. Input values for the concrete material were obtained from EC2 apart from fracture energy which was calculated using Model Code 2010, see section 9.2. Values are shown in Table 5-7. The input values for the plate and the anchoring pins are as shown in Table 5-2 and the pin-connectors as shown Table 5-4, both in section 5.1.2.

Table 5-7 Material properties for concrete in TRC panel model.

Compressive strength	f_{cm}	88 MPa
Tensile strength	f_{ctm}	4,8 MPa
Elastic modulus	E_{cm}	42 GPa
Fracture energy	G_f	163,4 N/m

5.2.3 Mesh and element types

All the mesh sizes and element types are the same as for Test Model 2 described in section 5.1.3. Figure 5-48 shows the mesh size of different components.

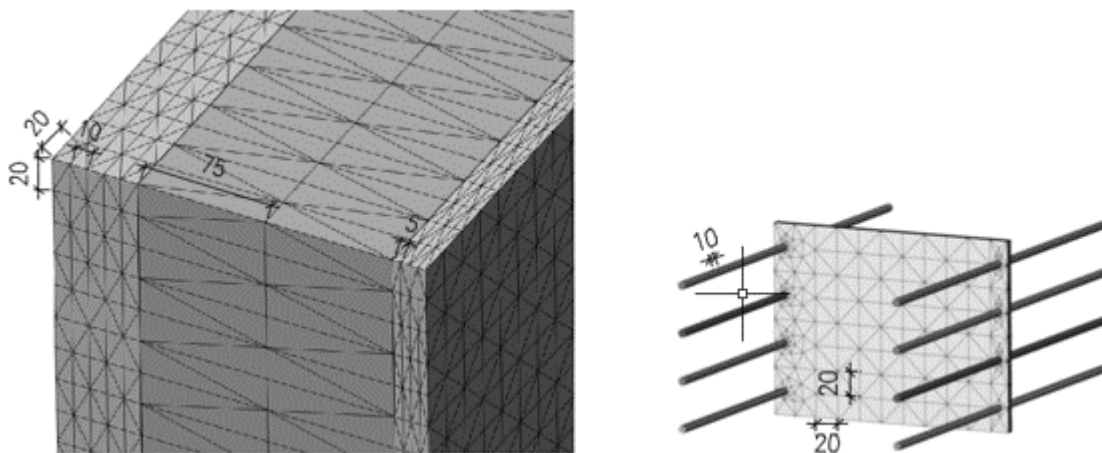


Figure 5-48 Mesh size of TRC panel model; dimension are in mm.

5.2.4 Boundary conditions

The boundary conditions of the TRC panel model were identical to Test Model 3, which seemed reasonable since the test model showed good correspondence to experimental results. Therefore the sandwich panel was supported on the bottom with prevention in x-, x- and z-direction and at the top in x-direction. A link was created where one node was chosen as master node and the other surrounding nodes were chosen as slave nodes. By implementing this link, all the slave node will have the same behaviour as the constrained master node. Consequently, the whole bottom surface acts as it is constrained in all directions and the top edge in the x-direction, see Figure 5-49.



Figure 5-49 Boundary conditions of the TRC panel model.

5.2.5 Loading and analysis method

The displacement control was used instead of the usual load control method. The main advantage of the displacement control is the ability to inspect what occurs after failure. A link as described in section 5.2.4 was implemented on the surface where the displacement is prescribed, see Figure 5-50. This prevents possible concrete crushing that can occur if the displacement is concentrated on one node. A 20 mm displacement in the z-direction was defined and the analysis ran 200 steps, where each step was 0,1 mm. The crack pattern and the failure modes of the concrete panel were then analysed as well as the load vs. displacement diagram. By looking at the crack pattern and failure modes it is possible to inspect what happens while the panel is being loaded and what part of the sandwich panel is failing at what load step. This information can be useful to further improve the connection system and to understand the overall behaviour and failure of the sandwich panel.

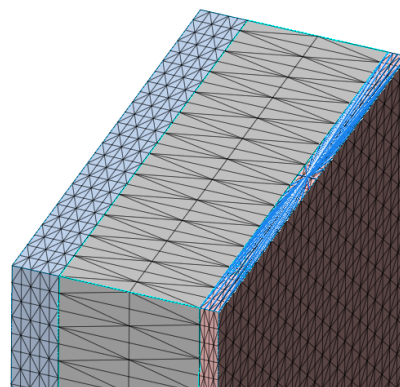


Figure 5-50 Load link on the TRC panel model.

5.2.6 Results

In Figure 5-51, a load vs. vertical displacement diagram from the numerical analysis is shown for the loading of the outer wythe of the TRC panel. The results show a stiff behaviour in first stage of loading until cracking initiates at approximately 33,6 kN load, causing a change in the curve leading up to approximately 37 kN maximum

capacity of the connection. The gradual descending capacity loss after first great stiffness loss indicates a very ductile response.

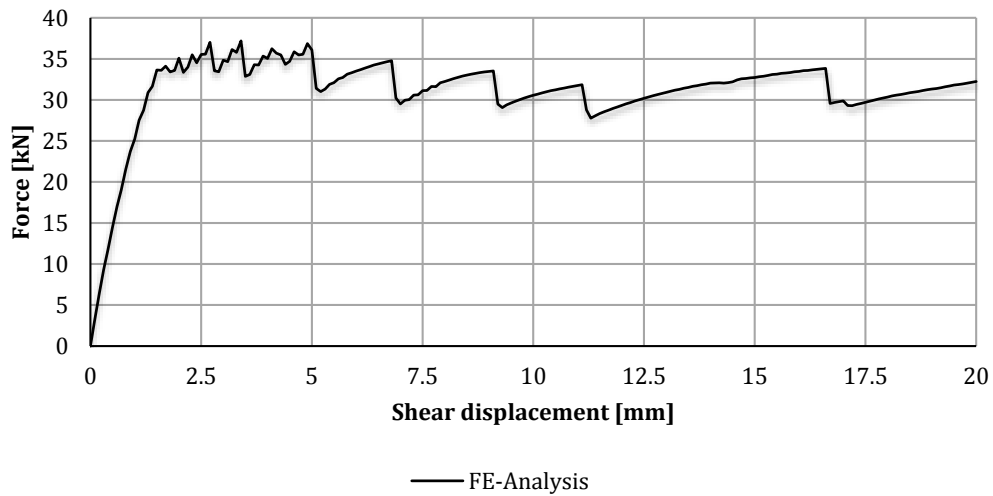


Figure 5-51 FE-results. Load vs. displacement of outer wythe, TRC panel model.

To be able to study the stress and crack distribution, the model was cut in half as shown in Figure 5-52. Afterwards, the insulation and the middle part of the plate were hidden to see both sides of the concrete wythes, thus allowing a more thorough inspection of stress concentrations and crack patterns.

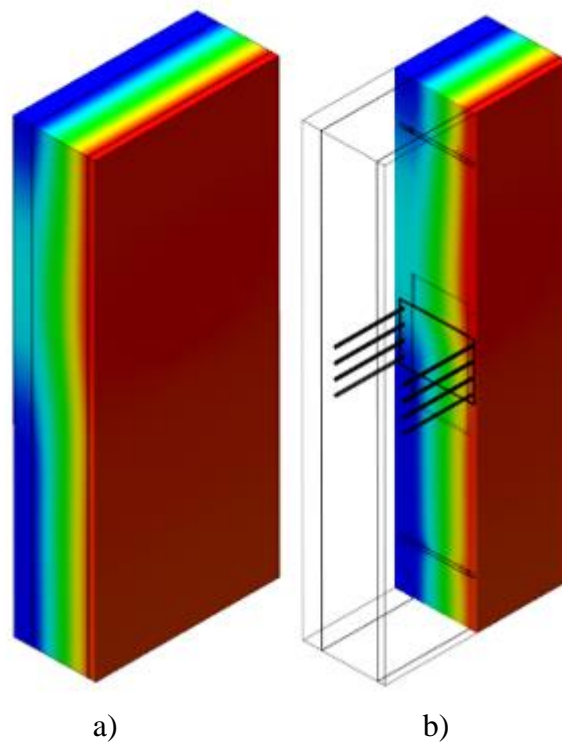


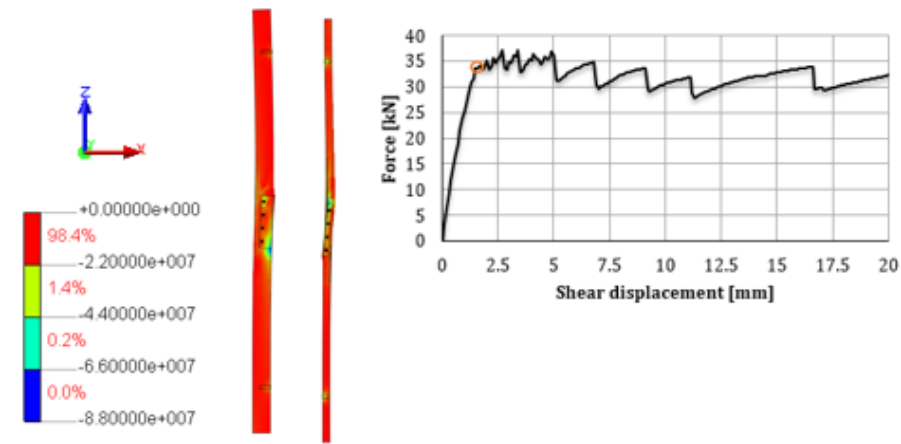
Figure 5-52 FE-model a) Full model, b) Sliced model.

The great loss of stiffness at approximately 33,6 kN load, indicates a failure of some sort. As can be seen on Figure 5-54 that first failure can be explained by crack initiation. It can be seen in Figures 5-54 and 5-55 that strain builds up above the connector plate in both wythes and leads to crack initiation horizontally throughout the wythe. In Figure 5-56, it can be seen how the strain increases and distributes more clearly horizontally in the y-direction which indicates cracking along the wythe above the connector. Figure 5-57 shows how the increased stress in the connector and wythes, followed by a sudden decrease in stiffness shown in Figure 5-58. The strain both above and below the connector is increasing at a fairly fast rate which points to even more cracking along the wythes. Figures 5-59 to 5-65 show very similar behaviour, the stress in the connector and wythes are getting larger followed by a sudden drop in stiffness which leads to an increase of strain and consequently more cracks.

From Figures 5-54 to 5-65, it can be seen that there are large stress concentrations on the compression side of the connector in the concrete. Those eventually lead to crushing of the concrete. It was however observed that before crushing occurred, horizontal cracking initiated in both wythes, shown in the strain distribution. When stress in the connecting plate and it's pins are examined it can be seen that the FRP material is only reaching approximately 45% of its ultimate strength and only around 20% of ultimate capacity when cracking of the concrete initiates.

From this discussion of the failure modes it can be concluded that such connecting device as is assumed in the model can provide a fully composite behaviour in such sandwich panel, since it has shown that the concrete wythes fail before the connector itself.

Concrete compressive stress, S3 [MPa]



Concrete strain, EXX [-]

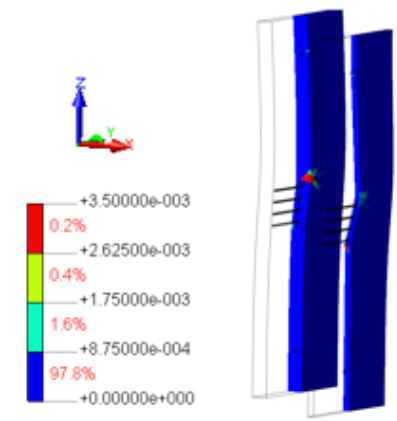


Plate connector, von Mises stress [MPa]

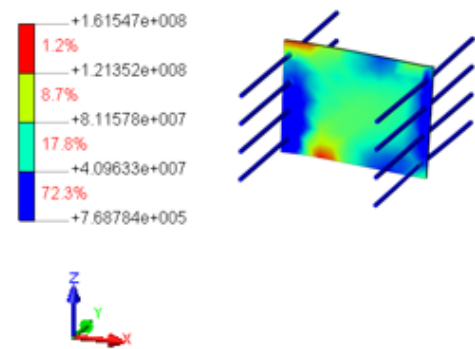


Figure 5-53 FE-results. TRC panel model. Before first crack initiation above connector plate in both wythes.

Concrete strain, EZZ [-]

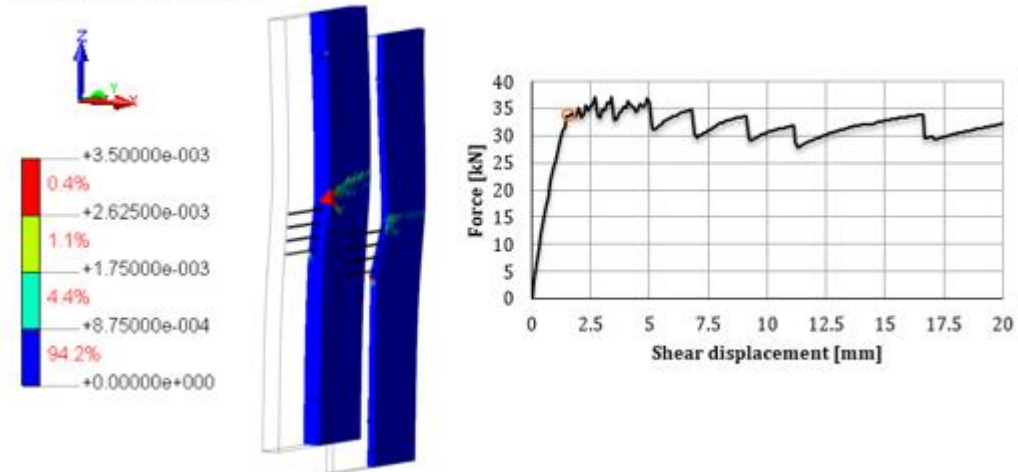
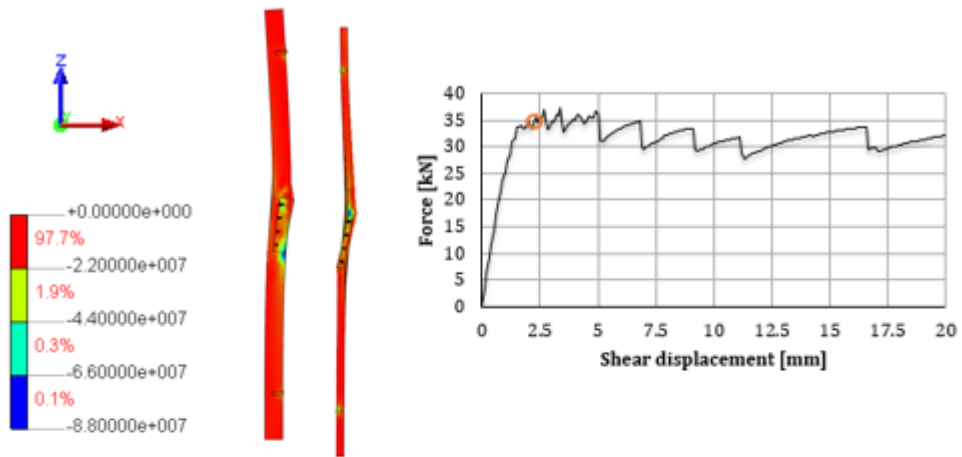


Figure 5-54 FE-results. TRC panel model. After first crack initiation above connector plate in both wythes.

Concrete compressive stress, S3 [MPa]



Concrete strain, EZZ [-]

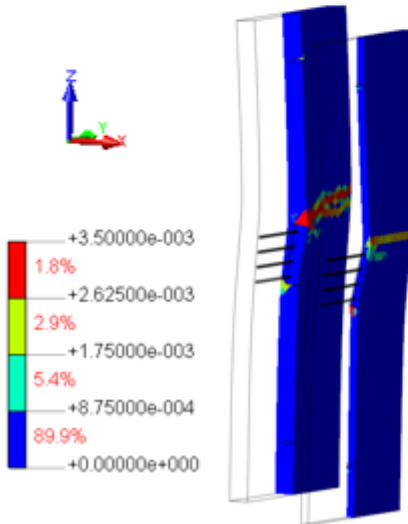


Plate connector, von Mises stress [MPa]

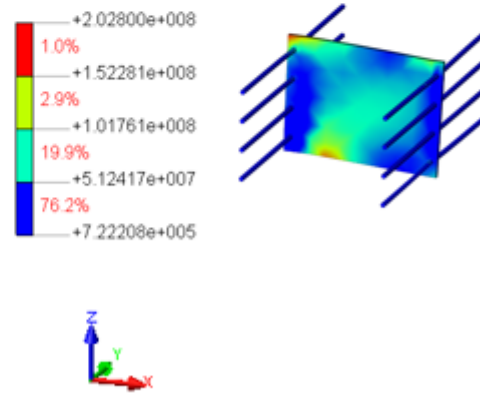
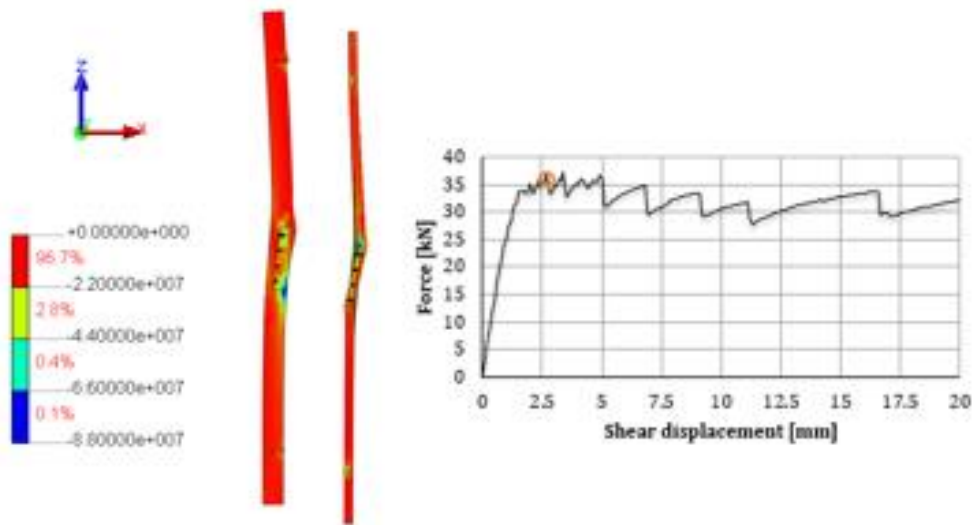


Figure 5-55 FE-results. TRC panel model, cracks propagates throughout the panels.

Concrete compressive stress, S3 [MPa]



Concrete strain, EZZ [-]

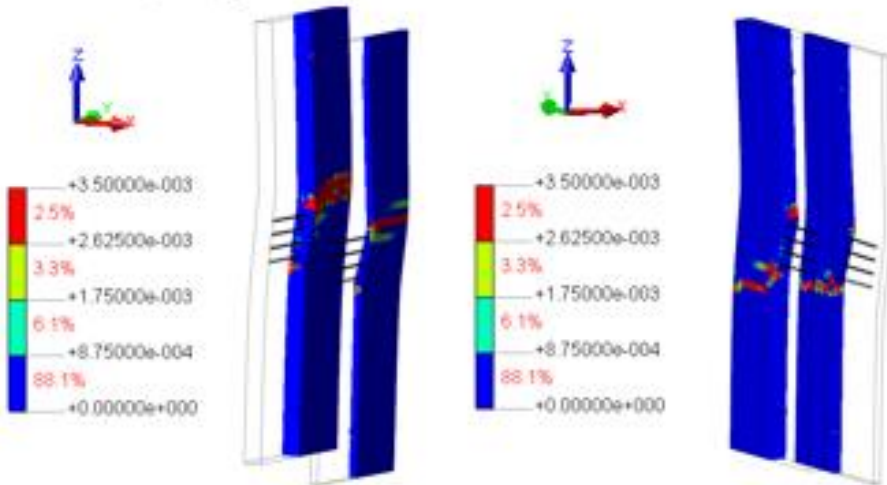


Plate connector, von Mises stress [MPa]

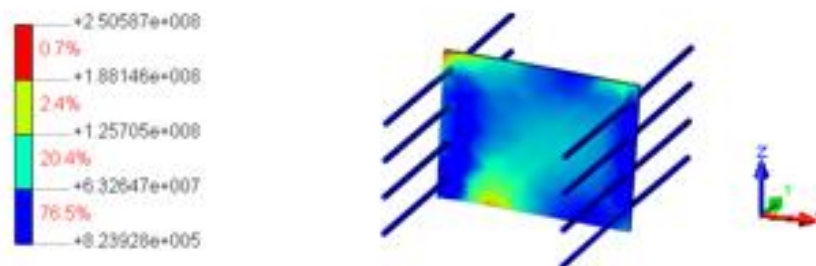
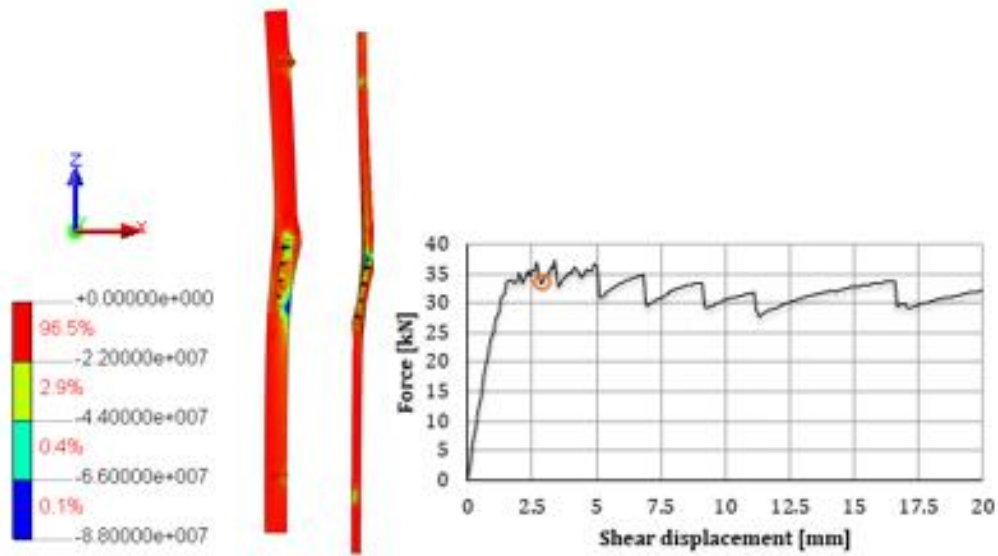


Figure 5-56 FE-results. TRC panel model, capacity reaches a peak, cracks propagates further.

Concrete compressive stress, S_3 [MPa]



Concrete strain, E_{ZZ} [-]

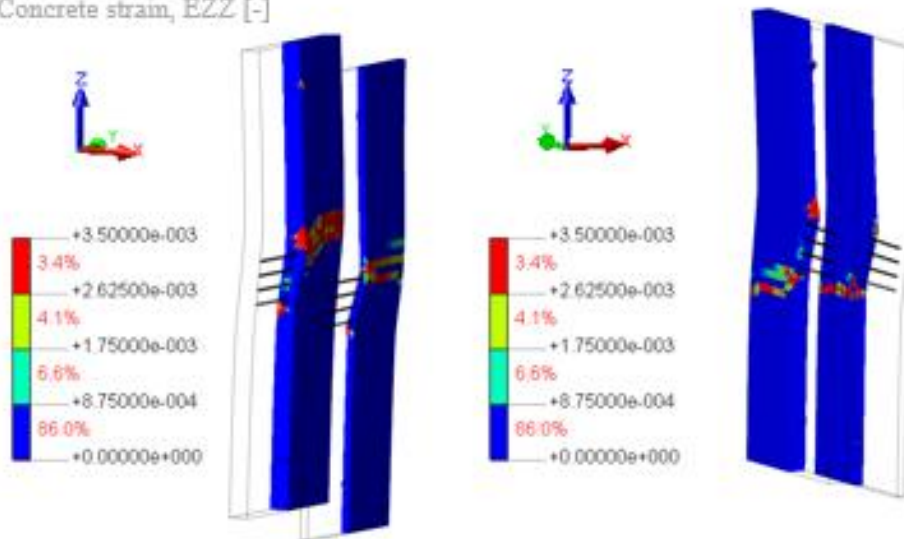


Plate connector, von Mises stress [MPa]

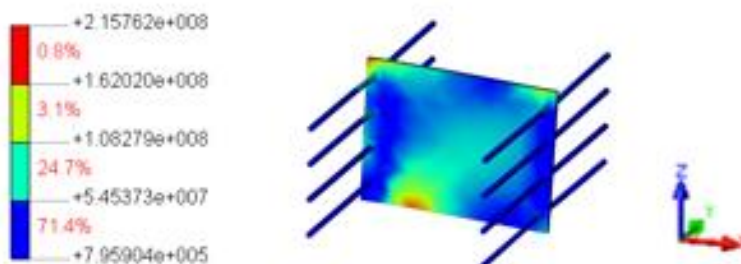
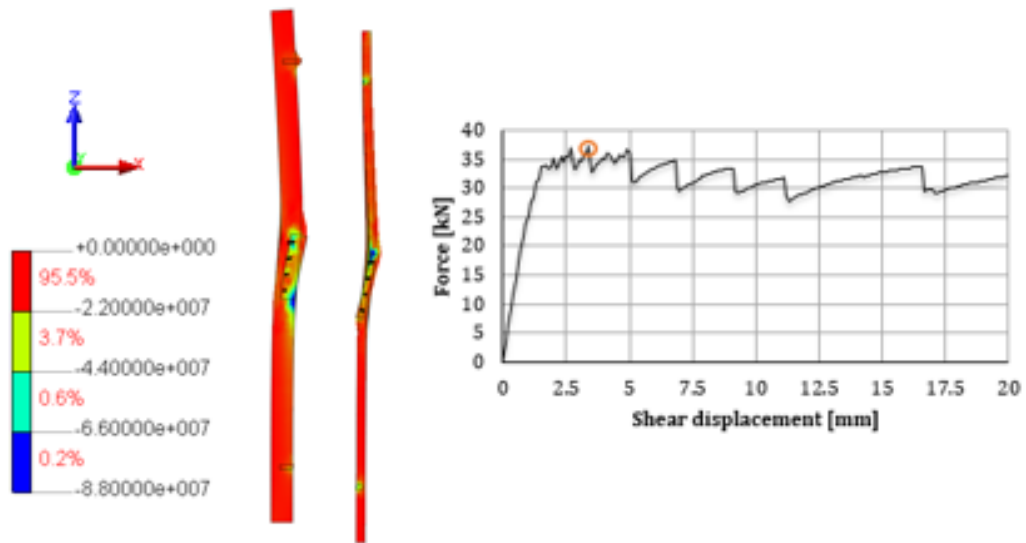


Figure 5-57 FE-results. TRC panel model, sudden loss of stiffness, cracks propagates further.

Concrete compressive stress, S_3 [MPa]



Concrete strain, E_{ZZ} [-]

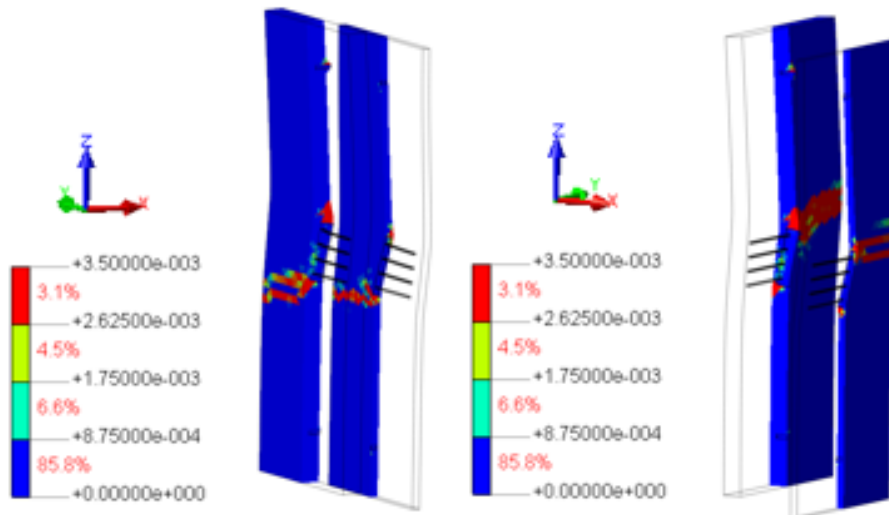


Plate connector, von Mises stress [MPa]

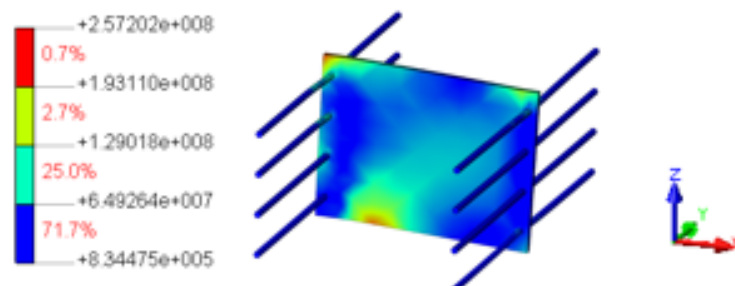
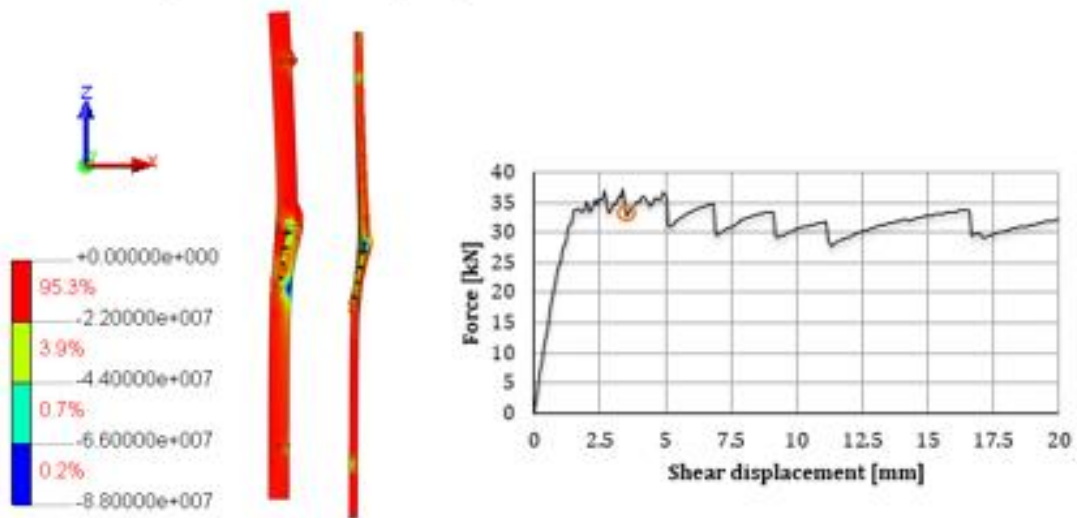


Figure 5-58 FE-results. TRC panel model, capacity reaches a peak, cracks propagates further.

Concrete compressive stress, $S3$ [MPa]



Concrete strain, EZZ [-]

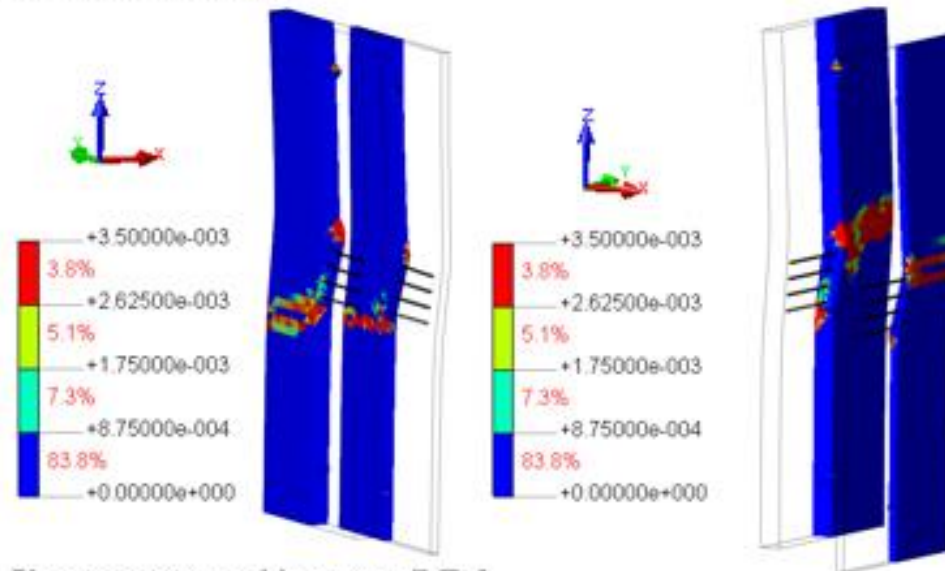


Plate connector, von Mises stress [MPa]

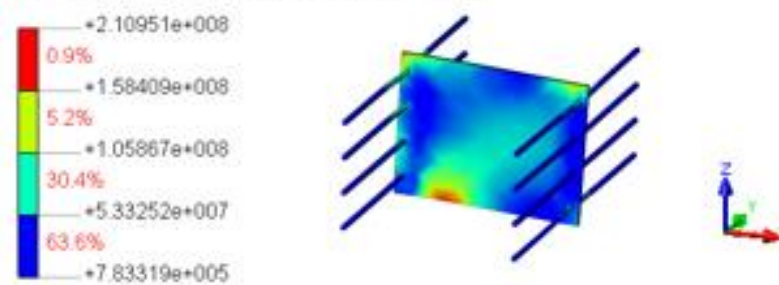
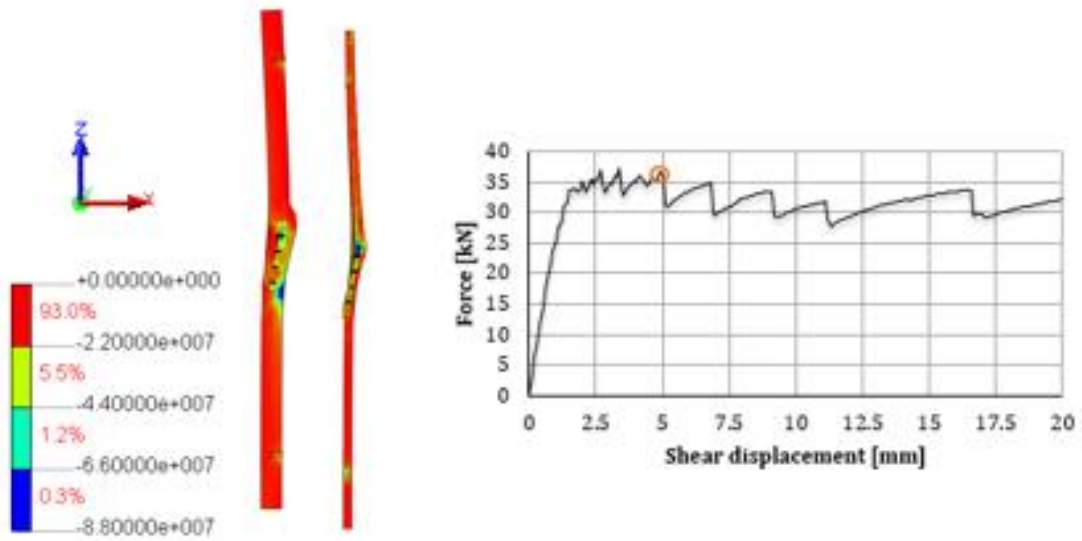


Figure 5-59 FE-results. TRC panel model, sudden loss of stiffness, cracks propagates further.

Concrete compressive stress, S_3 [MPa]



Concrete strain, E_{ZZ} [MPa]

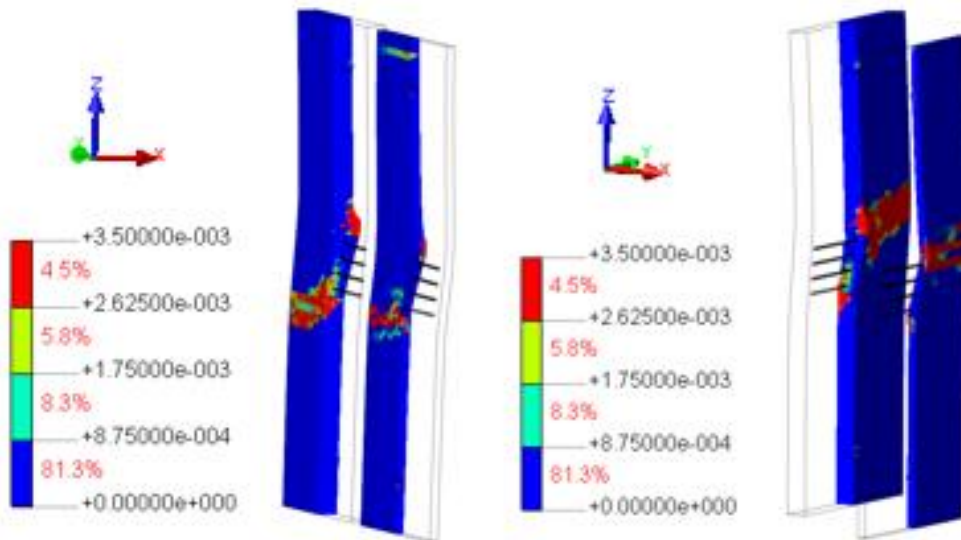


Plate connector, von Mises stress [MPa]

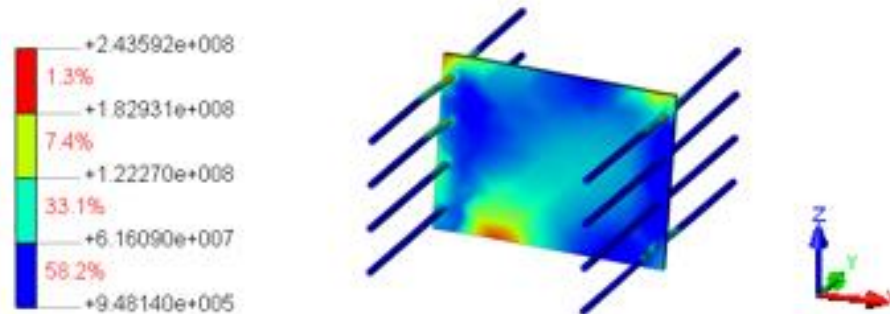
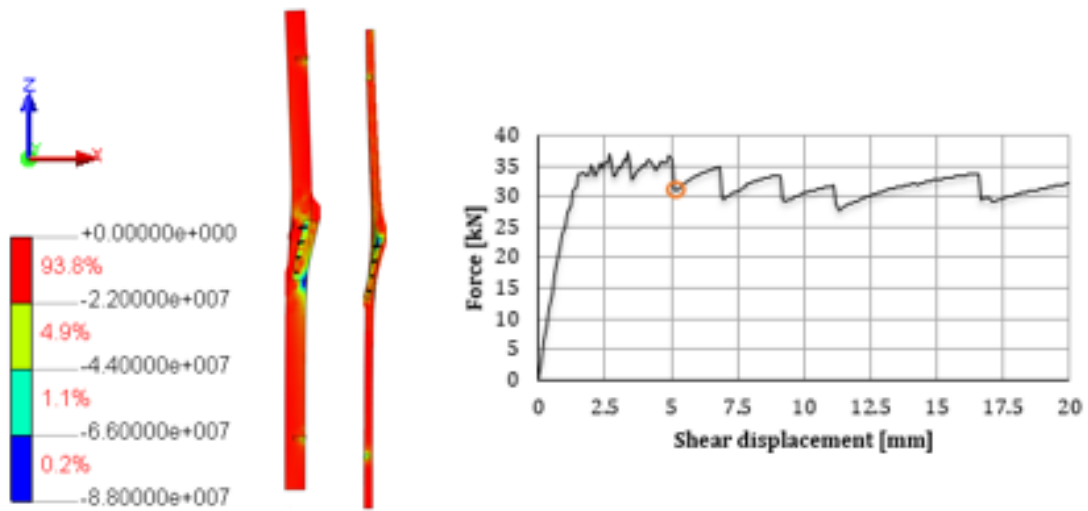


Figure 5-60 FE-results. TRC panel model, capacity reaches a peak, cracks propagates further.

Concrete compressive stress, $S3$ [MPa]



Concrete strain, EZZ [-]

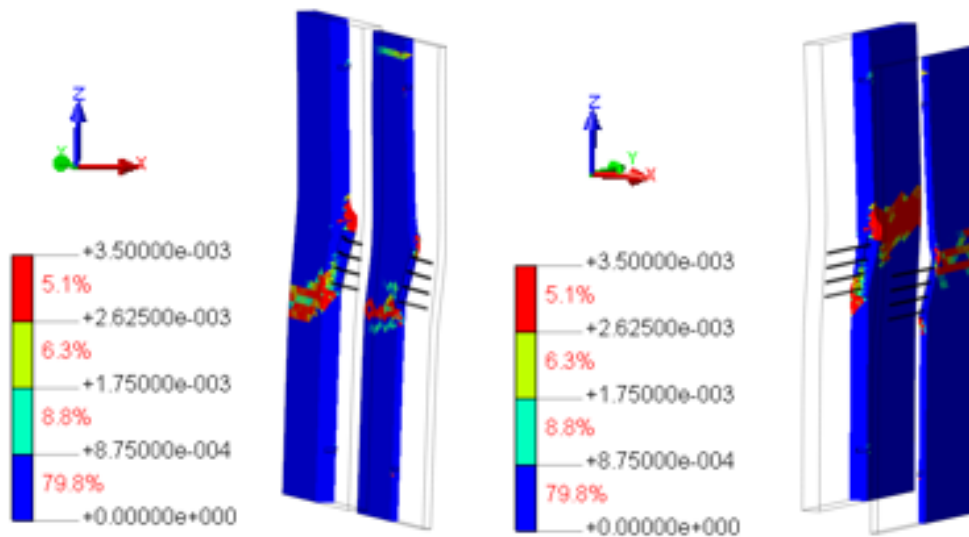


Plate connector, von Mises stress [MPa]

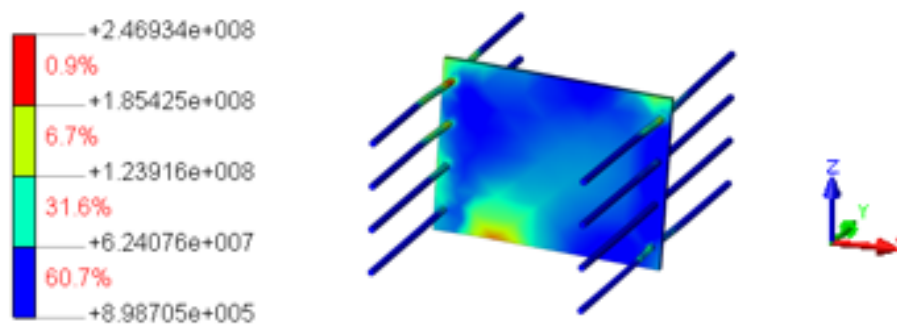
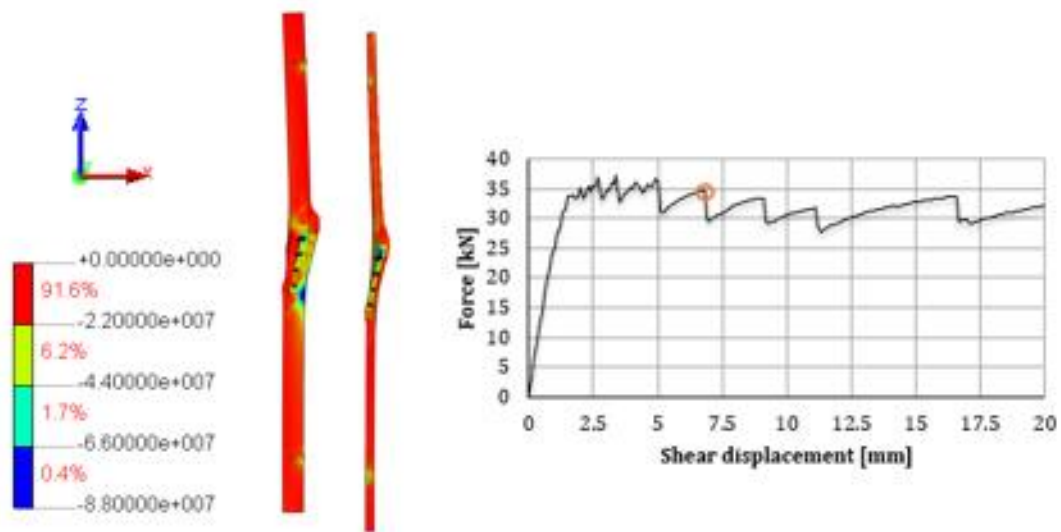


Figure 5-61 FE-results. TRC panel model, sudden loss of stiffness, cracks propagates further.

Concrete compressive stress, $S3$ [MPa]



Concrete strain, EZZ [MPa]

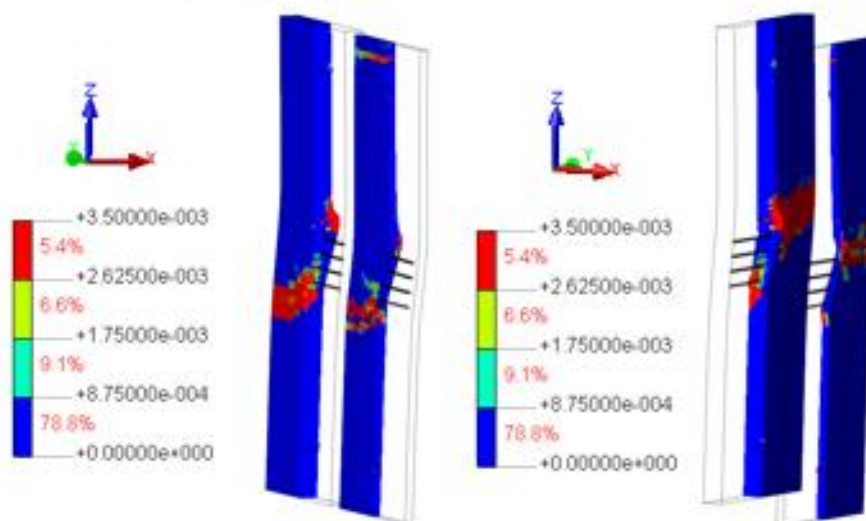


Plate connector, von Mises stress [MPa]

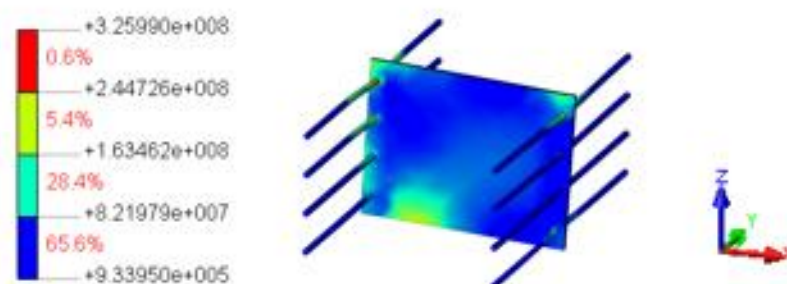
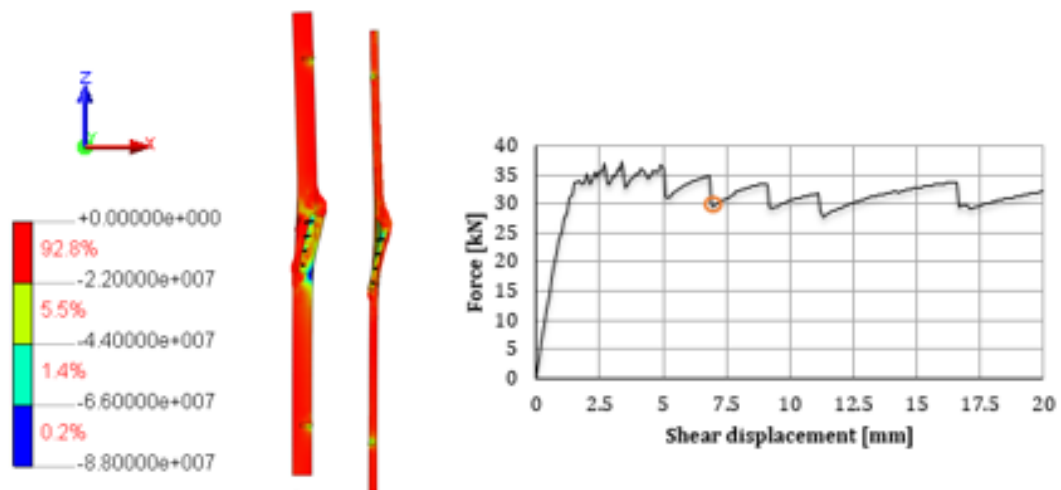


Figure 5-62 FE-results. TRC panel model, capacity reaches a peak, cracks propagates further.

Concrete compressive stress, $S3$ [MPa]



Concrete strain, EZZ [-]

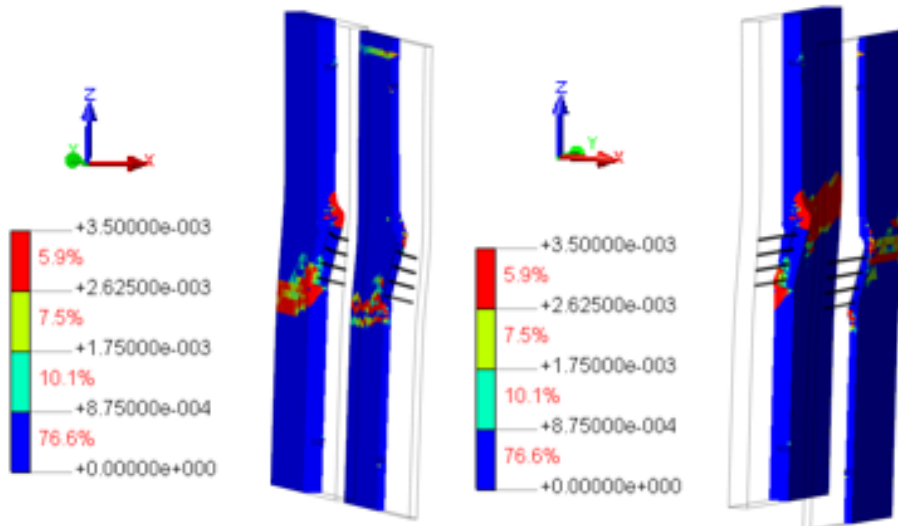


Plate connector, von Mises stress [MPa]

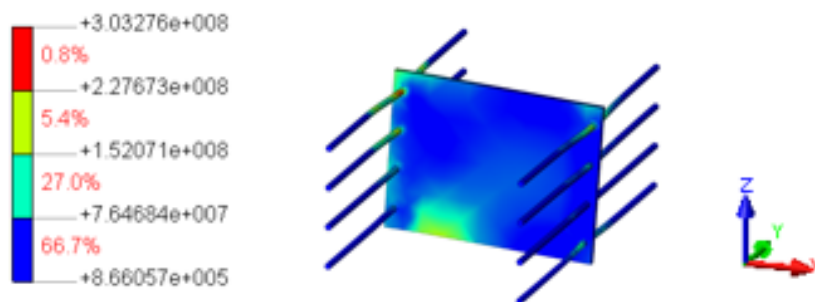
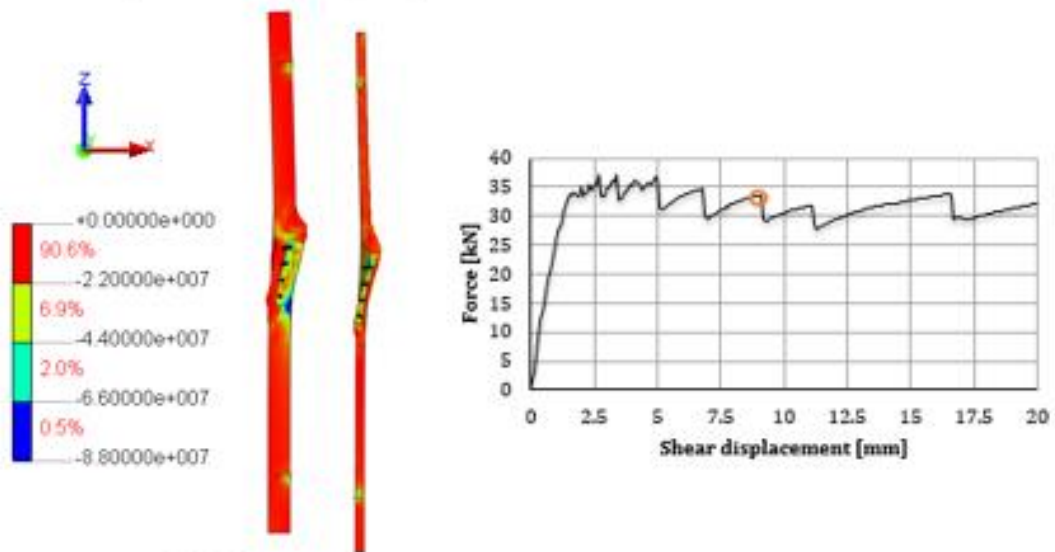


Figure 5-63 FE-results. TRC panel model, sudden loss of stiffness, cracks propagates further.

Concrete compressive stress, $S3$ [MPa]



Concrete strain, EZZ [-]

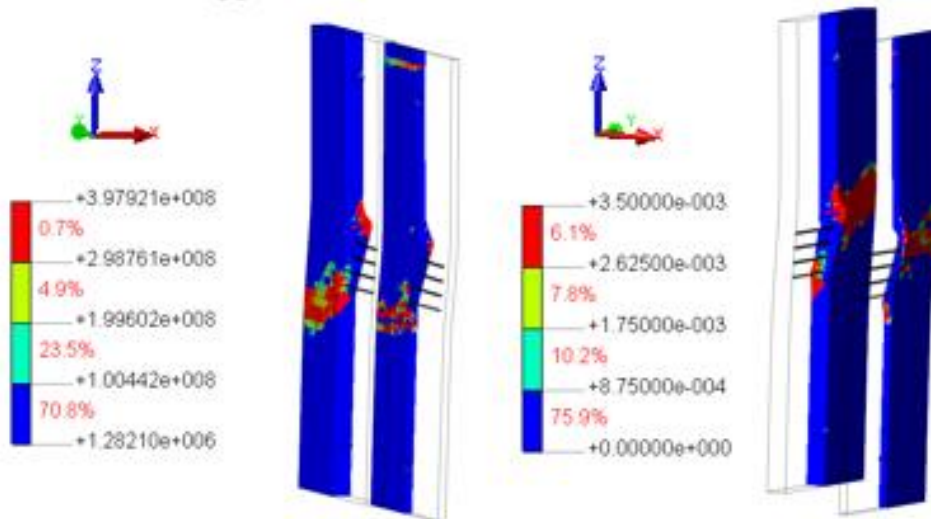


Plate connector, von Mises stress [MPa]

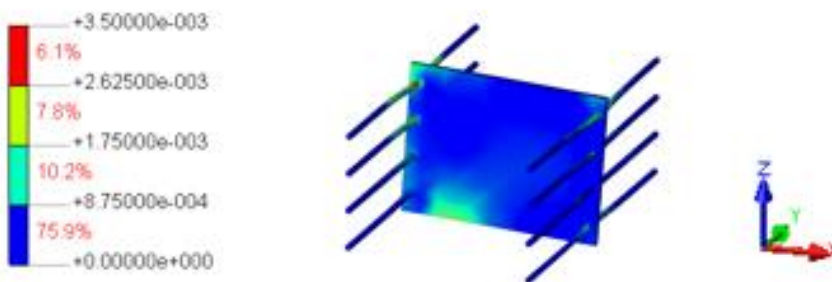
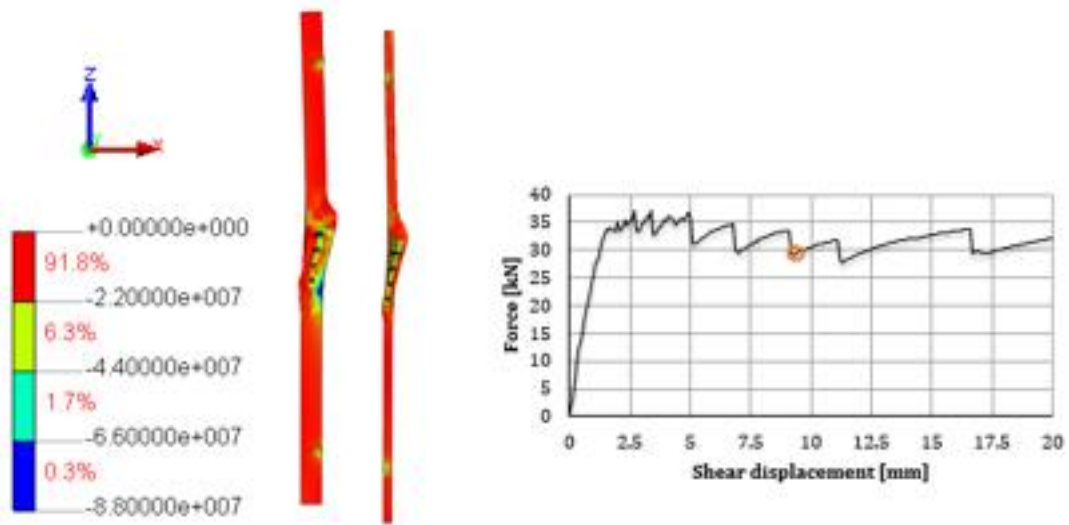


Figure 5-64 FE-results. TRC panel model, capacity reaches a peak, cracks propagates further.

Concrete compressive stress, S_3 [MPa]



Concrete strain, E_{ZZ} [-]

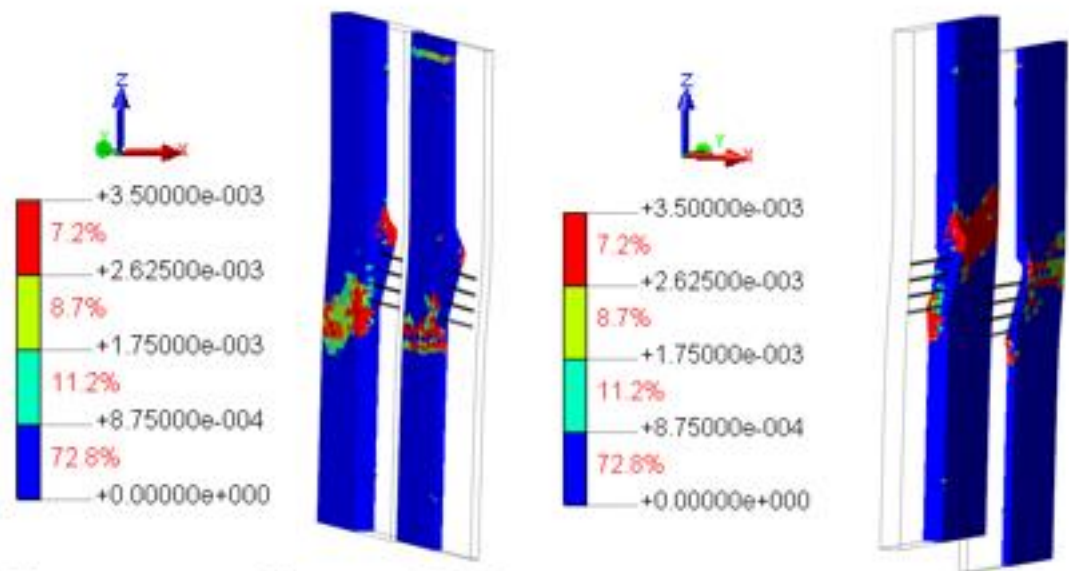


Plate connector, von Mises stress [MPa]

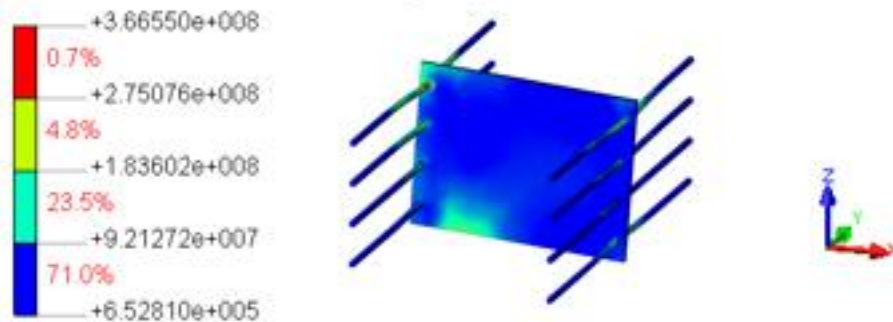


Figure 5-65 FE-results. TRC panel model, sudden loss of stiffness, cracks propagates further.

6 Discussions

As mentioned in section 5.1.5, when studying and comparing the structural behaviour of Test Model 1, with and without implementation of bond-slip, a big difference is obvious. Not only in the load vs. displacement curve but also in stress distribution and failure modes. Without bond-slip the full interaction between the connector and the concrete, as they share the same nodes in the FE-model, provides a robust fixation for the connector resulting in a very stiff behaviour. As stiffness tends to attract stresses, the stresses taken up by the connector are significantly higher than when the bond-slip relation is implemented. Furthermore, the strong bond enables higher utilization of the high strength FRP connector resulting in a higher ultimate capacity. Nevertheless, even though the model shows a very ductile behaviour, the high ultimate load leads further on to a brittle cracking and capacity loss which was not the case in the model with reduced bond strength.

After studying the shear traction reaction in the interface elements for both Test Models 1 and 2, it can be seen that neither model have reached their maximum values, as mentioned in section 5.1.6.3. This can be considered reasonable as the direct shear test on the panels mostly induce shear forces, which act in direction of the normal traction in the interface, perpendicular to the shear traction. Moreover, this explains why the normal stiffness input for the interface had such significant influence on the total stiffness behaviour.

In addition to inducing shear forces, the direct shear test also create a flexural load on the connector because of the eccentricity of loading to the supports. This flexural load is resisted by the fixed anchorage of the connector, creating pull-out tension at one side of the connector. This tension is taken up with shear traction reaction in the interface. As the flexure is proportionally small compared to the shear force the shear traction does not reach ultimate capacity as mentioned above.

From these discussions it can be assumed that by increasing the distance between wythes, thus increasing the eccentricity between load and support, one could expect greater flexural load and consequently larger pull-out tension in the connector. This means that with increased insulation thickness, the importance of including bonding behaviour in FE-modelling becomes greater.

This can be supported by the difference in maximum shear traction in Test Model 1, which was close to five times smaller than in Test Model 2, which has three times longer distance between wythes. The difference in geometry of the connectors and thus the interface can also affect this differences.

The TRC panel model shows a very stable behaviour with all component interacting as expected, while running analysis. As mentioned in 1.4, tests have not yet been conducted on a specimen with corresponding geometry and thus no results on its actual behaviour are available. Nevertheless, the model shows high ultimate capacity and a very ductile behaviour after failure, which implies that this is a promising design of a connection system for use in TRC sandwich panels.

7 Conclusions

7.1 Conclusions

After a study of reports regarding TRC, connectors and sandwich panels, four different FE-models were produced including one of a proposed connection system for a TRC sandwich panel. The material properties were obtained from reports and the manufacturer's data sheet, except for a few that had to be assumed or calculated.

By comparing 3D FE-test models with experimental results it was clear that the stiffness and ultimate strength was not limited by the tensile/compressive strength of the connecting devices or the concrete. The FE-test models showed considerable higher strength than the experimental results which suggested that some alterations needed to be done. After further research and several modifications of the FE-test model, the results indicated that the ultimate strength was greatly influenced by how the connectors and concrete interact. Thus, interface elements were added to the embedded parts of the connectors to mimic the bond-slip behaviour. Afterwards, the FE-test model showed a good correspondence to the test results which indicates that bond slip is truly an important aspect to include in the model.

Subsequently, a larger and more complicated model noted as TRC panel model was designed using the same modelling procedure as for the test models. Nonetheless, in this case bond slip was not implemented on the connector plate because of the anchoring bars which are mounted through the plate. However, bond slip was implemented on the pin connectors which are above and below the plate. Subsequently, the connection system can provide a fully composite behaviour in such TRC sandwich panel, since it has shown that the concrete wythes fail before the connector itself when the failure modes were inspected.

The geometry of the TRC panel model was based on other TRC sandwich panel experiments and the shape of the plate connector inspired by design of the Halfen shear plate connectors but with modified material properties and geometry. One of the challenges when selecting the connector system is the anchorage and embedment depth which are needed for the thin concrete wythes to avoid failures like pull-out. Because of the slenderness of the panel, it can be difficult to have a sufficient embedment depth while also maintaining an appropriate concrete cover.

At the time when this Master's thesis was published there were no experimental tests available to verify the TRC panel model, therefore a few test models were used to verify that the modelling procedure was right.

7.2 Further research

Since the TRC panel model only describes a part of a panel it would be interesting to model a full scale panel. Hence, it is possible to see a more realistic behaviour of the sandwich panel. Nevertheless, it is important to verify the TRC panel model first and compare it to experimental tests before the full scale panel is modelled.

Because this Master's thesis mainly focuses on two types of connectors for sandwich panels it would be interesting to model the other types which are mentioned in section 4 which are not studied in this Master's thesis. Furthermore, it would be possible to model different sizes and thicknesses of the connectors to see if that has any significant influence of the overall behaviour of the sandwich panel.

Further research on the bond-slip behaviour could also be done as well as more accurate calculations of the values for the bond-slip curve. By obtaining a more precise bond-slip curve it is possible to get even more realistic failure modes.

8 References

- Ancon©, 2015. Halfen sandwich panel anchor. *Ancon Building Products*. Available at: <http://www.ancon.co.nz/image/s7/content/11/sp-fa.jpg>.
- Anon, 2003. FEA bending analysis of TRC sandwich panels J . Finzel , U . Häußler-Combe Technische Universität Dresden - Institut für Massivbau , 01062 Dresden , Germany. *Engineering*, pp.1–9.
- Benayoune, a. et al., 2008. Flexural behaviour of pre-cast concrete sandwich composite panel - Experimental and theoretical investigations. *Construction and Building Materials*, 22, pp.580–592.
- Benayoune, a. et al., 2007. Response of pre-cast reinforced composite sandwich panels to axial loading. *Construction and Building Materials*, 21, pp.677–685.
- Benayoune, A. et al., 2008. Flexural behaviour of pre-cast concrete sandwich composite panel - Experimental and theoretical investigations. *Construction and Building Materials*, 22, pp.580–592.
- Brameshuber, W., 2006. Report 36: Textile Reinforced Concrete, State-of-the-Art Report of RILEM TC 201. *RILEM Publications*, (July 2002).
- Composite Global Solution, 2011. Thermomass – Insulated Concrete Sandwich Panel. Available at: <http://www.compositeglobal.com/insulation/concrete-sandwich-panels>.
- Domone, P. & Illston, J. eds., 2010. *Construction Materials* 4th ed., Spon Press.
- Einea, A. et al., 1994. A New Structurally and Thermally Efficient Precast Sandwich Panel System.pdf.
- fib International Federation for Structural Concrete, 2010. *Fib bulletin 55: Model Code 2010*,
- Gopinath, S. et al., 2014. Pre-fabricated sandwich panels using cold-formed steel and textile reinforced concrete. *Construction and Building Materials*, 64, pp.54–59. Available at: <http://www.sciencedirect.com/science/article/pii/S0950061814003857>.
- Hanjari, K.Z., Kettil, P. & Lundgren, K., 2011. *Modelling the structural behaviour of frost- damaged reinforced concrete structures*, *Structure and Infrastructure Engineering*,
- Häußler-Combe, U. & Hartig, J., 2007. Bond and failure mechanisms of textile reinforced concrete (TRC) under uniaxial tensile loading. *Cement and Concrete Composites*, 29, pp.279–289.

- Hegger, J. & Voss, S., 2008. Investigations on the bearing behaviour and application potential of textile reinforced concrete. *Engineering Structures*, 30, pp.2050–2056.
- J. Finzel & Häußler-Combe, U., 2003. FEA bending analysis of TRC sandwich panels. *Engineering*, pp.1–9.
- Kim, J. & You, Y.-C., 2015. Composite Behavior of a Novel Insulated Concrete Sandwich Wall Panel Reinforced with GFRP Shear Grids: Effects of Insulation Types. *Materials*.
- Mallick, P.K., 2008. *Fiber-Reinforced Composites: Materials, Manufacturing and Design*,
- Naito, C. et al., 2012. Performance and Characterization of Shear Ties for Use in Insulated Precast Concrete Sandwich Wall Panels. *ASCE Journal of Structural Engineering*, (January), pp.1–10.
- Obrien, E., Dixon, A. & Sheils, E., 2012. *Reinforced and Prestressed Concrete Design to EC2* 2nd ed., Spon Press.
- Portal, N.W., Lundgren, K. & Malaga, K., 2014. Evaluation of pull-out behaviour in textile reinforced concrete. , pp.97–102.
- Purnell, P. & Brameshuber, W., 2006. XIX TC 201-TRC (Textile Reinforced Concrete). , (July 2002).
- Shams, A., Hegger, J. & Horstmann, M., 2014. An analytical model for sandwich panels made of textile-reinforced concrete. *Construction and Building Materials*, 64, pp.451–459. Available at: <http://www.sciencedirect.com/science/article/pii/S0950061814003420>.
- Shams, A., Horstmann, M. & Hegger, J., 2014. Experimental investigations on Textile-Reinforced Concrete (TRC) sandwich sections. *Composite Structures*, 118, pp.643–653. Available at: <http://linkinghub.elsevier.com/retrieve/pii/S0263822314003791>.
- Sopal, G. et al., 2013. SHEAR TRANSFER MECHANISM OF CFRP GRIDS IN. , (December), pp.11–13.
- Thermomass®, 2012. Thermomass ® | CC Series. , (150 mm).
- Williams Portal, N., 2013. *Sustainability and Flexural Behaviour of Textile Reinforced Concrete*, Available at: <http://publications.lib.chalmers.se/records/fulltext/182607/182607.pdf>.

9 Appendices

9.1 Appendix A – DIANA .dat file

```
: Diana Datafile (TRC panel model) written by Diana 9.5
Translated from FX+ for DIANA neutral file (version
1.2.0).
'UNITS'
LENGTH M
FORCE N
TEMPER CELSIU
'DIRECTIONS'
  1  1.00000E+00  0.00000E+00  0.00000E+00
  2  0.00000E+00  1.00000E+00  0.00000E+00
  3  0.00000E+00  0.00000E+00  1.00000E+00
'MODEL'
GRAVDI 3
GRAVAC -9.81000E+00
'COORDINATES'
2227  2.60000E-02  6.50000E-02  5.43750E-01
2228  2.45000E-02  6.50000E-02  5.46348E-01
2229  2.15000E-02  6.50000E-02  5.46348E-01
116148  8.37339E-02  3.32258E-01  9.91434E-01
116149  9.79953E-02  3.25571E-01  3.05736E-01
116150  1.44238E-01  3.15890E-01  8.08904E-01
116151  1.70569E-01  2.80049E-01  9.61380E-01
'MATERI'
  1 NAME "Elastic_concrete"
    MCNAME CONCR
    MATMDL TSCR
    ASPECT
    POISON 2.00000E-01 % Poisson's ratio
    YOUNG 4.20000E+10 % Elastic modulus
    DENSIT 2.50000E+0 % Density
    TOTCRK ROTATE % Rotating crack model
    CRACKB 2.00000E-02 % Crack bandwidth
    TENCrv HORDYK % Tensile curve
    REDCRV NONE
    POIRED NONE
    GF1 1.63400E+02 % Fracture energy
    TENSTR 4.80000E+06
    COMCRV MULTLN % Multilinear,mod.Thorenfeldt
    COMSTR 8.80000E+07 % Compressive strength
    COMPAR 0.00000E+00 0.00000E+00 -4.20000E+06 -
1.00000E-04
-8.40000E+06 -2.00000E-04 -1.26000E+07 -
3.00000E-04
```

5.00000E-04	-1.68000E+07	-4.00000E-04	-2.10000E+07	-
7.00000E-04	-2.51990E+07	-6.00000E-04	-2.93980E+07	-
9.00000E-04	-3.35950E+07	-8.00000E-04	-3.77880E+07	-
1.10000E-03	-4.19750E+07	-1.00000E-03	-4.61500E+07	-
1.30000E-03	-5.03050E+07	-1.20000E-03	-5.44300E+07	-
1.50000E-03	-5.85080E+07	-1.40000E-03	-6.25180E+07	-
1.70000E-03	-6.64310E+07	-1.60000E-03	-7.02090E+07	-
1.90000E-03	-7.38040E+07	-1.80000E-03	-7.71590E+07	-
3.33561E-03	-8.02070E+07	-2.00000E-03	-8.28680E+07	-
3.03508E-02	-8.50610E+07	-1.63184E-02	-8.66990E+07	-
6.06830E-02	-8.77000E+07	-4.52125E-02	-8.76000E+07	-
9.26475E-02	-8.19170E+07	-7.65532E-02	-7.32710E+07	-
1.24888E-01	-6.24050E+07	-1.08802E-01	-5.06550E+07	-
1.56494E-01	-3.94290E+07	-1.40815E-01	-2.97100E+07	-
1.86931E-01	-2.18900E+07	-1.71879E-01	-1.59120E+07	-
2.15975E-01	-1.14910E+07	-2.01632E-01	-8.28490E+06	-
2.43584E-01	-5.98340E+06	-2.29955E-01	-4.33780E+06	-
2.69833E-01	-3.16100E+06	-2.56873E-01	-2.31700E+06	-
2.94846E-01	-1.70910E+06	-2.82487E-01	-1.26880E+06	-
3.18776E-01	-9.48000E+05	-3.06940E-01	-7.12810E+05	-
3.41757E-01	-5.39290E+05	-3.30377E-01	-4.10480E+05	-
3.63935E-01	-3.14250E+05	-3.52940E-01	-2.41930E+05	-
3.85418E-01	-1.87270E+05	-3.74755E-01	-1.45720E+05	-
4.06315E-01	-1.13950E+05	-3.95934E-01	-8.95440E+04	-
4.26714E-01	-7.06920E+04	-4.16572E-01	-5.60600E+04	-

4.46688E-01	-4.46490E+04	-4.36750E-01	-3.57090E+04	-
4.66302E-01	-2.86740E+04	-4.56537E-01	-2.31140E+04	-
4.85608E-01	-1.87030E+04	-4.75990E-01	-1.51880E+04	-
5.04650E-01	-1.23770E+04	-4.95160E-01	-1.01200E+04	-
5.23467E-01	-8.30200E+03	-5.14085E-01	-6.83200E+03	-
5.42089E-01	-5.64000E+03	-5.32801E-01	-4.66900E+03	-
5.60544E-01	-3.87700E+03	-5.51336E-01	-3.22800E+03	-
5.78853E-01	-2.69500E+03	-5.69716E-01	-2.25600E+03	-
5.97037E-01	-1.89400E+03	-5.87960E-01	-1.59300E+03	-
6.15111E-01	-1.34400E+03	-6.06086E-01	-1.13600E+03	-
6.33088E-01	-9.62000E+02	-6.24110E-01	-8.17000E+02	-
6.50982E-01	-6.96000E+02	-6.42045E-01	-5.93000E+02	-
6.68801E-01	-5.07000E+02	-6.59900E-01	-4.34000E+02	-
6.86556E-01	-3.72000E+02	-6.77686E-01	-3.20000E+02	-
7.04252E-01	-2.76000E+02	-6.95411E-01	-2.38000E+02	-
7.21898E-01	-2.06000E+02	-7.13081E-01	-1.78000E+02	-
7.39498E-01	-1.54000E+02	-7.30704E-01	-1.34000E+02	-
7.57058E-01	-1.17000E+02	-7.48283E-01	-1.02000E+02	-
7.74582E-01	-8.90000E+01	-7.65824E-01	-7.80000E+01	-
7.92073E-01	-6.80000E+01	-7.83332E-01	-6.00000E+01	-
8.09536E-01	-5.20000E+01	-8.00808E-01	-4.60000E+01	-
8.26972E-01	-4.00000E+01	-8.18257E-01	-3.60000E+01	-
8.44385E-01	-3.10000E+01	-8.35681E-01	-2.80000E+01	-
2	NAME	"Pin_connector"		
	YOUNG	4.00000E+10		
	POISON	2.00000E-01		
	YIELD	VMISES	% Von Mises yield criterion	
	YLDVAL	9.48000E+08	% Yield value	

```

3 NAME "Insulation_XPS"
  YOUNG 5.00000E+03
  POISON 2.00000E-01
4 NAME "FRP_Plate"
  YOUNG 4.00000E+10
  POISON 2.00000E-01
  YIELD VMISES
  YLDVAL 9.48000E+08
5 NAME "FRP_Bars"
  YOUNG 4.00000E+10
  POISON 2.00000E-01
  YIELD VMISES
  YLDVAL 9.48000E+08
6 NAME "Textile_Reinforcement"
  YOUNG 2.40000E+11
  POISON 2.00000E-01
  YIELD VMISES
  YLDVAL 4.00000E+09
7 NAME "Interface"
  DSTIF 1.09000E+10 1.09000E+10
  BONDSL 3
  SLPVAL 0.00000E+00 0.00000E+00 1.09000E+07
1.00000E-03 6.00000E+06 2.00000E-03 3.00000E+06
2.00000E-02 0.00000E+00 4.00000E-02
8 NAME "XPS_Ortho"
  YOUNG 1.20000E+07 1.00000E+00 1.00000E+00
  POISON 0.00000E+00 0.00000E+00 0.00000E+00
  SHRMOD 1.00000E+00 1.00000E+00 1.00000E+00
  DENSIT 1.00000E+00
'GEOMET'
1 NAME "Interface"
  XAXIS 1.00000E+00 0.00000E+00 0.00000E+00
2 NAME "FRP_Bar"
3 NAME "FRP_Plate"
4 NAME "Concrete"
5 NAME "FRP_Pins"
6 NAME "XPS_Ortho"
7 NAME "Textile_Reinf"
  THICK 6.10000E-05 6.10000E-05
  XAXIS 0.00000E+00 1.00000E+00 0.00000E+00
'DATA'
1 NAME "Wythe"
2 NAME "FRP_Pins"
4 NAME "FRP_Plate"
5 NAME "FRP_Bar"
10 NAME "XPS_Ortho"
9 NAME "Interface"
6 NAME "Textile_Reinf"
'ELEMENTS'

```

```

CONNECT
659490 T18IF 52309 52316 52310 102613 102612 102611
% Interface elements
.
.
.
7215 TE12L 2557 2410 2415 2261
.
.
.
MATERI
/ 364286-428026 525016-562204 / 1
/ 659225-659489 / 2
/ 31424-39135 / 4
/ 7215-20274 / 5
/ 659490 659492 659493 659495 659497 659499-659512 659514
659516-659519
659522-659524 659526 659528 659530-659533 659535-659541
659543-659545
659547-659551 / 7
/ 659552-756527 / 8
DATA
/ 364286-428026 525016-562204 / 1
/ 659225-659489 / 2
/ 31424-39135 / 4
/ 7215-20274 / 5
/ 659552-756527 / 10
/ 659490 659492 659493 659495 659497 659499-659512 659514
659516-659519
659522-659524 659526 659528 659530-659533 659535-659541
659543-659545
659547-659551 / 9
GEOMET
/ 659490 659492 659493 659495 659497 659499-659512 659514
659516-659519
659522-659524 659526 659528 659530-659533 659535-659541
659543-659545
659547-659551 / 1
/ 7215-20274 / 2
/ 31424-39135 / 3
/ 364286-428026 525016-562204 / 4
/ 659225-659489 / 5
/ 659552-756527 / 6
'REINFORCEMENTS'
LOCATI
1 GRID
  PLANE 21654 21325 21389 23279
2 GRID
  PLANE 42652 42653 42654 42655
3 GRID
  PLANE 42656 42657 42658 42659

```

```
MATERI
/ 1-3 / 6
GEOMET
/ 1-3 / 7
DATA
/ 1-3 / 6
'LOADS'
CASE 1
NAME "Load"
DEFORM
52271 TR 3 -2.00000E-02
```

9.2 Appendix B - Material properties calculations

Test Model 1

Concrete

$$f_{cm,1} := 47.4 \quad [\text{MPa}] \quad \text{Value stated in report}$$

Calculated values from fib Model Code 2010

$$\Delta f := 8 \quad [\text{MPa}]$$

$$f_{ck,1} := f_{cm,1} - \Delta f = 39.4 \quad [\text{MPa}]$$

Fracture energy

$$G_F := 73 \cdot f_{cm,1}^{0.18} = 146.205 \quad [\text{N/m}]$$

Tensile strength

$$f_{ctm} := 0.3 \cdot f_{ck,1}^{\frac{2}{3}} = 3.474 \quad [\text{MPa}]$$

Modulus of elasticity

$$E_{c0.1} := 21500 \quad [\text{MPa}]$$

$$\alpha_E := 1$$

Assuming quartzite aggregates

$$E_{ci,1} := E_{c0.1} \cdot \alpha_E \cdot \left(\frac{f_{ck,1} + \Delta f}{10} \right)^{\frac{1}{3}} = 3.612 \times 10^4 \quad [\text{MPa}] \quad E_{cm,1} := E_{ci,1}$$

FRP Plate

Reduced material properties for embedded part of connector

Pullout

$$F_{\text{report}} := 15.3 \text{ kN} \quad \text{Pullout capacity. Value from producer of connector}$$

$$f_{y,FRP} := 827 \text{ MPa}$$

$$E_{FRP} := 30 \text{ GPa}$$

$$A_{CCconn} := [38\text{mm} - (2 \cdot 2.5\text{mm})] \cdot 9.5\text{mm} = 313.5 \cdot \text{mm}^2$$

$$F_{ult.CC} := f_{y.FRP} \cdot A_{CCconn} = 259.265 \cdot \text{kN}$$

$$\text{Ratio}_{FRP} := \frac{F_{report}}{F_{ult.CC}} = 0.059$$

$$f_{y.FRP.reduced} := f_{y.FRP} \cdot \text{Ratio}_{FRP} = 48.804 \cdot \text{MPa}$$

$$E_{FRP.reduced} := E_{FRP} \cdot \text{Ratio}_{FRP} = 1.77 \cdot \text{GPa}$$

Test model 2

Concrete

Values stated in report

$$f_{ck.cube.2} := 65.1 \quad [\text{MPa}]$$

$$E_{cm2} := 37.23 \quad [\text{GPa}]$$

$$\text{ratio}_{cyl.cube} := \frac{67}{55} = 1.218 \quad \text{For concrete C55/67 in EC}$$

$$f_{ck.2} := \frac{f_{ck.cube.2}}{\text{ratio}_{cyl.cube}} = 53.44 \quad [\text{MPa}]$$

Calculated values from fib Model Code 2010

$$f_{cm.2} := f_{ck.2} + \Delta f = 61.44 \quad [\text{MPa}]$$

Fracture energy

$$G_{F.2} := 73 \cdot f_{cm.2}^{0.18} = 153.195 \quad [\text{N/m}]$$

Tensile strength

$$f_{ctm.2} := 0.3 \cdot f_{ck.2}^{\frac{2}{3}} = 4.256 \quad [\text{MPa}]$$

FRP Pin

Reduced material properties for embedded part of connector

Pullout

$$F_{\text{report.2}} := 8.5 \text{ kN} \quad \text{Pullout capacity. Value approximated from graph}$$

Pullout calculations with given equation

$$k_2 := 8.6$$

$$t_{TM.2} := 25$$

$$F_{\text{calc.TRC}} := k_2 \cdot t_{TM.2}^{1.5} \cdot f_{cm.2}^{0.5} = 8.426 \times 10^3$$

Tensile strength of pin

$$f_{y.FRPin} := 948 \text{ MPa}$$

$$E_{FRPpin} := 30 \text{ GPa}$$

$$A_{pin} := 9.8 \text{ mm} \cdot 5.7 \text{ mm} = 55.86 \cdot \text{mm}^2$$

$$F_{ult.pin} := f_{y.FRppin} \cdot A_{pin} = 52.955 \cdot \text{kN}$$

$$\text{Ratio}_{FRppin} := \frac{F_{calc.TRC}}{F_{ult.pin}} = 0.159 \frac{1}{N}$$

$$f_{y.FRppin.reduced} := f_{y.FRppin} \cdot \text{Ratio}_{FRppin} = 150.846 \frac{1}{N} \cdot \text{MPa}$$

$$E_{FRppin.reduced} := E_{FRppin} \cdot \text{Ratio}_{FRppin} = 4.774 \frac{1}{N} \cdot \text{GPa}$$

Reinforcement Grid

Equivalent thickness of textile reinforcement in Test Model 2 for input in DIANA

$$A_{tr} := 1.83 \text{ mm}^2 \quad \text{Cross-sectional area of single textile yarn}$$

$$s_{tr} := 30 \text{ mm} \quad \text{Spacing of yarns}$$

$$A_{tr.1m} := \frac{A_{tr} \cdot 1 \text{ m}}{s_{tr}} = 61 \cdot \text{mm}^2 \quad \text{Area pr. meter}$$

$$t_{eq} := \frac{A_{tr.1m}}{1 \cdot \text{m}} = 6.1 \times 10^{-5} \cdot \text{m} \quad \text{Equivalent thickness of reinforcement}$$

TRC panel model

Concrete C80/90. Material properties obtained from EC2

Fracture energy

From fib Model Code for Concrete Structures 2010

$$f_{cm.TRC} := 88 \quad [\text{MPa}]$$

$$G_{F.TRC} := 73 \cdot f_{cm.TRC}^{0.18} = 163.429 \quad [\text{N/m}]$$